

An Investigation into Present Sand Control Testing Practices for SAGD Wells

by

Omar Kotb

A thesis submitted in partial fulfillment of the requirements for the degree of

Master of Science

in

Petroleum Engineering

Department of Civil & Environmental Engineering

University of Alberta

© Omar Kotb, 2019

Abstract

Heavy oils and extra heavy oils in Alberta that are currently extracted through thermal recovery primarily employ Steam Assisted Gravity Drainage (SAGD). Sand control devices (SCDs) such as Slotted Liners (SLs) and Wire Wrap Screens (WWSs) have been used extensively in wells producing from unconsolidated formations such as the McMurray and Clearwater formations. Currently, utilization of sand control testing technology in the laboratory is gaining significant attention from the industry due to its ability to assess the performance and design of SCDs.

Since 1938, researchers have been developing sand control testing setups to evaluate the performance and develop design criteria for SCDs for different well conditions. However, it was only in the past decade that sand control testing began being employed for SAGD wells. Generally, researchers have aimed to apply sand control testing technologies in SAGD condition with varying setups and procedures to either evaluate comparatively the performance of different SCDs or investigate the effect of one testing parameter on the SCD performance. However, little focus has been given towards examining how the differences in testing setups and procedures affect the results and thus, the conclusions on SCDs performances. This shortcoming can cause significant difficulties in understanding as to what extent each study is simplifying the SAGD conditions and how their results are comparable to other setups.

The focus of this study is to improve the understanding of the current SRT setups and procedures in the literature on the sanding and flow performance results of the SCDs in SAGD and identify their limitations. Subsequently, the appropriate improvements are suggested, tested, and evaluated to overcome these limitations. The improvements should be supported either by superior testing performance or better representation of SAGD well-operating conditions based on developing an

understanding of sanding in SAGD through a literature review. Another aim of this study is to characterize SAGD reservoir oil sands and improve established techniques for replicating reservoir oil sands for sand control testing purposes.

A new sand control testing facility was developed, capable of conducting multiphase flow tests with multi-slot slotted liner coupons under different axial stress magnitudes. A testing procedure was designed to allow the representation of sanding in SAGD conditions while accommodating varying field conditions. The setup was used to evaluate the testing performance by introducing new procedures and testing parameters compared to previous testing practices in the literature. The sanding performance was assessed based on measuring the cumulative sand produced at the end of the test. The pore and slot plugging were evaluated by comparing the pressure responses of the sand-pack and the near-coupon region.

The work starts with the characterization oil-sands samples received from the McMurray Formation in the Long Lake field. The characterization was conducted in terms of PSD, grain shape, and mineral composition. Next, the characterization data was used to replicate the oil sand samples using commercial sands. Sieve analysis was conducted to validate the success of the replication process.

SRT testing parameters were gradually changed from a prominent testing approach in the literature developed by Hycal labs to the new procedure. The sanding test results indicate that fluid flow rate is the most influential testing parameter in SRT testing followed by the packing technique, stress magnitude, and brine salinity. Analysis of pressure data revealed that the moist tamping packing technique results in a significant increase in porosity and uniformity of the sand-pack. Besides, the effect of stress was found to be small on pressure drop, for the stress ranges in this testing program.

Furthermore, lowering the salinity from 10,000 ppm to 350 ppm was found to significantly increase fines migration and production, which led to higher pressure drops across the sample.

Preface

This thesis is an original work by Omar Kotb. No part of this thesis has been previously published.

Dedication

This dissertation is dedicated to my dearest family, Mr. Nasser Kotb, Dr. Maha Kamal and

Mr. Yasser Kotb.

Acknowledgements

I want to express my sincere appreciation to Dr. Alireza Nouri, for his valuable guidance, support, and kind help throughout my master program. I greatly appreciate the opportunity to pursue my research under Dr. Nouri's supervision. He has always been accessible and willing to help me with my research. I have learned from him the skill of critical thinking and rigorous attitude towards research.

I would like to express my deepest gratitude to my family. I much appreciate their unconditional love and support for me. I also want to thank my friends Ilyas El Kindi, Fritjof Bruns, Samer Hmoud and Basem Zakaria.

I want to also thank my colleagues, Dr. Morteza Roostaei, Dr. Mohammed Haftani, Dr. Mahmoud Salimi, Arian Velayati, Jesus Montero, Chenxi Wang, as well as RGL's Dr. Vahidoddin Fattahpour and Dr. Mahdi Mahmoodi and Nexen CNOOC's Noel Devere-Bennett, for providing feedbacks for this research. I am also thankful to the Todd Kinnee, Engineering Technologist, for his help and assistance in setting up the laboratory facility.

I would also like to thank all my committee members, Dr. Hassan Dehghanpour, Dr. Nobuo Maeda, and Dr. Japan Trivedi for their valuable suggestions to improve my thesis.

I gratefully acknowledge the financial support provided by RGL Reservoir Management Inc. matched by the Natural Sciences and Engineering Research Council of Canada (NSERC) through their Collaborative Research and Development (CRD) Grant program.

Table of Contents

Abstract.....	ii
Preface.....	v
Dedication	vi
Acknowledgements	vii
Table of Contents	viii
List of Tables	xiv
List of Figures.....	xv
CHAPTER ONE: Introduction	1
1.1 Background	1
1.2 Problem Statement	1
1.3 Research Objectives	2
1.4 Research Hypothesis	2
1.5 Research Methodology.....	3
1.6 Significance of the Work.....	4
1.7 Thesis Structure.....	5
Chapter 2- Literature Review.....	6
2.1 Introduction	6
2.2 Sanding Problems in SAGD.....	7
2.3 Sand Control Methods.....	9
2.3.1 Controlling drawdown.....	9
2.3.2 Chemical based sand control	10
2.3.3 Mechanical based sand control.....	10
Slotted liners	11
Wire wrapped screens.....	12
Precise punched screens	13
Gravel packs	14
2.4 Failure Mechanisms for SL and WWS	15

2.4.1 Intolerable sand production	15
2.4.2 Slot and near-slot pore plugging.....	16
2.5 Influential Factors in SCD Performance	17
2.5.1 Fluid flow rates	17
2.5.2 Fluid phases	18
2.5.3 Sand grain characteristics	19
Sand grains size	19
Sand grain shape	20
2.5.4 Stress.....	21
2.5.5 Salinity and pH	21
2.5.6 Miscellaneous factors	22
2.6 Sand-Retention Tests and Setup Variations in Literature	23
2.5.1 Slurry SRT	23
2.5.2 Prepack SRT	25
Conventional SRT	26
Pre-packed SRT with Stress (SRTS).....	27
Full-Scale Completion Tests (FCT)	27
2.6 Case Study: Hycal Labs Sand Control Testing Setup and Procedures	29
2.6.1 Testing setup and procedure	29
Testing setup.....	29
Testing procedure	30
2.6.2 Setup and procedural limitations and their implications on the SCD evaluation.....	31
2.7 Summary	33
Chapter 3: Long Lake Field-McMurray Formation Oil Sand Characterization and Replication	34
3.1 Introduction	34

3.2 Preparation and Cleaning of Field Oil Sands Samples	35
3.3 Surface Texture of Particles	36
3.4 Characterization and Replication of PSD.....	41
3.4.1 Measurement and description of PSD	41
3.4.2 Characterization of oil sands PSD	42
3.4.3 Replication based on PSD	45
3.5 Shape Factor Characterization and Replication	48
3.5.1 Shape factors description.....	50
Sphericity.....	50
Aspect ratio.....	50
Convexity.....	51
3.5.2 Characterization of particle shape	52
3.5.3 Matching grain shape.....	52
3.6 Compositional Analysis	56
3.6.1 Oil sands fines compositional analysis.....	56
3.6.2 Replication of fines based on compositional analysis	60
3.7 Conclusion.....	60
Chapter 4: Experimental Setup and Testing Procedure	61
4.1 Introduction	61
4.2 Experimental Setup	61
4.2.1 Fluid injection unit.....	62
4.2.2 Sand-pack cell and SCD holder.....	62
4.2.3 Load frame.....	63
4.2.4 Data acquisition and monitoring unit	63
4.2.5 Sand and fines production measurement unit.....	63
4.2.6 Backpressure unit	64
4.3 Testing Material and Components	64

4.3.1 Representative sand	64
4.3.2 Representative fluids	65
Brine	65
Oil	67
Gas	68
4.3.3 Liner coupons	68
4.4 Testing Plan	69
4.5.2 Sand-pack packing	70
4.5.3 Sand-pack saturation	71
4.5.4. Representative stress conditions	71
4.5.5 Fluid injection rates	72
4.6 Test Measurements and Uncertainty Analysis	78
4.7 Test Repeatability	79
4.7 Conclusion	81
Chapter 5: Effect of SRT Testing Procedure and Parameters on Sand Production and Fines Migration	82
5.1 Introduction	82
5.2 Replication Test	82
5.2.1 Introduction	82
5.2.2 Testing program	83
5.2.3 Results and discussion	83
5.3 Effect of Using Moist Tamping Packing Technique	87
5.3.1 Introduction	87
5.3.2 Testing program	87
5.3.3 Results and discussion	88
5.4 Effect of Using Representative Stress	91
5.4.1 Introduction	91

5.4.2 Testing program.....	92
5.4.3 Results and discussion.....	92
5.5 Design of Flow Steps	95
5.5.1 Introduction	95
5.5.2 Testing program.....	95
5.5.3 Results and discussion.....	98
5.6 Effect of Using Representative Salinity	100
5.6.1 Introduction	100
5.6.2 Testing program.....	100
5.6.3 Results and discussion.....	101
5.7 Conclusion.....	104
Chapter 6: Conclusions and Recommendations for Future Work	106
6.1 Main Results and Contributions.....	106
6.2 Experimental testing limitations.....	107
6.3 Recommendations for Future Work	107
6.3.1 Investigation into how laboratory sand production relates to field production.....	107
6.3.2 Investigating how conducting HT-HP sand control testing differs from the simplified version	108
6.3.3 Investigating how to practically and accurately quantify fines migration in multiphase flow conditions	108
6.3.4 Investigating how to practically measure and isolate relative permeability effects from fines migration effects in multiphase flow conditions.....	108
6.3.5 Effect of stress isotropy on sand production	109
6.3.6 Effect of slot width, geometry, and density on completion induced skin in injection wells	109
References	110
Appendix A: Determining Stress During Saturation	125

Appendix B: Flow Rate Estimation.....	127
Appendix C: Initial Absolute Permeability	130
Appendix D: Friction Approximation Across the Core	131

List of Tables

Table 2-1. Summary of the SCD pass/fail criteria for slurry testing in the literature.....	25
Table 2-2. Schematic of Hycal labs multiphase flow setup (Bennion et al. 2007).....	31
Table 3-1. PSD descriptors of sands used in testing.....	48
Table 3-2. XRD Rietveld analysis results of the oil sands samples.....	57
Table 3-3. XRD Rietveld analysis results of the commercial fines samples	60
Table 4-2. Test matrix.....	70
Table 4-3. Effective flow factors to calculate testing flow rates	75
Table 4-4. Testing parameters of the replication test.....	80
Table 5-1. Testing program (Packing).....	88
Table 5-2. Testing program (Stress)	92
Table 5-3. Testing program (Fluid Flow Rate).....	96
Table 5-4. Testing program for salinity test.....	101
Table A-1. Lab constants and assumptions during saturation	125
Table B-1. Lab and field constants and assumptions.....	127
Table B-1. Field production information	127
Table C-3. Scenarios of effective flow represented in the testing	128
Table C-4. Scenarios of effective flow represented in the testing	128
Table C-5. Steam rate calculations	129
Table C-1. Initial permeability of the sand pack of each test	130
Table D-1. Mechanical properties of University of Alberta (UofA) and Hycal setup and sands	131

List of Figures

Figure 2-1. Illustration of the SAGD process (Dang et al. 2013).....	9
Figure 2-2. Different slot geometries and distributions (Guo 2018)	12
Figure 2-3. Wire wrapped screens (Zhang 2017)	13
Figure 2-4. Illustration of how bridging happens in WWS (Right) and PPS (Left).....	14
Figure 2-5. Illustration of the hydrodynamic forces and frictional forces aiding and preventing sand production, respectively, through a liner slot.....	16
Figure 2-6. Schematic illustrating a typical slurry setup	24
Figure 2-7. Demonstration of the downhole scenarios simulated by prepack SRT (left) and slurry SRT (Right) (Montero et al. 2018)	25
Figure 2-8. Conventional Pre-Packed Sand Retention Test (SRT) (Montero et al. 2018)	28
Figure 2-9. Pre-packed SRT with Stress (SRTS) (Montero et al. 2018)	29
Figure 2-10. Schematic of Hycal labs multiphase flow SRT setup (Bennion et al. 2007).....	31
Figure 3-1. Flowchart linking relationship between sand characterization and sand control testing	35
Figure 3-2. Image and schematics of Soxhlet extraction setup used in this work.....	36
Figure 3-3. SEM images of the field and commercial sands for different size classes	41
Figure 3-4. PSD of sands from the formation of interest analyzed by Hycal compared to the analysis conducted herein	43
Figure 3-5. Uniformity and sorting coefficients versus D10 of the sand samples from the formation of interest acquired from different wells.....	44
Figure 3-6. Uniformity and sorting coefficients versus D50 of the sand samples from the formation of interest acquired from different wells.....	44
Figure 3-7. The relationship between fines and clay content in gathered oil sand samples from McMurray Formation in Long Lake	45

Figure 3-8. PSD curves of oil sands analyzed by Hycal by LPSA (blue), oil sands used in Hycal testing (black), Long Lake samples characterized in the University (green), and commercial sands available (red)	46
Figure 3-9. Diagram of the PSD replication technique.....	47
Figure 3-10. A comparison between the target (Batch 3) and replica PSD from the replication process.....	47
Figure 3-11. A qualitative measurement of shape (Powers 1953).....	49
Figure 3-12. A guide for assigning roundness and sphericity values to a particle (Krumbein and Sloss 1951).....	49
Figure 3-13. Schematic illustrating maximum and minimum feret diameters of a sand grain.....	51
Figure 3-14. Schematic illustrating concept of convexity	51
Figure 3-15. From left to right aspect ratio, sphericity, and convexity of oil sand samples versus depth.....	52
Figure 3-16. Oil sands and commercial sand convexity (a) and cumulative distribution (b) of convexity with the available commercial sands.....	53
Figure 3-17. Oil sands and commercial sand sphericity (a) and cumulative distribution (b) of sphericity with the available commercial sands.....	54
Figure 3-18. Oil sands and commercial sand aspect ratios (a) and cumulative distribution (b) of aspect ratio with the available commercial sands	55
Figure 3-19. SEM image and EDS analysis of oil sands sample at a depth of 225 m.....	57
Figure 3-20. SEM image and EDS analysis of oil sands sample at a depth of 215 m.....	58
Figure 3-21. SEM image and EDS analysis of oil sands sample at a depth of 219 m.....	58
Figure 3-22. SEM image and EDS analysis of oil sands sample at a depth of 206 m.....	59
Figure 3-23. Close up SEM images of trace minerals in the fines of oil sands samples	59
Figure 4-1. Schematic of the SRT setup	61
Figure 4-2. Target sand (Batch 2 & 3 of Hycal testing) and the sand replica	65

Figure 4-3. STIFF diagram comparing field samples to brine used to testing by Hycal labs and University of Alberta	67
Figure 4-4. Measured oil viscosity for Long Lake field as a function of temperature	67
Figure 4-5. Multi-slot coupon as a cut-out of a slotted liner	68
Figure 4-6. (a) An image of a multi-slot 0.016-to-0.020 coupon, (b) schematic cross section of a rolled top slot	69
Figure 4-7. Hycal original rates used with their setup	73
Figure 4-8. Hycal upscaled rates used with the University of Alberta setup.....	73
Figure 4-9. Schematic view to illustrate how variations of sub-cool in a SAGD well can result in fluid flow variations along the length of the well	76
Figure 4-10. Non-contributing sections of a slotted liner	76
Figure 4-11. The methodology for setting representative liquid flow rates	77
Figure 4-12. A diagram illustrating the new methodology for setting representative gas flow rates	77
Figure 4-13. Liquid and gas rates for the University testing procedure	78
Figure 4-14. Concept of the pressure gradient in the context of testing setup presented herein ..	79
Figure 4-15. Pressure gradients for repeatability tests.....	80
Figure 4-16. Normalized sand production in repeatability tests	81
Figure 5-1. Normalized produced sand of replication test with sand produced by Hycal testing	84
Figure 5-2. Compares the pressure gradients across the cell of Hycal tests employing sand-pack of Batch 2 with the pressure gradients of the replication test on the 153 μm (0.006 inch) WWS....	85
Figure 5-3. Near-coupon pressure gradients of Hycal’s SRT using different SCDs reported in (Devere-Bennett 2015).....	86
Figure 5-4. Near-coupon pressure gradients of Hycal’s SRT using different SCDs reported in (Devere-Bennett 2015).....	87

Figure 5-5. Normalized produced sand in testing on sand-packs by moist tamping and Hycal packing techniques.....	89
Figure 5-6. Porosity distribution across the sand-pack after stress was applied (A: Bottom and E: Top).....	90
Figure 5-7. Porosity distribution across the sand-pack before stress was applied (A: Bottom and E: Top).....	90
Figure 5-8. Pressure gradient across the sand-pack in SRT testing packed by moist tamping and Hycal’s packing technique.....	91
Figure 5-9. Normalized sand production under 60 and 350 psi axial stress	93
Figure 5-10. Effect of axial stress on pressure gradient across the top and middle segments of the sand-pack at 350 and 60 psi	94
Figure 5-11. Effect of stress on pressure gradient across the near-coupon region of the sand-pack	94
Figure 5-12. The maximum liquid flow rates used in testing stages of Hycal and the University	97
Figure 5-13. Water cuts used in testing stages of Hycal and the University	97
Figure 5-14. The maximum gas flow rates used in testing stages of Hycal and the University...	97
Figure 5-15. The maximum liquid flow rates employed by Hycal and the University for SL testing	98
Figure 5-16. Normalized sand production by SRT testing at different flow rates.....	99
Figure 5-17. Pressure gradient associated with the new procedure	100
Figure 5-18. Normalized sand production by SRT testing with a brine of salinity of 350 ppm and 10,000 ppm	101
Figure 5-19. Location of the brine sampling port in the SRT setup	102
Figure 5-20. Solid concentration in brine under the coupon at different testing stages	103
Figure 5-21. Pressure gradient of the top and middle sections of the SRT sand-pack while injecting with brine salinity of 350 and 10,000 ppm	103

Figure 5-22. Pressure gradient of the near-coupon section of the sand-pack for brine salinity of 350 and 10,000 ppm..... 104

Figure 5-23. Summary of the effect of different testing parameters on the sand production 105

Figure A-1 Modified illustrations of the phenomena of bed fluidization (De Nevers 1999) 125

Nomenclature

D	Diameter of Particle Size
D ₁₀	Sieve opening size that retains 10% of the particles in a sample
D ₅₀	Sieve opening size that retains 50% of the particles in a sample (Median size on the PSD curve)
D ₉₀	Sieve opening size that retains 90% of the particles in a sample
D ₉₅	Sieve opening size that retains 95% of the particles in a sample
dp	Pressure drop
P _{real}	Perimeter of sand grain projection
P _{gradient}	Pressure gradient
A	Area of sand grain projection
S	Sphericity
AR	Aspect Ratio
L	Length of Core-holder
P _{EQPC}	Circle Equivalent parameter of Sand Grain Projection

List of Abbreviations

CHOPS	Cold Heavy Oil Production with Sand
CNRL	Canadian Natural Resources Limited
DAQ	Data Acquisition
DIA	Dynamic Image Analysis
EDS	Electron Dispersive Spectroscopy
ESP	Electric Submersible Pump
FCT	Full-Scale Completion Test
GP	Gravel Pack
LPSA	Laser Particle Size Analysis
OFA	Open Flow Area
PPS	Precise Punched Screen
PSD	Particle Size Distribution
SAGD	Steam Assisted Gravity Drainage
SC	Sorting Coefficient
SL	Slotted Liner
SEM	Scanned Electron Microscope
SPF	Slots Per Foot
SRT	Sand Retention Test
SRTS	Sand Retention Test with Stress
UC	Uniformity Coefficient
UofA	University of Alberta
WWS	Wire-Wrapped Screen
XRD	X-Ray Diffraction

CHAPTER ONE: Introduction

1.1 Background

Canada proven heavy oil reserves are estimated to be around 165.7 billion barrels and ranked third worldwide behind only Saudi Arabia and Venezuela (AER 2018). The surface mineable oil sands are just above 20% of the total oil sands area. Therefore, non-minable resources must be recovered by in-situ techniques (CAPP 2018). In-situ thermal recovery by Steam Assisted Gravity Drainage (SAGD) accounted for almost 50% of total bitumen production in 2017.

SAGD is an oil extraction process where two parallel wells are drilled into a target reservoir. Steam is injected from the top well (injection well) to heat the bitumen and reduce its viscosity. With the help of gravity, heated bitumen flows toward the bottom well (production well) and then is pumped to the surface (Albahlani and Babadagli 2008).

The SAGD technology is typically drilled into unconsolidated sand formations. Sand production is a significant problem in SAGD operations owing to the unconsolidated nature of the formation. Sand control devices (SCD) are employed to control the sand production in the SAGD process. The most popular SCD choices are slotted liners and wire-wrap screens. Traditionally, the design criteria for SCDs were either based on empirical correlations or field experience. However, recently there has been a growing interest in employing so-called sand control laboratory tests to aid in the selection and design of SCDs for SAGD operations.

Typically, sand control testing aims to replicate wellbore liner conditions closely. The testing is employed to help the optimal SCD selection and design with some simplifying assumptions for practicality. These assumptions stem from either simplifications or unknown field conditions. Test assumptions should always be re-evaluated, and practical measures should be put in place to remedy them.

1.2 Problem Statement

Since 1938, researchers have been developing sand control testing setups to evaluate and help develop design criteria for SCDs (Coberly 1938). However, it was only in the past decade that sand control testing began being employed for the SCD evaluation in SAGD wells (Bennion et al.

2008). Researchers have aimed to apply sand control testing technologies for SAGD with various setups and procedures to either evaluate comparatively the performance of different SCDs or investigate the effect of testing parameters on the SCD performance. However, little focus has been given towards examining how the differences in testing setups and procedures affect the results and thus, the conclusions on SCDs performances. The outcome is difficulties in understanding to what extent each study is simplifying SAGD conditions and how their results are comparable to other setups.

This study investigates the SAGD sand control testing setups and procedures. Following that, improvements are suggested on some of the limitations identified in the previous testing in equipment and procedures. A new multiphase flow Sand Retention Testing (SRT) facility is built, and a testing procedure is developed capable of overcoming limitations in capturing multi-slot interactions, sand-pack preparation, sand-pack stress, setting different fluids injection rates, and preparing the representative brine. Testing was performed to quantify the importance of each improvement on test performance.

1.3 Research Objectives

The primary objective of this study is to improve the current multiphase sand control testing practices for SAGD production wells and to compare them with preceding setups and procedures for sand control testing. The current testing procedures in SAGD applications are reviewed, and their limitations are identified. Subsequently, the appropriate improvements are suggested, tested, and evaluated to solve these limitations. The improvements should be supported by better representation of SAGD well-operating conditions. In this study, the effect of the suggested improvements on testing performance is evaluated in terms of pressure response and sand production by conducting comparative testing.

A secondary objective of this investigation is to characterize SAGD reservoir oil sands and improve established techniques for replicating reservoir oil sands for sand control testing purposes.

1.4 Research Hypothesis

Conducting SRT with different setups should not result in different conclusions given the procedure is followed precisely and test parameters scaled properly. Replicated sand with same

uniformity coefficient and deviation within SCD manufacturing tolerance should exhibit sanding and plugging during sand control testing comparable to the original sand. However, SRT results can result in misleading conclusions about the liner design if testing parameters such as fluid rates, stress magnitude, brine salinity and pH are not representative of the wells of interest.

For the same slot width and particle size distribution (PSD), an increase in fluids injection rate should cause more sanding. The higher injection rate is accompanied by higher interstitial velocities, steeper pressure gradients, hence, stronger drag forces on the sand near the slots, therefore, more sanding.

Increasing the stress levels during testing is expected to reduce porosity and increase interstitial velocities thus, stronger fines migration. The increase in interstitial velocity will increase drag forces on sand bridges and act as a destabilizing force leading to sand production. However, this effect may be offset by stronger sand bridges resulting from mobilized friction forces between the grains caused by the higher stresses (grain interlocking).

Reducing the salinity of the brine in the test is expected to increase fines migration and result in a higher pore plugging and pressure drop. This can be attributed to the deflocculation of clay materials caused by the low ionic strength of the solution which eases their migration in the pore spaces and, accordingly, accumulates in the pore throats.

1.5 Research Methodology

This research starts with an attempt to replicate multiphase testing conducted by previous researchers. A newly developed testing apparatus is used capable of conducting three-phase testing and capturing the multi-slot interactions. In this way, testing elements of the previous SRT practices in the literature can be examined, and new improvements suggested. Next, the improvements are applied one by one to assess their impact(s) on testing results. The testing elements, which are considered in this investigation, are the packing technique, applied stress magnitude, flow rates, and brine salinity. However, before the investigation can commence, characterization and then, replication of the sand used in the previous testing in terms of particle size distribution, fines content, grain shape, and mineral composition needs to be performed.

The research steps can be stated as follows:

1. Examine and identify possible deficiencies in the previous testing setups and procedures established for representing sand production in multi-phase flow conditions for SAGD production wells.
2. Design, build, test, debug, and verify repeatability of a novel experimental setup. The new facility should be capable of performing prepack sand control testing under multiphase flow condition and be representative of SAGD production well while overcoming previous SRT setups equipment limitations.
3. Use data about sand control testing conducted by Hycal, the provider of sand control testing service, provided by Nexen CNOOC to identify a possible test for replication.
4. Characterize sand samples from the reservoir tested previously and then, replicate the sand using commercial sands based on particle size distribution, fines content, grain shape, and mineral composition.
5. Replicate the testing conditions used by Hycal and analyze the results.
6. Develop a new testing methodology that overcomes procedural deficiencies in the past testing setups.
7. Investigate the impact of gradually-applying the different elements of the new testing methodology to assess their effect on the results.

1.6 Significance of the Work

In Alberta, millions of dollars are annually spent on well interventions and remediation to increase the performance of sand control completions or re-complete the wells in which failed screens are detected. Estimations indicate that in Alberta around 15-45% of wellbore costs are related to the wellbore completion (Athabasca Oil Corporation, 2015a, 2015b; Petroleum Service Association of Canada, 2015). Due to the importance of selecting appropriate and cost-effective screens for the well, several evaluations and design techniques have been developed over the years.

Improper design of slotted liners can prompt a massive sand production, low flow efficiency, and severe liner erosion. Each of these problems can be extremely costly and can result in the loss of well productivity or poor well performance. A better understanding of sand control design procedure can lead to improved well completion, reduced well failures, and enhancement of wellbore performance.

This work introduces a new laboratory testing methodology for conducting practical and reliable multiphase sand control testing to simulate operational conditions of SAGD producer wells in laboratory conditions. The comparison between the performance between the newly developed setup and other setups in the literature helps identify the critical features in the experimental design that most prominently affect the results. Identifying these features will help SCD designers assess whether a given experimental setup sufficiently simulates the SAGD well conditions.

1.7 Thesis Structure

This thesis is made up of six chapters:

- Chapter 1 presents an overview of the problem, outlines the scope of the work, and approaches to tackling the problem.
- Chapter 2 describes the relevant literature on SAGD and the factors affecting sand production in SAGD production wells, as well as an overview of laboratory sand control testing setups in the literature. Besides, experimental setups and results of previous researchers' sand control testing for a SAGD well are presented and discussed.
- Chapter 3 details the methodology adopted to characterize and replicate the sand used in the SAGD sand control testing case as mentioned earlier, discussed in Chapter 2, in terms of particle size distribution, fines content, particles shape, and mineral composition.
- Chapter 4 presents the experimental setup, testing plan as well as the associated testing material, and procedure.
- Chapter 5 presents and discusses the testing results in terms of sand production and pressure responses. This chapter quantifies the significance of improvement in the testing technique involving packing technique, stress magnitude applied, fluid rates employed, and brine salinity in comparison to the previous testing techniques for SAGD wells.
- Chapter 6 summarizes the critical findings of this work and suggests ideas for future studies.

Chapter 2- Literature Review

2.1 Introduction

The oil reserves in Canada are ranked third in the world. However, 162 of the 170 billion barrels of Canada's reserves are in the form of bitumen (CAPP 2018), and the conventional oil reserves are declining rapidly (Butler 1998).

Exploitation of bitumen resources is challenging. Most of the bitumen reserves located in northern Alberta, such as the Cold Lake, Peace River, Wabasca, and Athabasca reservoirs, are classified as unconsolidated sands and therefore, require non-conventional and costly exploitation schemes.

Open-pit mining is used to exploit the bitumen from shallow reservoirs in Alberta by operators such as Suncor energy, CNRL, and Canadian Oil Sands Ltd. (Roberts and Abbakumov 2014). Mining has limited potential in exploiting the reserves since open pit mining can be only technically and economically viable for shallow deposits and thus, make up less than 20 % of Alberta's bitumen production (AER 2018). Furthermore, oil sand mining entails high environmental costs in the form of landscape destruction and water usage reaching ten times the produced bitumen.

Another bitumen exploitation technique is cyclic steam stimulation (CSS), which involves injecting steam into a well followed by a soaking period and then, production (Bybee 2003). Although CSS is more environmentally friendly than open pit mining as it involves minimal landscape disruption and the ratio of 1:1 for water used to oil produced, the ultimate recovery can be relatively low around 25 % (Jimenez 2008). Also, the high injection pressures of steam during the injection stage followed by soaking can cause cyclic and thermal stresses around the wellbore, which could lead to wellbore failure (Albahlani and Babadagli 2008).

Cold Heavy Oil Production with Sand (CHOPS) has been implemented to exploit heavy oil in Alberta such as the Wolflake project. However, this technique involves operational costs reaching 15-20 % resulting from handling of produced solids with a low ultimate recovery of less than 10 % (Dusseault 2002).

Steam Assisted Gravity Drainage (SAGD) is the most promising technology for bitumen exploitation due to its low landscape impact and low water used to oil produced ratio compared to

open pit mining ratio (Lightbown 2017). Besides, it has been successfully implemented in more than ten commercial projects majority of which are in Athabasca, Canada (Jimenez 2008), combined with a high average ultimate recovery of over 50 % (Handfield et al. 2009), which makes SAGD superior to other in-situ techniques.

This chapter will discuss sanding in SAGD wells and factors affecting it as well as measures employed to reduce sand production. Subsequently, the chapter discusses different versions of sand control testing in the literature and their ability to simulate SAGD well conditions. Finally, an in-depth discussion of Hycal labs setup and procedure will be presented.

2.2 Sanding Problems in SAGD

Roger Butler and his colleagues introduced the SAGD technology during the late 1970s (Butler 1998). SAGD is a thermal in-situ production process where horizontal wells are drilled in parallel 5 meters apart into a bitumen reservoir. Steam is generated and then, injected into the reservoir through the shallower injection well. The steam mobilizes the viscous bitumen by flowing to the perimeter of the steam chamber and through conduction and convection, heats the oil to reduce its viscosity. The decrease in viscosity allows gravity to drain the oil due to the density difference between steam and denser oil into the deeper production well in which a mixture of oil and brine is pumped to the surface using an artificial lift method. Figure 2-1 illustrates the process of SAGD described above.

In SAGD, start-up stage steam is circulated in both wells to heat the near-wellbore region and establish communication between the injection and production wells. The circulation period ranges from 3 to 5 months to bring the inter-well formation region to between 50 °C and 100 °C and to create enough fluid mobility to establish communication (Sheng, 2013). In addition, one needs to consider the steam hammering effect occurring during the heating up phase (Irani 2013). This phenomenon can cause massive pressure perturbations in the near-wellbore region during the start-up stage and destroy any inter-granular cohesive bonds around the wellbore. Due to the unconsolidated nature of sands in SAGD operated reservoirs, sand production can occur if the installed Sand Control Device (SCD) opening size is not compatible with the formation sand properties as was reported by multiple authors (Kaiser et al. 2000; Slack et al. 2000).

Once production is underway, a sub-cool between 20-40 °C (Edmunds 2000, Gates and Leskiw 2010) is maintained between the injector and producer to form a pool of liquid around the production well called steam trap. This liquid level is vital in SAGD operations as it prevents a steam breakthrough from the injector, which can result in reduced energy efficiencies among a myriad of other issues such as sand production (Gates and Leskiw 2010). However, a steam breakthrough has been observed in multiple instances in SAGD wells especially in the well heel region due to poor drilling (Brooks and Tavakol 2012), completion design, and operational practices (Irani 2013) resulting in high potentials for massive sand production.

Although SAGD is poised to be the primary means of exploiting in-situ oil sand reserves in Alberta, it still faces serious challenges. In a case study concerning Hangingstone field in Alberta, improper design and operations of SCD in two SAGD wells resulted in workovers due to excessive sand production (Spronk et al. 2015). As reported in the literature, sand production above 3-4% of mass produced can be problematic to surface processing facilities (Burton et al. 2005). In addition, it was reported that sand production could be detrimental to Electrical Submersible Pump (ESP) lifetime if concentrations are above 1% (Devere-Bennett 2015). One of the significant challenges is how to limit sand production to acceptable levels reliably and economically. One approach to tackle this challenge is to use sand control testing of possible SCDs under in-situ representative conditions to SAGD well throughout its lifetime. This work aims to investigate the currently-employed testing techniques and then, develop improvements to the testing parameters and assess their significance on sand production under multiphase flow conditions.

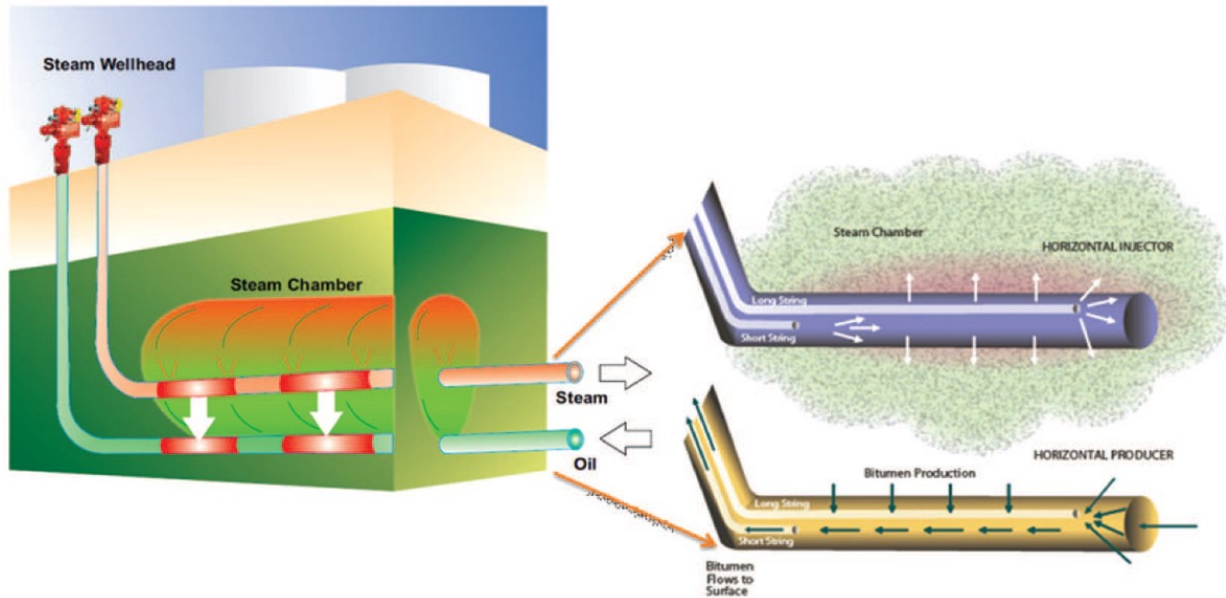


Figure 2-1. Illustration of the SAGD process (Dang et al. 2013)

2.3 Sand Control Methods

Multiple sand control approaches have been developed and implemented in unconsolidated formations. Several studies have suggested methodologies for choosing the SCD compatible with the target formation starting with simple design matrix up to complex multiple-criteria-decision-making techniques such as AHP, TOPSIS, and ELECTRE (Tausch and Corley 1958; Farrow et al. 2004; Latiff 2011; Khomehchi et al. 2015; Shahsavari and Khomehchi 2018).

Generally, sand control approaches in the literature can be classified into three categories; controlling drawdown, mechanical based control, and chemical based sand control. The optimum sand control method for a given problematic well is one that reduces sand production to tolerable levels with minimal resistance to fluid flow at the lowest economic cost. Each approach will be explained, and their previous applications in SAGD wells will be reviewed in the sections below.

2.3.1 Controlling drawdown

Controlling drawdown across the sand face is achieved by restricting the production rates within bounds that result in tolerable sanding rates. This technique has been employed successfully in weakly to intermediately consolidated sandstones (Papamichos and Malmanger 1999). The critical sand free rate can be identified either by increasing/decreasing the rate gradually till the sand-free

production is observed (Aggour et al. 2007) or through analysis of log and core data to identify rock strength model and corresponding critical drawdown (Santarelli et al. 1989).

The process of identifying the critical or sand-free production rate is based on trial and error and must be repeated as reservoir conditions change since factors such as water-cut, shut-in frequency, and pressure depletion all affect the sanding phenomena (Vaziri et al. 2006). Besides, the sand free rate is often lower than the maximum production rate possible, and thus, the well loses its productivity. This sand control approach is not feasible in SAGD wells owing to the unconsolidated nature of typically targeted formations and an already low fluid flux rate of SAGD wells.

2.3.2 Chemical based sand control

Chemical sand control involves injecting a fluid that either cements the sand grains, such as a thermosetting and thermoplastic resin (Matanovic et al. 2012) or influences the zeta potential of the sand grains by nanoparticles resulting in agglomeration of sand matrix (Singh et al. 2014; Mishra and Ojha 2016). Chemical sand control has been somewhat successful in vertical wells in conventional oil (Haavind et al. 2008) and gas reservoirs. It has been reported that consolidating agents are capable of performing sand control at temperatures up to 350°C (Wan 2011).

A significant concern in chemical consolidation techniques is the permeability impairment occurred by cementing or consolidating sands. Kalgaonkar et al. (2017) report 30% reduction in permeability, which is similar to the value reported by other studies (Carlson et al. 1992; Marfo et al. 2015). Moreover, chemical sand control is only applicable in a well with short formation pay (say, about five meters) due to placement challenges. Thus, chemical methods are not feasible sand control options with horizontal SAGD wells (Wan 2011).

2.3.3 Mechanical based sand control

Multiple designs of mechanical sand control equipment have been developed in the oil and gas industry. However, this work will only discuss the sand control equipment that either has been implemented or has the potential of being applied in SAGD wells. These are namely slotted liners (SL), wire-wrapped screens (WWS), precise punch screens (PPS) and gravel-packing (GP).

Slotted liners

Slotted liners are liners with machined slots of specified width, length, distribution density, and geometry along the liner. They are low-cost sand control solutions often employed in low economics and well-sorted sand reservoirs producing at a low rate and high viscosity oil by horizontal wells (Kaiser et al. 2000; Matanovic et al. 2012). The in-situ bitumen reserves in Canada are classified as unconsolidated sand and therefore, requires SCD for acceptable sand production with slotted liners and WWS used most widely (Sheng 2013). Slotted liners have been commonly employed in SAGD for their notable mechanical strength along with lower price per foot compared to other sand control devices for long horizontal well completion.

Slot width and geometry is a crucial controllable factor that determines slot plugging and thus, liner lifetime. Three main slot geometries exist namely straight, rolled top, and keystone (Bennion et al. 2008), which are shown in Figure 2-2. Straight cut slots have a uniform width across the liner thickness, which is manufactured by a single blade plunge. On the other hand, the rolled top and seamed slots have varying slot width across the liner thickness and thus, allow easier passage of sand grains, which reduces plugging potential. The decreased plugging potential of keystone and rolled top compared to straight cut has been reported in the literature (Bennion et al. 2008; Roostaei et al. 2018b). The keystone slot is manufactured by two blade plunges in the liner while the rolled top slot is an improved version of the straight cut slot where concentric stresses are applied on the surface of the outer side of slot causing it to deform about 1 mm inwards plastically.

Another problem contributor to slotted liner plugging is corrosion products (Romanova and Ma 2013). However, developments in SL coating such as High-Phosphorus Ni-P coating have shown promising results in reducing corrosion and scaling extending lifetime of the liners (Sun et al. 2018).

An analytical evaluation concluded that SL slot density is more influential on inflow resistance than slot width (Kaiser et al. 2000). Based on Computational Fluid Dynamics (CFD) studies conducted on slotted liners, it was found that an Open to Flow Area (OFA) above 3% would not influence the flow distribution within the SAGD well and the reservoir as the changes in the velocity profile was insignificant (Sivagnanam et al. 2017). However, for slotted liners in SAGD wells, OFA is limited to a maximum of 1.5% for mechanical integrity considerations due to thermal stresses (Hara 2015). Thus, owing to the low OFA, recent field studies have shown that

slotted liners have higher plugging potential than WWS (Romanova and Ma 2013). For instance, a field case study reported that the SAGD well drawdown performance difference reached 1000 kPa on average when compared to WWS and premium screens which ranged between 80 to 200 kPa (Spronk et al. 2015).

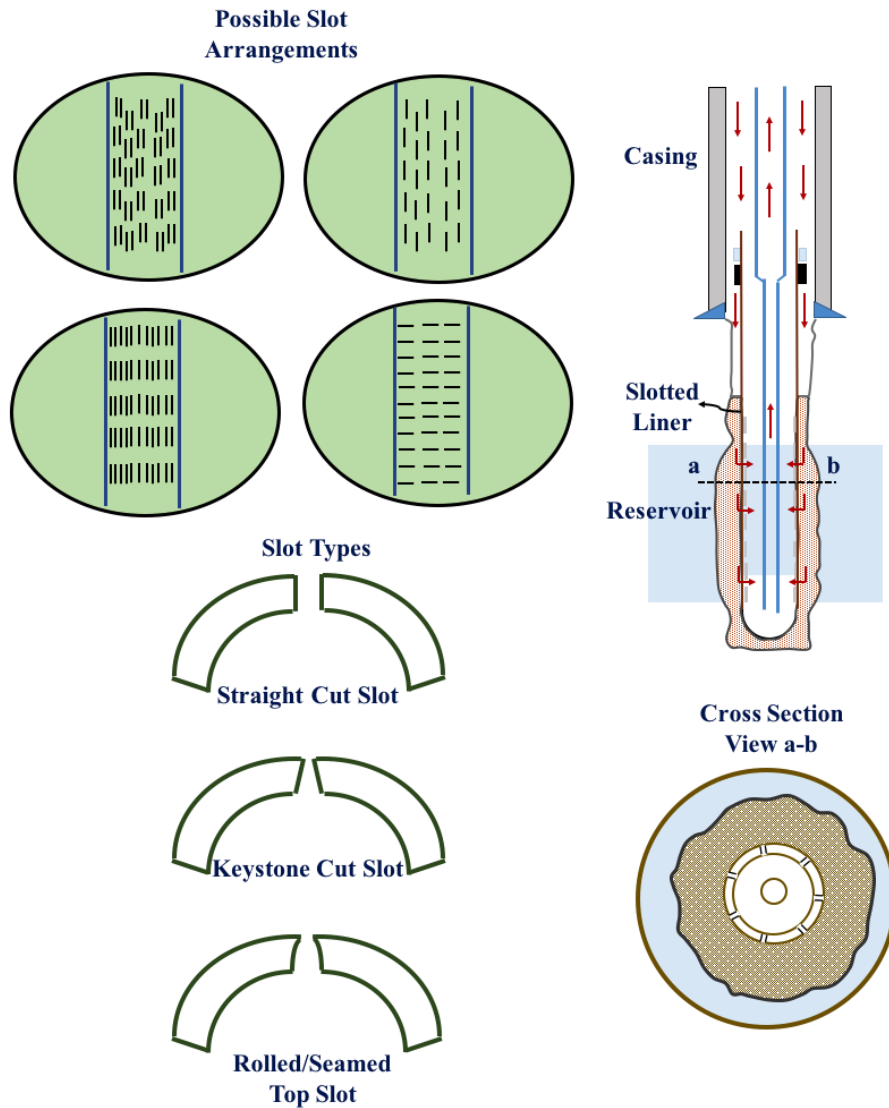


Figure 2-2. Different slot geometries and distributions (Guo 2018)

Wire wrapped screens

WWS was first introduced and patented in 1973 (Layne and Gerwick 1973). Conventionally, WWS is made up of an outer jacket, which is manufactured on special wrapping machines. The trapezoidal cross-sectional stainless-steel wire is wrapped and welded into longitudinal rods to

form a single helical slot. These rods are, then, secured to a perforated base pipe (Bellarby 2009) as shown in Figure 2-3. Other variations include shrink-fit pipe-based and rod-based.

WWS with OFA of 6-12% surpasses the 1-3% OFA offered by SL (Spronk et al. 2015), which allows less resistance to flow and lower flow velocities at the sand bridges and thus, less sanding potential (Suman et al. 1983; Bellarby 2009). The wires' trapezoidal cross section creates a slot, which is narrow at the screen surface and wider at the interior that reduces its plugging potential. The WWS offers stable and reliable sand control with an average working lifetime of 8 to 10 years (Zhang 2017).

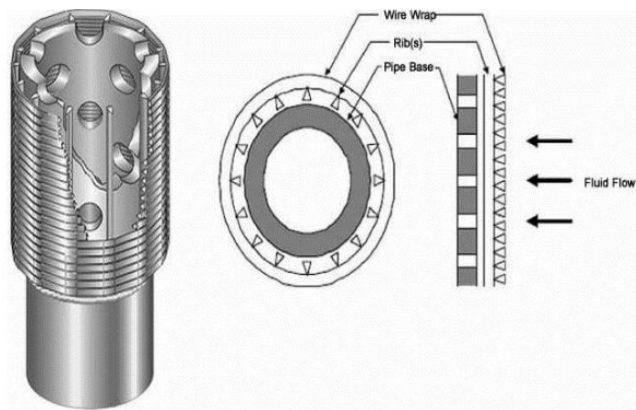


Figure 2-3. Wire wrapped screens (Zhang 2017)

Precise punched screens

Precise punch screens are gaining attention in SAGD operations (Spronk et al. 2015). The screen is made up of a stainless-steel outer screen punched to a specific depth to create two apertures between the original and punched plates, which are rolled into a jacket and welded on to a base pipe. The screen is durable against corrosion (Yang and Macaraeg 2013). In a recent study, laboratory testing was conducted to compare the performance of PPS and SL, and the results indicated that PPS had less plugging potential owing to its OFA of 6-14%, which is 3-7 times higher than that of SL (Zhang 2017). Besides, due to the base pipe, PPS was shown to possess at least four times the mechanical strength of SL, providing better resistance to liner collapse (Zhang 2017). In addition, its 90° angle offers better support to the arches formed and reducing sand production compared to WWS or SL, which are limited to 20° due to manufacturing constraints (Zhang 2017).

Another study (Fattahpour et al. 2018) conducted prepack SRT testing representative of SAGD conditions, to compare the performance of SL, WWS, and PPS. They concluded that PPS performance was superior to SL and WWS in terms of sand production; however, the PPS showed high pressure drop for the same slot aperture at low flow rates, which they attributed this to the higher tortuosity of the flow path in PPS screens.

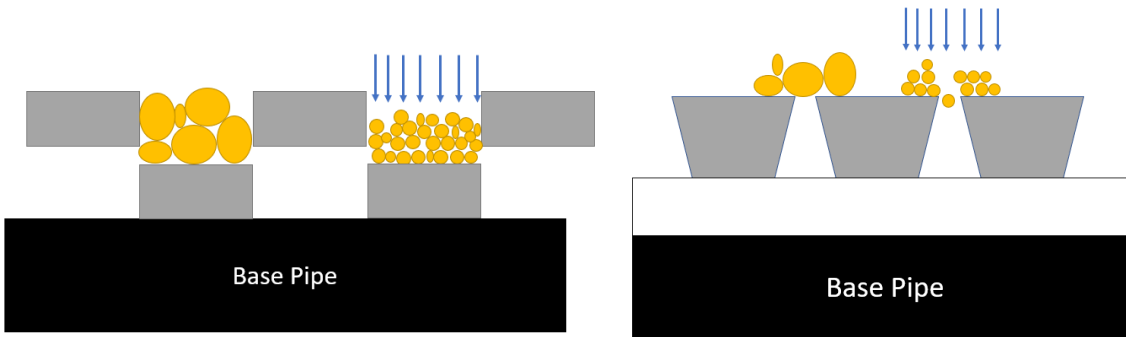


Figure 2-4. Illustration of how bridging happens in WWS (Right) and PPS (Left)

Gravel packs

Gravel packing creates a permeable down-hole filter of sands supported by a liner that allows fluid production and prevents the sand production. Gravel packing is also a useful technique to reduce the fines migration towards the wellbore by lowering the near wellbore velocities and provides a high-permeability graveled zone around the liner/screen (Sparlin 1969). The implementation can be summarized as injecting a slurry of accurately-sized gravel slurry in a carrier fluid into the annular space between a screen and open-hole or casing. Although, historically, gravel-packs were restricted to short-length target formations due to proppant transport and placement limitations. Recently, the alternate path technology was developed and applied for intervals up to about 1000 m (Yeh et al. 2008; Barry et al. 2008). Also, the successful installation of a gravel pack in 1000-2000 m in heavy oil wells using advanced friction reducers and lightweight proppants was reported (Colbert et al. 2017).

The pack performance can be compromised with fines invasion and pore plugging (Bellarby 2009). Recently, a laboratory investigation was conducted to assess the performance of gravel pack in SAGD conditions, which was inconclusive, as more testing was needed. Although gravel packs

are technically feasible in horizontal wells, no attempt was found in the literature of using gravel packs in SAGD wells, which can be attributed to the economic limitations.

2.4 Failure Mechanisms for SL and WWS

2.4.1 Intolerable sand production

Generally, sand production occurs when the hydrodynamic forces such as fluid flow induced drag forces overcome the stabilizing forces caused by inter-granular friction and cohesive bonding through cementing material such as clays. Figure 2-5 shows a schematic of sand bridges near a slot and illustrates the hydrodynamic forces and frictional forces aiding and preventing sand production, respectively. There are five scenarios where sand production can occur in a wellbore (Morita and Boyd 1991), which are listed below:

1. Unconsolidated/uncemented sands (applies to the majority of SAGD wells);
2. Weakly/intermediately consolidated sands with water breakthrough;
3. Abnormally high and anisotropic lateral tectonic forces in strongly consolidated formations;
4. Reservoir pressure depletion in relatively strongly consolidated formations;
5. Steep flow rate change or excessively high production rates.

Sand failure in the scenarios above can be summarized into two mechanisms (Morita et al. 1989b). The first is the shear failure, which occurs due to excessive shear stress in the near wellbore region. The second failure mechanism is due to tensile failure caused by drag forces on sand grains by the pressure differentials created by the flowing fluids. Multiple well and field scale phenomena or events can aid the failure by either mechanism. For instance, reservoir pressure depletion exacerbates the shearing. Also, fines migration can restrict conduits available for fluids flow, resulting in higher pressure drawdown and increases the tendency of sand production due to tensile failure (Santarelli et al. 1989). Besides, cyclic stress due to fluctuating production rates can result in rock fatigue, reducing the rock strength and easing sand production by both failure mechanisms (Morita et al. 1989a).

Sand production in a problematic well can be classified qualitatively into three categories based on the manner of sand production (Veeken et al. 1991). The first is transient sand production,

which refers to a short high-sanding episode stemming from sudden changes in production operations such as perforation, acid clean up, and sudden production rate change. The second category is continuous sand production, which refers to a constant level of sanding that associates with specific well-operating conditions. The last category is catastrophic sanding where sand production level increases rapidly accompanied by a steep decrease in fluid production culminating in well death. An extremely steep production rate increase can trigger this type of sanding.

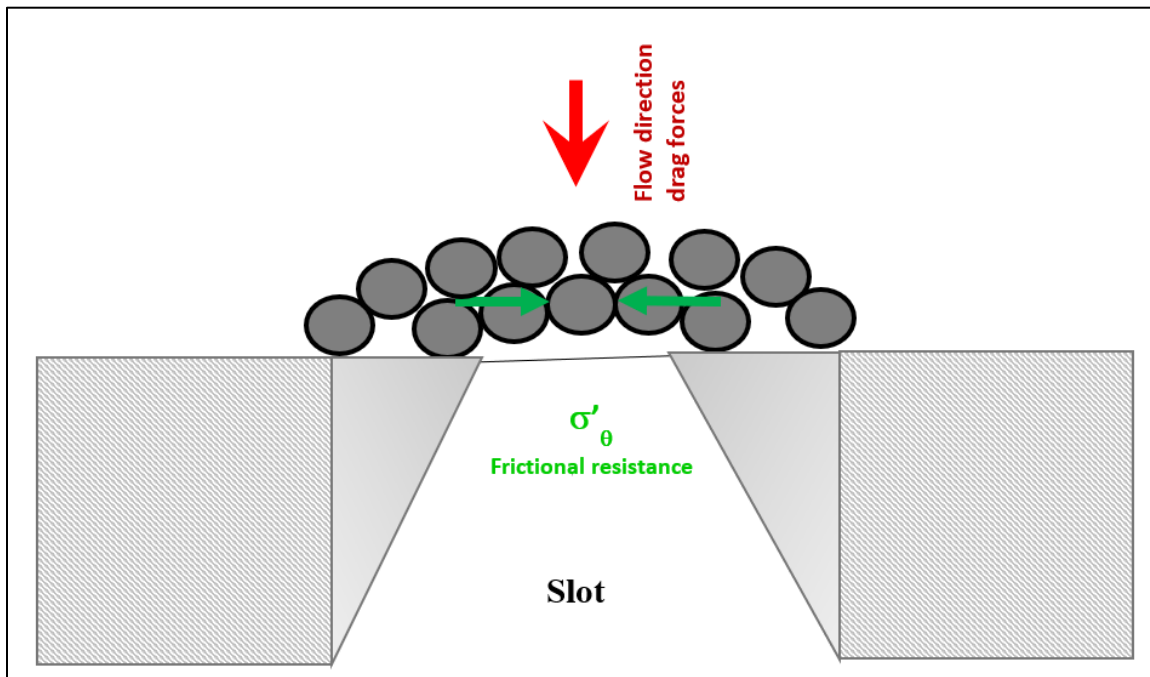


Figure 2-5. Illustration of the hydrodynamic forces and frictional forces aiding and preventing sand production, respectively, through a liner slot

2.4.2 Slot and near-slot pore plugging

Ideally, installation of an SCD will have no impact on productivity of a well (Parlar et al. 2016). In SAGD wells, SCDs have been reported to be prone to plugging of the slots and near slots porous media and can result in productivity impairment of the well. The productivity impairment caused by installing SCDs can be classified into three sources:

- The first, resulting from plugging of the SCD screen slots, is due to corrosion, scale deposition, and trapped sands and fines in the slots (Bennion et al. 2008; Romanova and Ma 2013).
- The second is attributed to the extra pressure drop in the near-SCD region caused by pore plugging due to fines migration and other products such as asphaltene precipitation. Multiple factors affecting pore plugging by fines migration have been studied in the literature such as slot width and density (Mahmoudi et al. 2016b), stress (Guo et al. 2018), and fluid pH and salinity (Khilar and Fogler 1998).
- The third source of extra pressure drop is due to flow choking and convergence as fluid flows towards the slots instead of an open hole, which is affected by the OFA of SCD, and slot distribution, and geometry (Kaiser et al. 2000; Mahmoudi et al. 2017).

Further discussions of factors affecting failure due to plugging are presented in the following sections.

2.5 Influential Factors in SCD Performance

2.5.1 Fluid flow rates

High fluid flow rates have been linked to SCD failure due to sand production (Stein et al. 1974) and low productivity (Spronk et al. 2015). Therefore, a careful selection of SCD compatible with the expected well production rates is essential.

High flow velocities around the wellbore result in high-pressure drops, increase the drag forces on sand grains, and increase the sanding potential. The flow rate that causes sanding in a given well is called the critical sanding rate and can be determined by slowly increasing the flow rate till sand production is observed (Stein et al. 1974).

The same concept of critical flow rate was also found true when researchers investigated factors affecting fines migration. For fines migration, however, electrochemical forces due to surface changes also play a prominent role in fines mobilization due to the high particle surface area to the particle mass ratio. For instance, in low pH and high salinity environment, the critical flow rate at which fines migration would occur could not be observed experimentally (Khilar and Fogler 1998; Mahmoudi et al. 2016a).

2.5.2 Fluid phases

Fluid saturations in the multiphase environment, as seen in SAGD wells, influence sand production. In field operations, sand production has been regularly associated with water breakthrough (Veeken et al. 1991). The effect of water saturation on sand production can be explained through two reasons; 1) cohesive capillary effects and 2) chemical interactions with the formation.

Multiple water-formation chemical reactions can aid in sanding through either the Rebinder effect, in which the sand surface energy is altered, and the shape and size of cementation material are physically changed, or locally increasing the pressure gradients as for the case of expansion of swelling clays (Han and Dusseault 2002).

Experimental studies show that capillary cohesive forces have a stabilizing effect on sand bridges (Bruno et al. 1996; Papamichos et al. 2010). It has been reported that capillary cohesion provides stability to the unconsolidated sands at irreducible water saturation. This cohesion is eliminated as water breakthrough occurs and water saturation increases above the irreducible water saturation, resulting in sand production. An analytical analysis was conducted to develop a model that quantifies the effect of water saturation on sand capillary cohesion (Han and Dusseault 2002). However, the analytical model has several terms not easily quantifiable such as water saturation and is made with simplifying assumptions, for instance, the sand grains are assumed perfectly spherical.

Multiphase fluid saturations can affect the fines migration (Civan 2016). Laboratory investigations concluded that fines migration in multiphase liquid flow environment, generally, has lower fines migrations than that observed in single phase flow environment (Muecke 1979; Sarkar and Sharma 1990). Formulation and experimental verification of a model describing the formation damage by fines migration under multiphase flow and allows capturing the effect of wettability and transfer of particles between phases as it was observed that particles tend to concentrate in the wetting phase (Liu and Civan 1993, 1994, 1995, 1996; Civan 2016).

Although steam trap has been used in horizontal SAGD producers to prevent injected steam circulation, steam breakthrough has been reported, especially at the heel of the horizontal well (Edmunds 2000) due to high drawdown of the producer and at the toe, due to drilling in low

competency section of the formation, which creates a loss circulation zone (Brooks and Tavakol 2012). Steam breakthrough can cause massive sand production through the erosion of the SCD liner (Toma et al. 1988; Das 2005, 2007). While Zhu et al. (2016) reported that dry steam breakthrough could not erode liner steel based on C-factor erosion calculations, steam condensate and the sand particles entrained by the steam can cause erosion. Haugen et al. (1995) reported that the erosion severity due to transported sand dramatically depends on the fluid velocity. Accordingly, a steam breakthrough in SAGD wells creates a high fluid velocity compared to liquid flow and thus, causes the liner to be more susceptible to erosion and removal of the corroded film. Removal of the corroded film due to erosion will expose fresh metal of the screen, which causes the continuation of the corrosion/erosion cycle and ultimately the development of a failure (Procyk et al. 1998; Hallman et al. 2015). No attempt of quantification of steam breakthrough at the liner could be found in the literature.

2.5.3 Sand grain characteristics

Sand grains size

Sand grains size is commonly represented by particle size distribution, which is a distribution of the constituting grains' measure of size. The sand PSD analysis can be conducted in the lab using sieve analysis, hydrometer analysis, Laser Particle Size Analysis (LPSA), sonic sifting, and Dynamic Image Analysis (DIA). Another approach to estimate grain size in a formation of interest is to correlate well logging data to sand size. Oyeneyin (1988) correlated log derived permeability, sand-size standard deviation from sets of core data to mean grain size of a particular formation based on Krumbein and Monk's equation. The fitting of the correlation parameters was based on Gaussian elimination technique. The developed workflow was implemented successfully in the unconsolidated sands of the Niger Delta. However, it should be noted that the PSD measurement by different techniques produces dissimilar results due to the unique and non-spherical features of sand grains, in addition to the assumptions associated with each measurement technique.

In the literature, the PSD is used as the primary parameter for choosing the sand control technique (Tiffin et al. 1998; Price-Smith et al. 2003) and for designing the opening size. In most SCD sizing criteria, PSD of the reservoir sands is sometimes the only or main design criteria. Some design criteria used discrete points in the PSD to set the opening size of the SCD such as Coberly (1938), which found that stable bridges would always form given the SCD aperture is less than D10 and

that above $2xD_{10}$ no stable sand bridging would occur and thus, is the upper limit for sizing. Furthermore, Rogers (1971) and Suman et al. (1983) suggested that WWS and SL aperture should be sized using D_{10} . Gillespie et al. (2000) concluded that for WWS and PPSs, $2xD_{50}$ and $2.5xD_{50}$, respectively, should be regarded as the maximum aperture width. Other design criteria incorporated the shape and distribution of the PSD such as Constien and Skidmore (2006) which included the Uniformity Coefficient (UC) with the D_{50} for plotting master curves to be used in sizing. More recent design criteria incorporated other elements such as plugging tendency (Mahmoudi 2016) and stress (Guo 2018) in their design criteria, however, PSD always played an essential role in sizing of SCD. Thus, by reviewing all the design criteria in the literature, one can conclude that PSD plays a vital role in the sand production and proper PSD characterization is essential to effective sand control management.

$$UC = \frac{D_{60}}{D_{10}} \quad (2.1)$$

$$SC = \frac{D_{90}}{D_{10}} \quad (2.2)$$

Sand grain shape

The shape of grains varies and is affected by the distance of sediment transported before sedimentation, mineral composition, chemical, and mechanical processes after sedimentation (Wentworth 1919). Historically shape factors such as roundness and sphericity were quantified visually (Krumbein and Sloss 1951), which was subjective to the evaluator's evaluation. However, improvements in image acquisition and analysis capabilities allowed practical use of mathematical definitions of sand grain size. Shape quantification factors such as sphericity, aspect ratio, and convexity among others have been reported in the literature (Wadell 1935; Krumbein and Sloss 1951; Janoo 1998; Pan 2002; Rodríguez et al. 2013).

Several studies reported that sand grain shape can affect rock hydraulic and mechanical behavior (Witt and Brauns 1983; Shinohara et al. 2000; Cho et al. 2006; Rousé et al. 2008; Cox and Budhu 2008; Göktepe and Sezer 2010), which, in turn, affect sand production. For instance, Cox and Budhu (2008) analyzed grain shape using fractal techniques and concluded that sands with higher convexity have a higher frictional angle. In addition, Rousé et al. (2008) found that roundness affects the maximum and minimum porosity as well as the friction angle of a sand-pack.

Furthermore, using triaxial compression test, Shinohara et al. (2000) concluded that the friction angle of a specimen increases when angularity of grains increases and the initial porosity decreases, which were attributed to an increase in the grains interlocking effect.

2.5.4 Stress

Several historical studies documented that increasing stress levels in a formation reduced sand production. Clearly et al. (1979) found that arch size decreased thus, stability increased with increasing stress levels and that most stable arches formed under minimum vertical stress and maximum horizontal stress. In addition, another study, recently, reported a prepack Sand Retention Test with Stress (SRTS) laboratory investigation and concluded that sand production decreases with increasing stress, however, the magnitude of reduction in sand production decreases at the higher stress levels, i.e., the effect of stress on sand control is more critical at low-stress levels (Guo et al. 2018).

The formation stress magnitude, on the other hand, has a detrimental effect on fines migration and pore plugging. Coşkuner and Maini (1990) reported that at high-stress levels the critical velocity to plug pore throats by mobilized fines decreases as stress magnitude increases. Another study developed an extended fines migration test, which involved injecting 40,000-60,000 pore volumes of the core under different stress levels and reported that retained permeability decreased with increasing stress levels, resulting in an increase in fines migration. Recently, researchers used an SRTS setup to represent SAGD wells and reported that as stress level increases, more fines migration occurs resulting in increased skin (Guo 2018).

2.5.5 Salinity and pH

A study investigating the effect of salinity on rock strength reported that rocks saturated with higher salinity brine exhibited higher strength than low salinity saturated rock (Huang et al. 2018). However, another study used a conventional SRT setup to conduct a sensitivity analysis on the effect of pH and brine salinity on sand production with unconsolidated sand, similar to that in SAGD wells, concluded that sand production remained relatively constant while varying pH and salinity (Mahmoudi et al. 2016a).

Several laboratory studies established a correlation between increased fines migration and permeability reduction with decreasing salinity and increasing pH levels in the injected brine

(Khilar and Fogler 1998; Bennion et al. 2008; Mahmoudi et al. 2016a; Mahmoudi 2016). The mechanisms are describing permeability reduction by clays through migration, swelling, and swelling-induced migration was proposed by Mohan et al. (1993). Through lab testing, Khilar and Fogler (1984) hypothesized the existence of a critical salt concentration (CSC) below which fines release and migration will start to occur. Moreover, they reported that fines migration is more sensitive to monovalent cations concentration compared to bivalent cations. Others studied physicochemical factors of clay particles stability and transport in sandstone porous media and concluded that the zeta potential and electrical double layer properties are the main factors controlling the clay mineral behavior (Khilar and Fogler 1998; Sokolov and Tchistiakov 1999). Liu et al. (2017) tested the effect of salt concentration on permeability reduction in sand samples with different clay minerals and concluded that montmorillonite led to the largest permeability reduction, followed by kaolinite, and illite.

In addition, several researchers documented the effect of injected brine pH on the permeability of porous media (Mungan 1965; Simon et al. 1976; Kia et al. 1987; Leone and Scott 1988; Valdya and Fogler 1992) and concluded that salinity and pH changes are interrelated and therefore, must be addressed simultaneously and that high pH is detrimental to permeability. Researchers (Bennion et al. 2008; Mahmoudi et al. 2016a), investigating SCD performance with the clays mineralogy and concentrations typically found in SAGD well formations, showed that brine salinity and pH have a severe impact on plugging tendency of SCDs.

2.5.6 Miscellaneous factors

In SAGD systems, steam can also react chemically with bitumen and rock minerals through aquathermolysis and generate corrosive gases such as hydrogen sulphide, carbon oxides, as well as hydrogen, and methane (Hoffmann et al. 1995; Wen et al. 2007). These corrosive gases can aid plugging and failure of the installed SCD. Kapadia et al. (2011) conducted simulations to model aquathermolysis in SAGD reservoirs and concluded that lower steam injection pressures would enable better energy utilization and lower hydrogen sulfide emissions.

It has been reported that steam hammering can occur in SAGD wells, which could possibly cause sand production (Irani 2013). Steam hammering occurs when steam is isolated by liquid, and high

enough heat transfer is occurring to cause rapid condensation, which causes the vapor void to collapse producing a destructive pressure pulse.

2.6 Sand-Retention Tests and Setup Variations in Literature

Sand control testing generally aims to evaluate the performance of SCDs under lab conditions representative of field conditions of interest. The performance is usually evaluated in terms of sand production and flow resistance through pressure drop measurement. Sand control testing conducted in the literature can be categorized into two groups: slurry tests (Coberly 1938; Underdown et al. 1999; Gillespie et al. 2000; Hodge et al. 2002; Constien and Skidmore 2006; Mathisen, et al. 2007; Chanpura et al. 2011; Ballard and Beare 2012); and prepack tests (Markestad et al. 1996; Ballard and Beare 2003, 2006; Williams et al. 2006; Bennion et al. 2008; Chanpura et al. 2011; Agunloye and Utunedi 2014; Romanova et al. 2014; Devere-Bennett 2015; Hara 2015; Romanova et al. 2015; Mahmoudi 2016; Fattahpour et al. 2016; Anderson 2017; Fattahpour et al. 2018). Based on a review of the literature, there is no agreed upon standard procedure for sand control testing. The testing setup design and testing procedure are highly subjective to the researchers' understanding of the well conditions simulated and to what measure can be reasonably simplified without an adverse effect on results.

2.5.1 Slurry SRT

In slurry SRT, a slurry of solids and fluids is injected into an empty cell towards the SCD coupon. A typical slurry setup consists of slurry preparation unit, test cell, and effluent collection unit as shown in Figure 2-6. In slurry sand control testing, a homogenized mixture of fluids and sand at specific concentrations, rates, and viscosities are injected towards an SCD under evaluation (Ballard et al. 1999). This testing is meant to represent sand production in a strong formation, or early production life of weakly consolidated formation wherein for both scenarios: (1) the sand face is separated from the liner, (2) no stress is exerted by the formation on the liner, (3) slurry with low solid concentration flows towards the SCD (Ballard and Beare 2003; Chanpura et al. 2011).

The produced sand and slot plugging, observed through pressure build-up across the coupon, are used to measure the performance of the SCD tested. The testing setup and parameters such as the selection of carrier fluid viscosity (Ballard and Beare 2012), slurry sand concentration (Ballard

and Beare 2003, 2006, 2012; Chanpura et al. 2011), injection rate (Wu et al. 2016; Ballard, Kageson-Loe, and Mathisen 1999), and SCD specification (Ballard and Beare 2003) can profoundly affect the test results. The success criteria of slurry testing are subjective to the test setup and the researcher’s experience with the conditions of the field under consideration. For instance, when considering the pressure drop, a value below 689 kPa (100 psi) is deemed to be acceptable by Burton and Hodge (1999) and Williams et al. (2006) while criticized by Chanpura et al. (2011) for being arbitrary and instead propose the use of a screen retained permeability. For sand production, Hodge et al. (2002) set the maximum limit of acceptable sanding at 0.12 lb/ft², which was determined by correlating their test performance with gas wells performance data that they had access to for specific fields in the United States, North Sea, and Indonesia. Table 2-1 summarizes the pass/fail criteria of slurry testing in the literature.

For SAGD, assuming the collapse of the sandface onto production liner before initiation of production is a valid assumption since the sands are mainly consolidated by the extra viscous bitumen, which loses its viscosity during the well start-up recirculation period (Fattahpour et al. 2016). Therefore, slurry SRT setups cannot be used to mimic sand production in SAGD conditions, and as a matter of fact, there is no attempt in the literature to simulate sand production in SAGD wells using slurry testing. Figure 2-7 illustrates the sandface scenarios simulated by both tests.

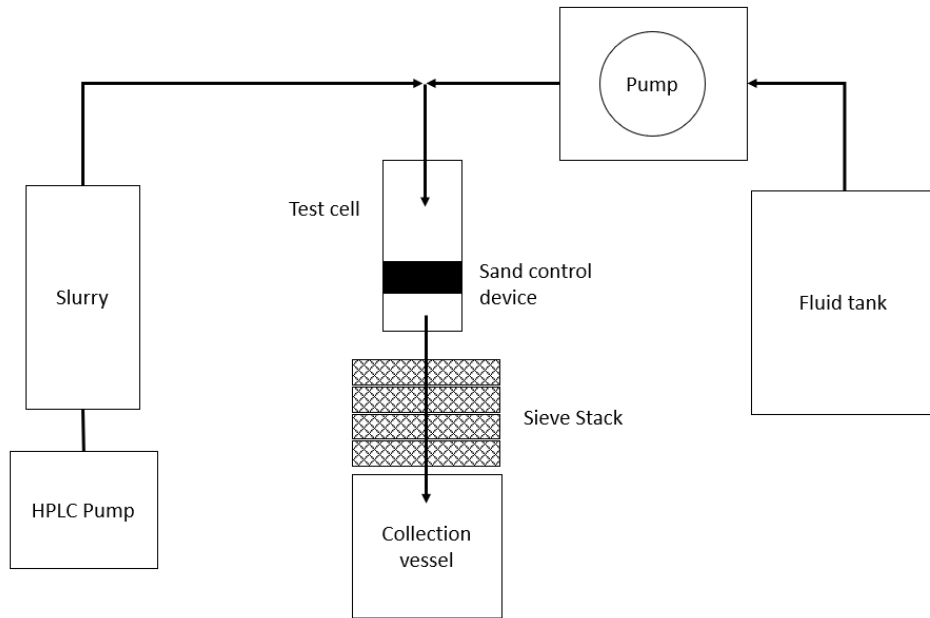


Figure 2-6. Schematic illustrating a typical slurry setup

Table 2-1. Summary of the SCD pass/fail criteria for slurry testing in the literature

Source	Sand production	Screen plugging	Produced Particle Size
(Hodge et al. 2002)	≤ 0.12 lb/ft ² of flow area	retained permeability $\geq 50\%$	-
(Williams et al. 2006)	≤ 6 % of effluent mass	$d_p < 689$ kPa (100 psi) across sand-pack and screen	$D_{50} \leq 50$ micron
(Constien and Skidmore 2006)	≤ 0.12 lb/ft ² of flow area	retained permeability $\geq 50\%$	$D_{50} \leq 50$ micron
(Adams et al. 2009)	≤ 0.15 lb/ft ² of flow area	retained permeability $\geq 50\%$	-



Figure 2-7. Demonstration of the downhole scenarios simulated by prepack SRT (left) and slurry SRT (Right) (Montero et al. 2018)

2.5.2 Prepack SRT

In prepack testing, the cell is filled with sand before establishing fluids flow towards the SCD coupon. The prepack test can more realistically represent SAGD well conditions. The reason is the sandface collapses onto the liner closing the annular gap during the well start-up period.

Researches on sand control testing for SAGD wells have employed a variation of the prepack SRT setup (Bennion et al. 2007, 2008; Romanova et al. 2014; Devere-Bennett 2015; Hara 2015; Williamson et al. 2016; Mahmoudi et al. 2016c; Fattahpour et al. 2016; Anderson 2017; Fattahpour et al. 2018). The collapsed region consists of high-porosity sands (Carlson 2003). The collapse is

due to the loss of viscosity of the bitumen caused by heating and oil sand thermal expansion (Fattahpour et al. 2016).

The prepack SRT testing procedure consists of first installing a coupon representative of the downhole liner. Then, a sand-pack is prepared over the evaluated SCD. A porous disc is placed on the top of the sand-pack to provide a uniform fluid injection during the test. Next, the sand-pack is saturated by flowing brine from the SCD side towards the sand-pack. It is crucial that the appropriate amount of stress is applied during the saturation phase to prevent fluidization of the sand-pack due to the counter-gravity drag force exerted by the saturating fluid (Ballard and Beare 2003). Once saturation is achieved, the test begins by injecting field fluids with representative properties and flow rates from the sand-pack towards the SCD. The injection stage can be conducted at either constant pressure differential or constant flow rate with the other being recorded. The sand is collected, and the flow rate or pressure drop is evaluated after the test to assess the SCD performance.

Prepack SRT setups can vary significantly in how they are representing the SCD liner performance in SAGD conditions. The variations in design and procedure can stem from the size of the setup, sand-pack preparation technique, SCD representation device, fluid properties, number of phases as well as the order of fluid phases injected and their associated rates, applied stress magnitude and anisotropy, and flow geometry towards the liner coupon. In this work, the setups are classified into three categories: conventional SRT, SRT with stress and full-scale tests with each explained in the following sections.

Conventional SRT

In this work, a prepack setup is considered conventional if the setup does not allow significant stress application, and also, only linear flow is simulated towards the coupon. A typical schematic of prepack SRT setup used to simulate SAGD producer conditions is illustrated in Figure 2-8. The setups in literature commonly consist of a fluid injection unit, core holder, sand trap, and pressure measurement and logging unit. In SAGD context, this setup was used by (Mahmoudi et al. 2016c) to come up with design criteria to optimize the slotted liner design to reduce plugging due to fines migration and sand production to within acceptable levels. The setup is meant to simulate the early life of SAGD production well where the near-liner region is made up of high-porosity collapsed sand under no stress.

Pre-packed SRT with Stress (SRTS)

SRTS setups have similar components when compared with the conventional SRT except for being capable of applying a controlled amount of stress on the sand-pack during the test. Figure 2-9 illustrates a schematic of a typical SRTS setup. In the context of SAGD operations, the application of different stress levels during testing allows simulation of various stages in the life of a well. Typically, a SAGD well liner will experience low stress during early production stages, but the stress will gradually increase with steam chamber expansion. The stress build-up is attributed to several phenomena such as reservoir thermal expansion, shear dilation, and poroelastic sand expansion (Fattahpour et al. 2016).

A majority of SRTS setups used in SAGD sand control testing only allow axial application of stress (Bennion et al. 2007, 2008; Romanova et al. 2014; Devere-Bennett 2015; Hara 2015), which limits the control on the confining lateral stress from the confining core holder. A more advanced setup, capable of conducting SRTS under controlled triaxial stress condition, was developed by Fattahpour et al. (2016). The setup was recently used to study the effect of stress on SCD performance and concluded that sand production decreases with increasing stress magnitude applied in the testing (Guo et al. 2018). However, no attempt was made to study the effect of stress anisotropy on sand production from SCDs.

Full-Scale Completion Tests (FCT)

A major criticism of conventional SRT and SRTS is that both setups simulate linear flow which is not the case in downhole wells where radial flow dominates the near-wellbore region. Testing setups that simulate radial flow are categorized as Full-Scale Completion Test (FCT) setups. Researchers developed prepack testing setups design to simulate radial flow by using a cylindrical liner for conventional oil (Chenault 1938) and gas wells (Jin et al. 2012). For SAGD wells only Anderson (2017) developed a setup that uses a 17.78 cm (7-inch) liner to simulate radial flow.

The FCT setups in the literature use a cylindrical liner in the center surrounded by sand where the fluid is injected from the side boundaries through baffles or dispersive filter medium to allow uniform radial flow. However, the comparison between the performance of SRTS and FCT shows general agreement in the results (Anderson 2017). Thus, indicating that radial flow afforded by FCT setup does not significantly impact the results compared to SRTS results and probably does not warrant the high cost of FCT testing.

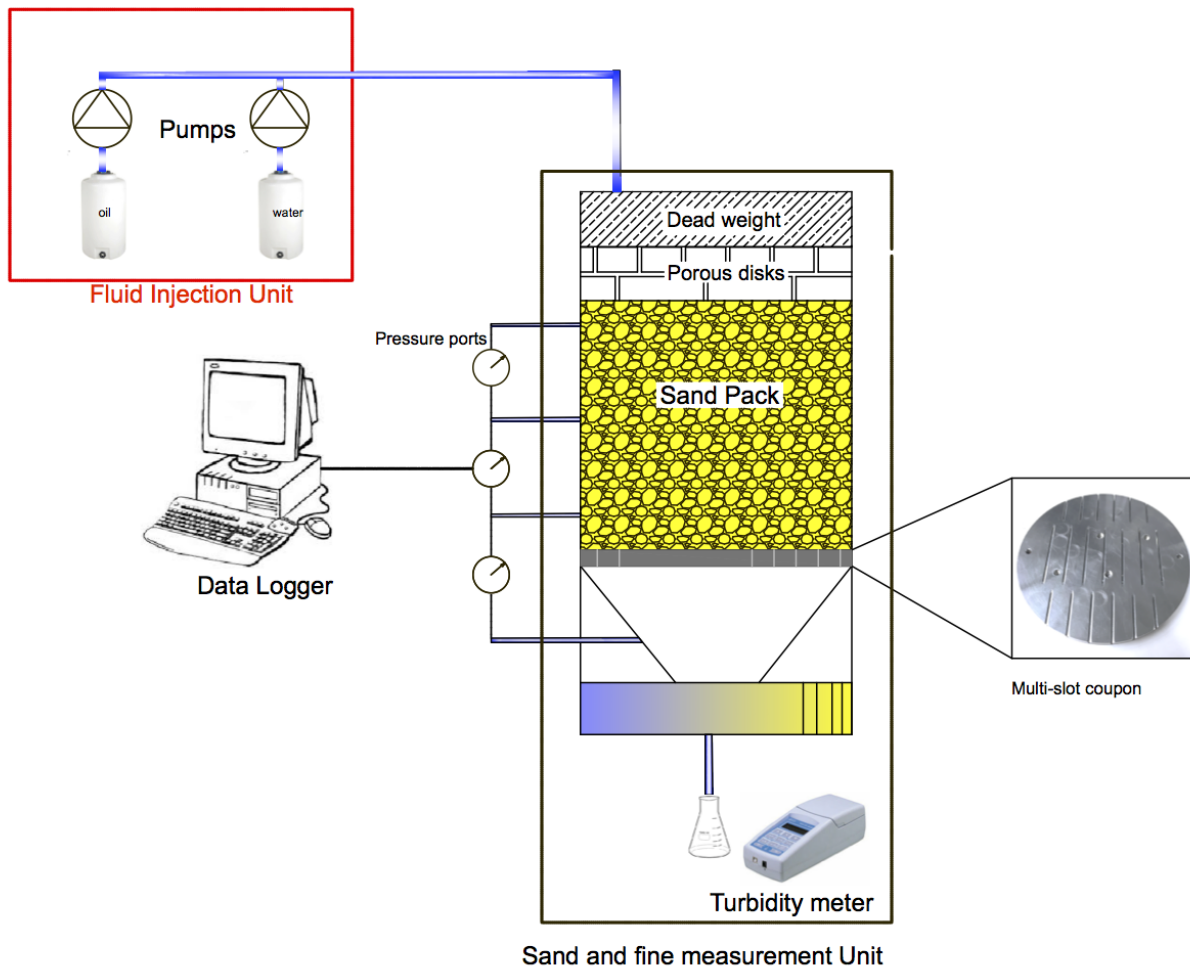


Figure 2-8. Conventional Pre-Packed Sand Retention Test (SRT) (Montero et al. 2018)

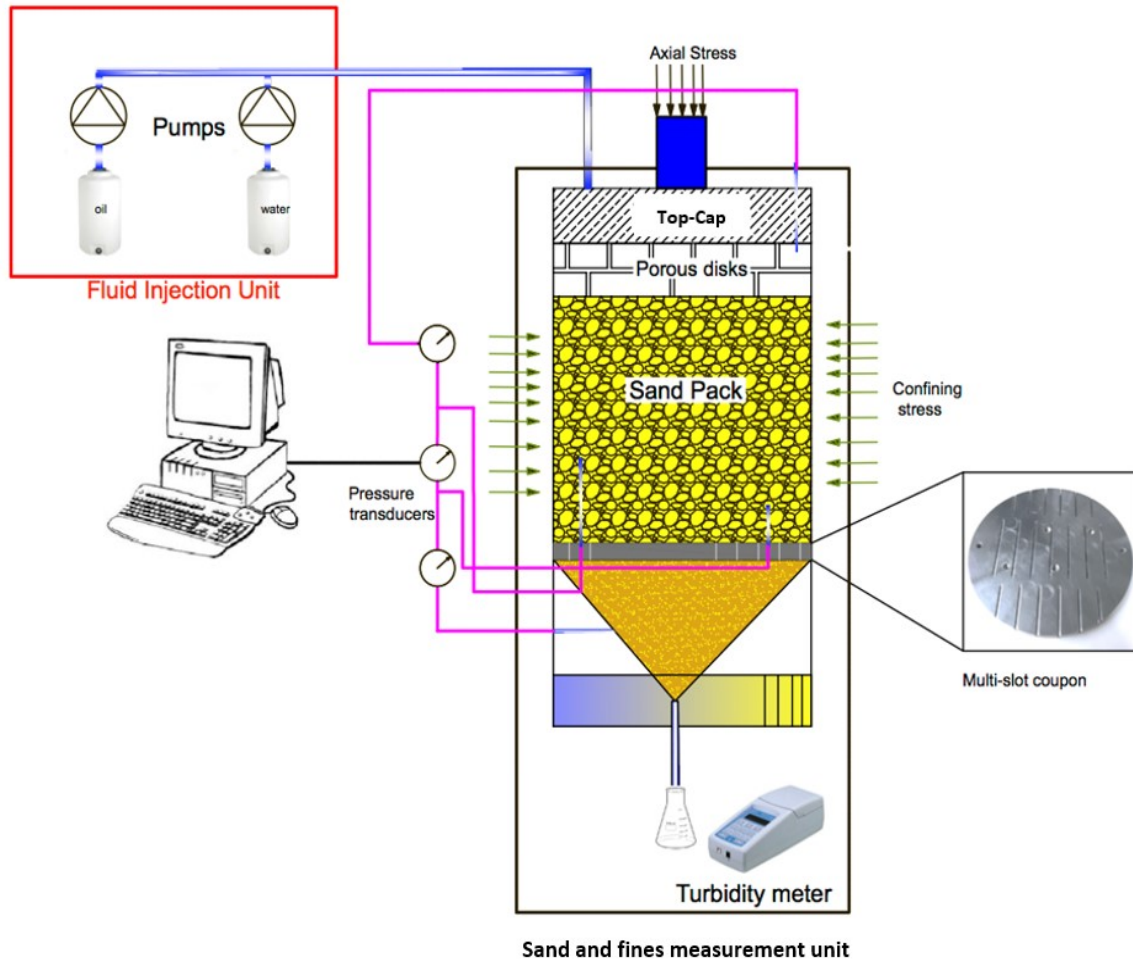


Figure 2-9. Pre-packed SRT with Stress (SRTS) (Montero et al. 2018)

2.6 Case Study: Hycal Labs Sand Control Testing Setup and Procedures

Hycal prepack setup was used by multiple researchers in assessing SCD performance under SAGD conditions (Bennion et al. 2008, 2009; Romanova et al. 2014; Devere-Bennett 2015). This section will give an overview and discussion of Hycal labs setup equipment and testing procedures, which are based on published literature and internal testing reports provided to Nexen CNOOC by Hycal labs.

2.6.1 Testing setup and procedure

Testing setup

Figure 2-10 shows the setup used to conduct multiphase flow prepack SRT in Hycal labs. The cell has sand-pack dimensions of 20 cm and 6.36 cm in length and diameter, respectively. Pressure

ports are placed at different points in the cell, which varies in position depending on the type of SCD tested. These pressure ports measure the pressure drop across the sand-pack and the SCD. For WWS the pressure drop across the sand pack is considered from the top of the sand pack till 2 cm (0.787 inch) above the coupon after which is considered the near-coupon section. Fluids are injected using highly accurate and pulsation-free positive displacement pumps. Fluid production is monitored in a four-phase separator, which records volumes of oil-water-gas and solids (sand and fines combined) production during the test.

Testing procedure

The following SRT testing procedure is used in Hycal labs (Weatherford Laboratories 2015):

6. Wet/dry sieve analysis of the cleaned formation oil sand samples by using the ASTM 136-A4A method.
7. Prepare a brine of 1% NaCl or 10,000 ppm and mineral oil of 15 cp.
8. Prepare coupon for testing by cutting a 5-cm-diameter section of field liner containing a single slot of the representative entry and exit dimensions for testing. Mount the coupon in a test cell configuration and install pressure taps above and inside the slot body.
9. Install coupon in core holder assembly; pour dry cleaned formation sand to the core holder space above the slotted coupon to form a pack approximately 20 cm in length by about 6.37 cm in diameter (about 1500 g of sand for each test).
10. Install top confining (injection end) piston in the apparatus and apply 3500 kPa axial confining pressure to the sand-pack to compress onto the top of the slotted coupon.
11. Evacuate pack for 24 hours to remove all residual gas. Saturate the sand-pack with brine using pressure (filtered to 0.5 microns).
12. Inject fluids in stages with the order and fluid rates shown in Table 2-2. The calculated rates are based on a liner length of 900 m, outer liner diameter of 17.8 cm, and well production rate of 500-1500 m³/day. Besides, 50 -90% plugging of SCD is assumed. For each test stage, the fluid phase(s) is injected from top to bottom until pressure drop stabilizes. Record pressure drops through the entire pack, on top of the slot and at the base of the slot. Note any sand production at each testing stage.

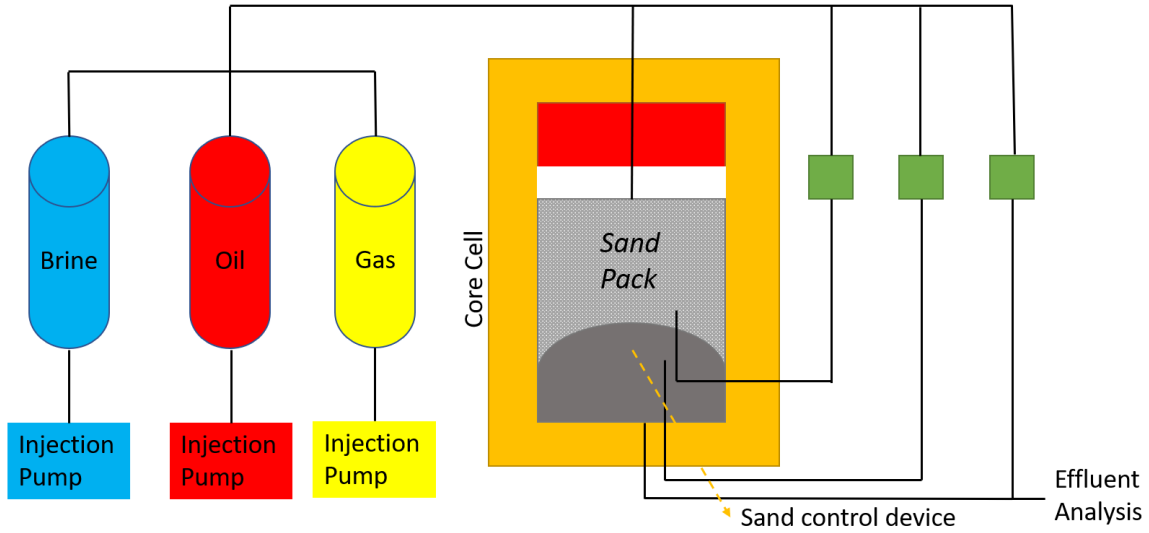


Figure 2-10. Schematic of Hycal labs multiphase flow SRT setup (Bennion et al. 2007)

Table 2-2. Schematic of Hycal labs multiphase flow setup (Bennion et al. 2007)

Weatherford Standard Flow Rates Oil, Water, Gas (cm ³ /hr)
40, 0, 0
80, 0, 0
120, 0, 0
160, 0, 0
160, 80, 0
160, 160, 0
160, 240, 0
160, 320, 0
160, 320, 10000
160, 320, 20000
160, 320, 30000
160, 0, 0

2.6.2 Setup and procedural limitations and their implications on the SCD evaluation

The volume of sand in Hycal labs cell is about 635 cm³, which is significantly lower than other SAGD prepack setups reaching up to 9200 cm³ (Mahmoudi 2016; Guo 2018). Random errors in sand-pack and coupon preparation can result in a higher impact on a small setup than a larger setup. Also, the fluid flow through the sand-pack and SCD coupon is linear flow, which is not the

best way to represent the pressure drop and capture convergence in wells since flow in the near well-bore region is considered radial flow (Anderson 2017).

Stress applied in every test using this testing setup is about 3500 KPa (500 psi). This value is chosen with no explanation provided and such a high amount is unusual since SAGD wells usually are under low-stress levels at the start of the well lifetime and increases as operations progress (Fattahpour et al. 2016). Using such high stress can cause underestimation of sand production in SRT for SAGD wells (Guo 2018).

Unlike other sand control testing failure criteria published in the literature (Ballard et al. 1999; Hodge et al. 2002), sand production and plugging failure criteria set by Hycal labs testing are not tied to wellbore data. This is a drawback with all sand control testing in the literature as the failure criteria are subjective to the operator and apply to specific field data. There are no established models connecting between the sand produced in the lab and the field.

The preparation of the sand-pack is conducted through the pouring of dry sand and then compacting axially. Testing performed in this work will show that this technique is not reliable, and reproducible pack preparation as the pouring rate is subjective to the test operator. In addition, pouring dry sands and fines will cause finer particles to be more concentrated at the bottom of the pack than the top by percolation of fine particles or vice versa due to elutriation segregation (Rhodes 2008), thus producing a non-homogenous sand-pack.

The methodology of choosing the magnitude of flow rates and the number of testing stages is subjective to the test operator understanding of the production conditions of the wells, which the test is to simulate. Representative fluid flow rates of different phases used in Hycal lab testing has been constant, regardless of the well and field conditions during SAGD operations with the exception of three low-rate tests reported by Devere-Bennett (2015). The testing parameters should account for such factors as reservoir heterogeneity, which cause non-uniform production and are unique to individual field cases.

Brines injected during Hycal tests use a salinity value of 10,000 ppm. The brine salinity in the testing should be linked to the brine salinity of the formation of interest. Brine salinity in the testing can significantly influence the fines migration, hence, the plugging of the pore structure (Khilar and Fogler 1998).

The coupons used to represent slotted liners are made up of a single slot, which neglects the effect of slot density on the inter-slot flow interaction and flow convergence. Flow convergence depends mainly on the opening size and slot density (Kaiser 2002; Mahmoudi et al. 2016a; Mahmoudi 2016), which is not captured when testing with single slot coupon.

2.7 Summary

Since the objective of this work is to investigate current sand control testing practices for SAGD wells, a good background in SAGD operators, sanding problems, influencing factors, and sand control testing is necessary.

This chapter started with an overview of the typical steps involved in SAGD operations and explained the significance of the sand production problem. A brief overview of sand control techniques was provided followed by the mechanisms and influencing factors such as fluid flow rate, fluid properties, sand properties, and stress levels, which affect plugging and sanding in SCDs. Next, the different versions of sand control testing setups in the literature were discussed, and their applicability to simulating SAGD conditions were critiqued. Subsequently, the mechanisms and influencing factors such as fluid flow rate, fluid properties, sand properties, and stress levels affecting the plugging and sanding in SCDs were discussed. The testing setup and procedure of Hycal labs used to investigate sand production in SAGD environment were presented, which are replicated in the subsequent chapters and eventually, the identified improvements are applied and tested.

Chapter 3: Long Lake Field-McMurray Formation Oil Sand Characterization and Replication

3.1 Introduction

Sand grain characterization focuses on particle size distribution (PSD) analysis, particle shape analysis, surface texture, and compositional analysis. As discussed in Chapter 2, previous researchers found that PSD, grain shape, and the composition of sand and fines influence the mechanical properties of granular media and therefore, sand production. Thus, it is essential to conduct characterization investigation to replicate the representative samples of oil sands in the reservoir of interest for having meaningful sand control testing. Figure 3-1 illustrates the steps of sand and fines characterizations and how it fit in the sand control testing process. Each step of characterization and replication will be discussed in this Chapter.

Several authors (Fattahpour et al. 2012; Younessi et al. 2012; Mahmoudi 2016) presented methodologies to replicate weakly-consolidated and unconsolidated sands by mixing a combination of commercial sands, fines, and cement. They validated their replication techniques by matching the unconfined compressive strength or shear strength of the replica with the original sand mixture.

Long Lake field is located 40 km southeast of Fort McMurray and is operated by Nexen CNOOC. The area of interest is south of the current development. The primary producing formation is the McMurray Formation. This chapter presents the characterization and replication recipe of the oil sands from Nexen, Long Lake by commercial sands through applying a modified version of the replication methodology developed by Mahmoudi (2016) for sand control testing.

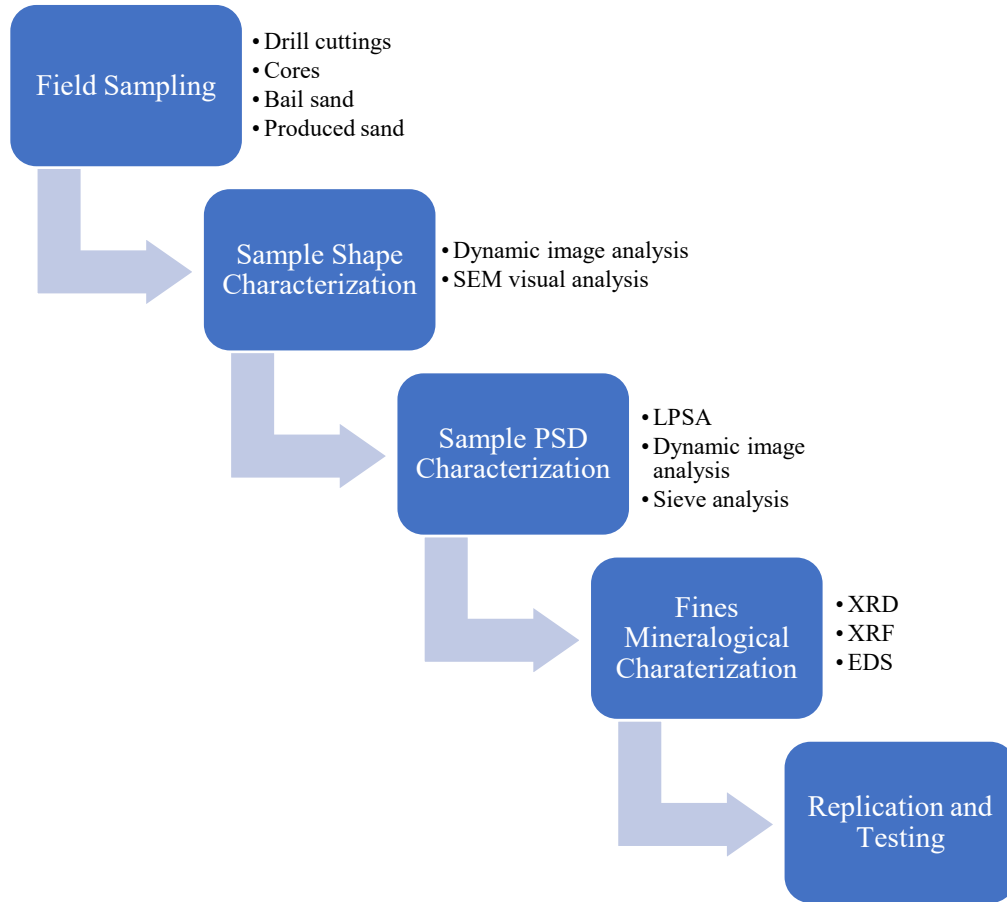


Figure 3-1. Flowchart linking relationship between sand characterization and sand control testing

3.2 Preparation and Cleaning of Field Oil Sands Samples

Five oil sand samples at five different depths in the McMurry formation were acquired from a well in the Long Lake field operated by Nexen CNOOC. For each sample, three subsamples were obtained and cleaned using the Soxhlet extraction setup shown in Figure 3-2.

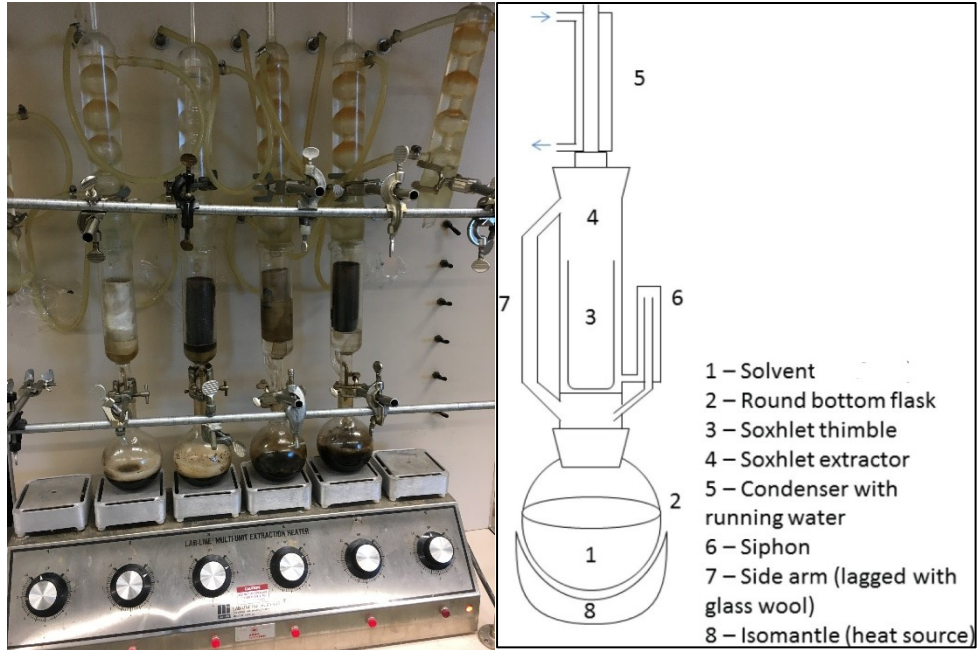


Figure 3-2. Image and schematics of Soxhlet extraction setup used in this work

The oil sand sample is placed in a polymer-based thimble then, into the extraction chamber. Toluene, as the extraction solvent, is placed in the boiling flask. Water is injected into the condensing chamber to allow reflux of the toluene vapor to pour into the oil sand sample. Once the toluene level in the extraction chamber reaches the height of the siphon arm, the dirty toluene is drained back to the boiling solvent. This process is allowed to repeat itself for 48 hours for each sample to produce oil-free sand. In the end, the oil-free sands are characterized for the characterization data to be used in the replication of oil sands for sand control testing purposes as will be explained in the following sections.

3.3 Surface Texture of Particles

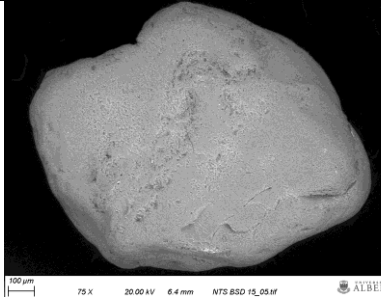
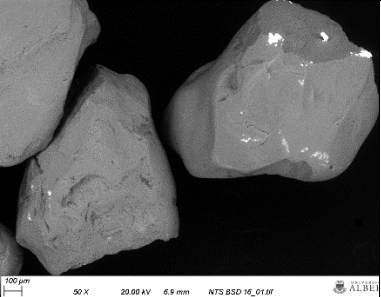
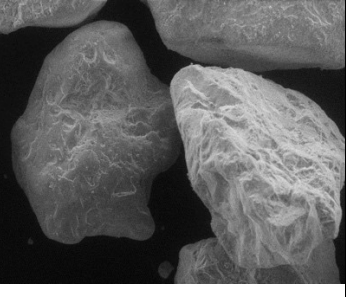
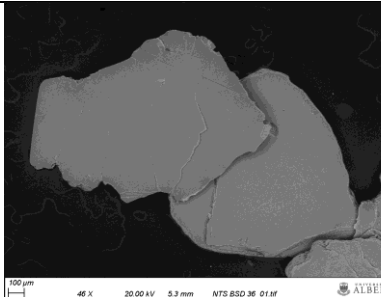
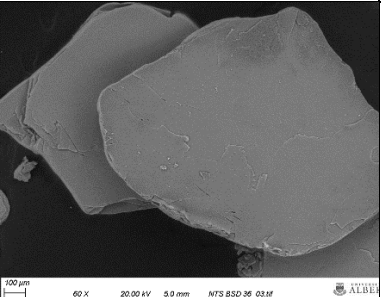
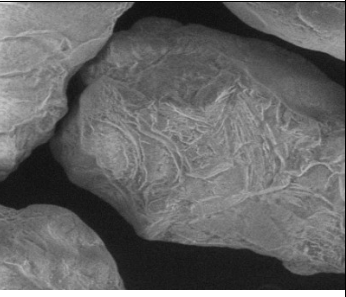
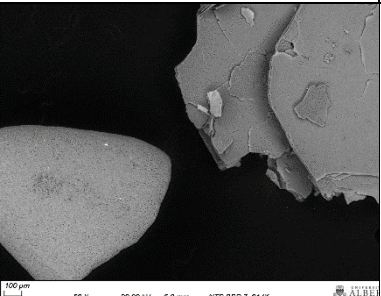
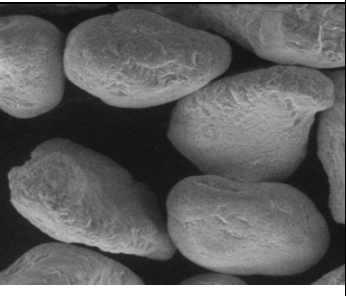
The surface texture of particles can influence the friction between the particles and thus, bridging and sand production. Surface texture is the recurring or unsystematic deviation from a nominal surface that makes up the 3-dimensional topography of a surface which includes roughness waviness, lay, and flaws (Bhushan 2000). However, quantifying the surface texture from images requires specialized equipment and can be quite challenging to perform accurately (Yang and Baudet 2016).

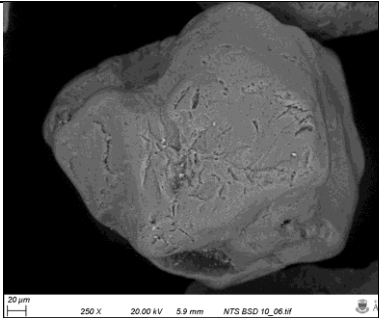
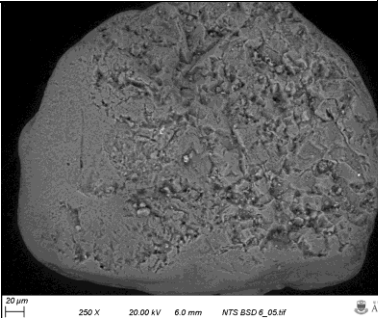
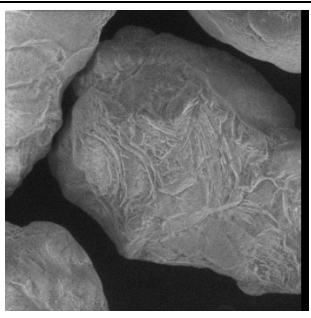
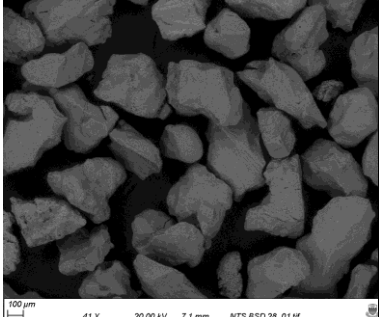
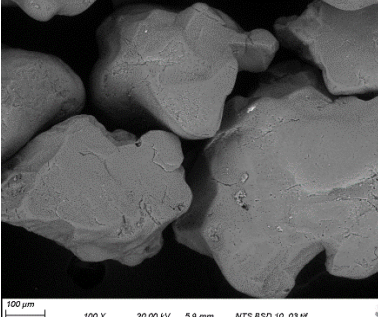
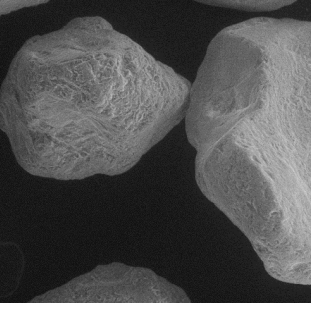
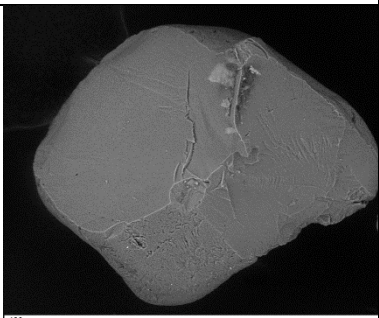
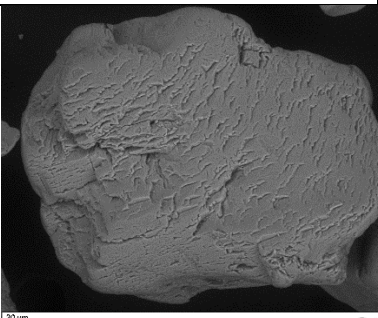
In this work, texture analysis and matching were done qualitatively. Oil sand and commercial sand grains at different size groups were chosen randomly and placed on a double-sided carbon tape. Then, the carbon tape is mounted on an aluminum stub and analyzed by ZEISS Sigma 300VP scanning electron microscope under backscattered electron mode.

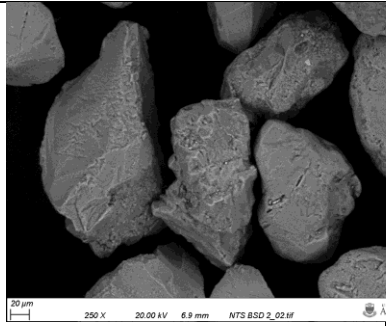
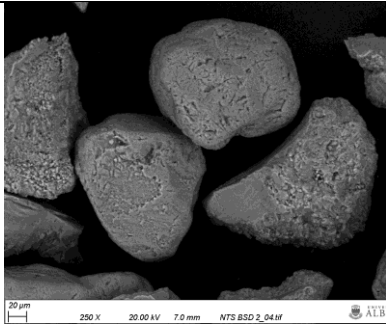
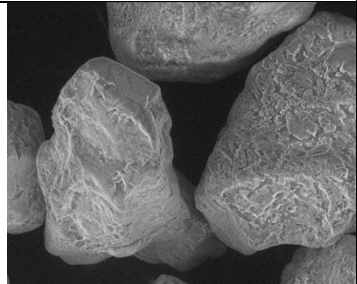
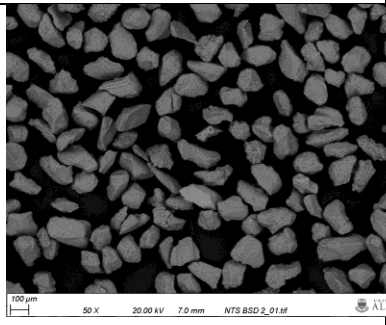
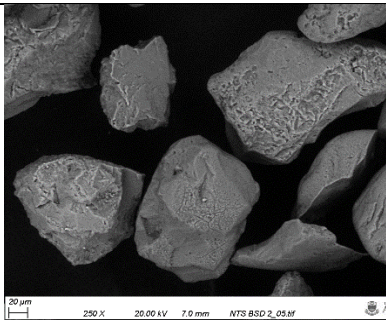
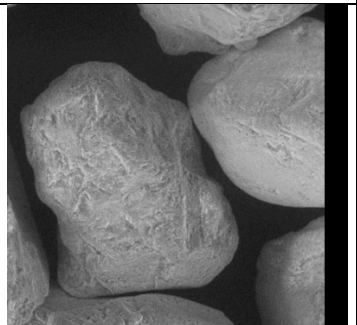
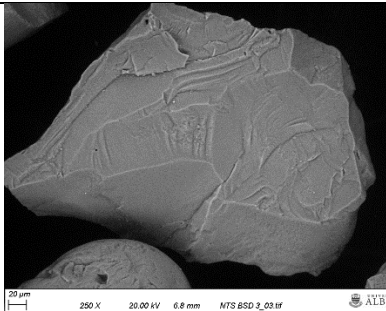
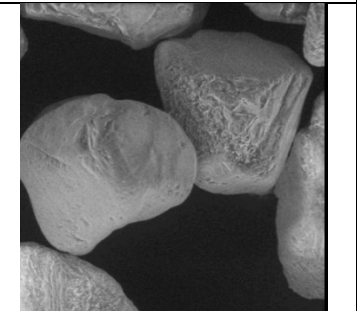
All sand size groups, as classified by Wentworth (1922), were represented in the texture analysis. The oil sand samples analyzed were first sieved at 850 and 630 μm (coarse sand), 500 and 315 μm (medium sand), 250 and 150 μm (fine sand), 125 and 75 μm (very fine sands), and finer than 44 μm (fines). The Scanned Electron Microscope (SEM) images of each size class are presented in Figures 3-3 along with the commercial sand SEM images for comparison.

For each size class, SEM imaging was conducted. It was noticed that the surface texture was progressively rougher for smaller particles for all the five oil sand samples provided by Nexen.

Based on the images, one can notice the presence of large mica particles (Figure 3-3 A3-A4), which are absent in the commercial sand. It also appears that the rounder the grains, the smoother the surface of the grain (Figure 3-3 A2 vs. A5). Besides, one can notice that, generally, the roughness of commercial sands is higher than that of oil sands.

	Oil-Sand samples	Commercial sands	
Coarse sands (500-1000 μm)			
	A1	A2	B1
			
	A3	A4	B2
			
	A5	A6	B3

	Oil-Sand samples	Commercial sands	
Medium sands (250-500 μm)	 <p>20 μm 250 X 20.00 kV 5.9 mm NTS BSD 10_06.tif</p>	 <p>20 μm 250 X 20.00 kV 6.0 mm NTS BSD 6_05.tif</p>	
	A7	A8	
	 <p>100 μm 41 X 20.00 kV 7.1 mm NTS BSD 28_01.tif</p>	 <p>100 μm 100 X 20.00 kV 5.9 mm NTS BSD 10_03.tif</p>	
	A9	A10	B5
	 <p>100 μm 190 X 20.00 kV 6.0 mm NTS BSD 6_02.tif</p>	 <p>20 μm 200 X 20.00 kV 7.0 mm NTS BSD 28_04.tif</p>	
	A11	A12	B6

	Oil-Sand samples	Commercial sands	
Fine sands (125-250 μm)			
	A13	A14	B7
			
	A15	A16	B8
			
	A17	A18	B9

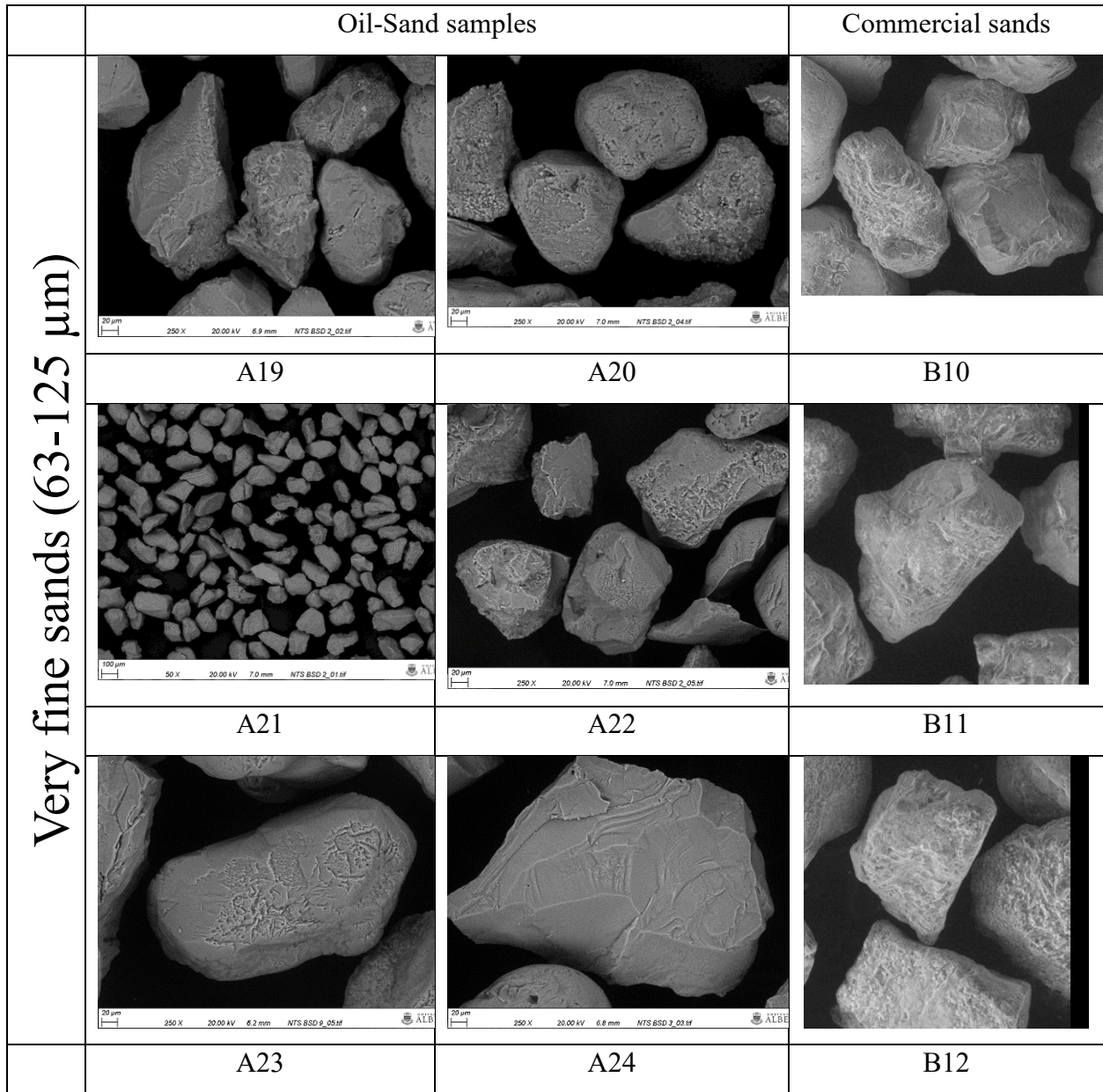


Figure 3-3. SEM images of the field and commercial sands for different size classes

3.4 Characterization and Replication of PSD

3.4.1 Measurement and description of PSD

Sand Particle Size Distribution (PSD) can be characterized based on size classes such as the classification table provided by Wentworth (Wentworth 1922). The PSD is usually presented in a curve to show the mass fraction passed or retained at each size class measurement increment as a

function of the mesh size measured. The PSD can be presented as a histogram or a cumulative distribution, however, plotting the cumulative distribution is standard practice for sand control design purposes.

Sand PSD for sand control purposes is mainly measured by sieve analysis (Ballard and Beare 2013), Laser Particle Size Analysis, LPSA (Devere-Bennett 2015), and Dynamic Image Analysis, DIA (Mahmoudi 2016). The PSD by using sieve analysis usually results in limited measuring points of the second smallest dimension of a sand grain (Beare and Ballard 2013). Also, the PSD can be measured by correlating physical phenomena to the size of particles such as light scattering for LPSA or settling velocity for the hydrometer. However, these techniques simplify the response to the behavior of spherical particle and thus neglect the complex dimensions of the shape of the grains. Advances in imaging and analysis have made the dynamic image analysis possible. DIA is preferred over other PSD quantification techniques since it allows the capture of the non-unique and non-spherical features of the sand grains.

Sand PSD curve, in the context of sand control, is usually characterized based on the size at various cumulative percentiles, uniformity, and sorting coefficient to describe the curve shape. Generally, PSD descriptors can be based on centering variables such as mean and median size or size spread descriptors such as standard deviation or sorting. The third type of curve description is shape variables such as kurtosis or uniformity constant (Manchuk et al. 2013). Other attempts to characterize the PSD are based on curve fitting and parametric distribution functions (Esmaelnejad et al. 2016; Bayat et al. 2017; Roostaei et al. 2018a).

In this work, the characterization of the PSD of the reservoir oil sands and commercial sands is based on curve fitting of measured PSD data with a moving average fitting technique and interpolation from the curve, which allows measurement of missing data points. Once fitted, the Uniformity Coefficient (UC), Sorting Coefficient (SC), and size corresponding to cumulative percentiles 1% to 100% can be calculated.

3.4.2 Characterization of oil sands PSD

According to Figure 3-4, the PSD of field samples acquired by the E&P Company operating in the field of interest closely resembles the PSD of the oil sand samples delivered to the sand control testing lab at the University of Alberta. The close match indicates that the samples are

representative of the formation of interest and further shape and compositional characterization of them would be representative of the formation of interest.

Hycal labs represented the oil sands in that formation to four batches. Comparing Hycal tested oil sands with the field PSDs showed that only Batch 2 and 3 are representative of field oil sands while Batch 0 and 1 are too fine compared with the majority of field oil sands PSDs.

Figure 3-5 plots the Uniformity Coefficient (UC) and Sorting Coefficient (SC) against the size of the finest 10th percentile. Results indicate that the SC and UC increase exponentially as the D10 decreases. In other words, coarser sands in this formation are more uniform. The same trend is visible in Figure 3-6, even if less pronounced when comparing the UC and SC with the size of the coarser 50th percentile. Furthermore, a linear relation is noticed when plotting and fitting a function between the clay and fines content of the oil sand samples presented in Figure 3-7.

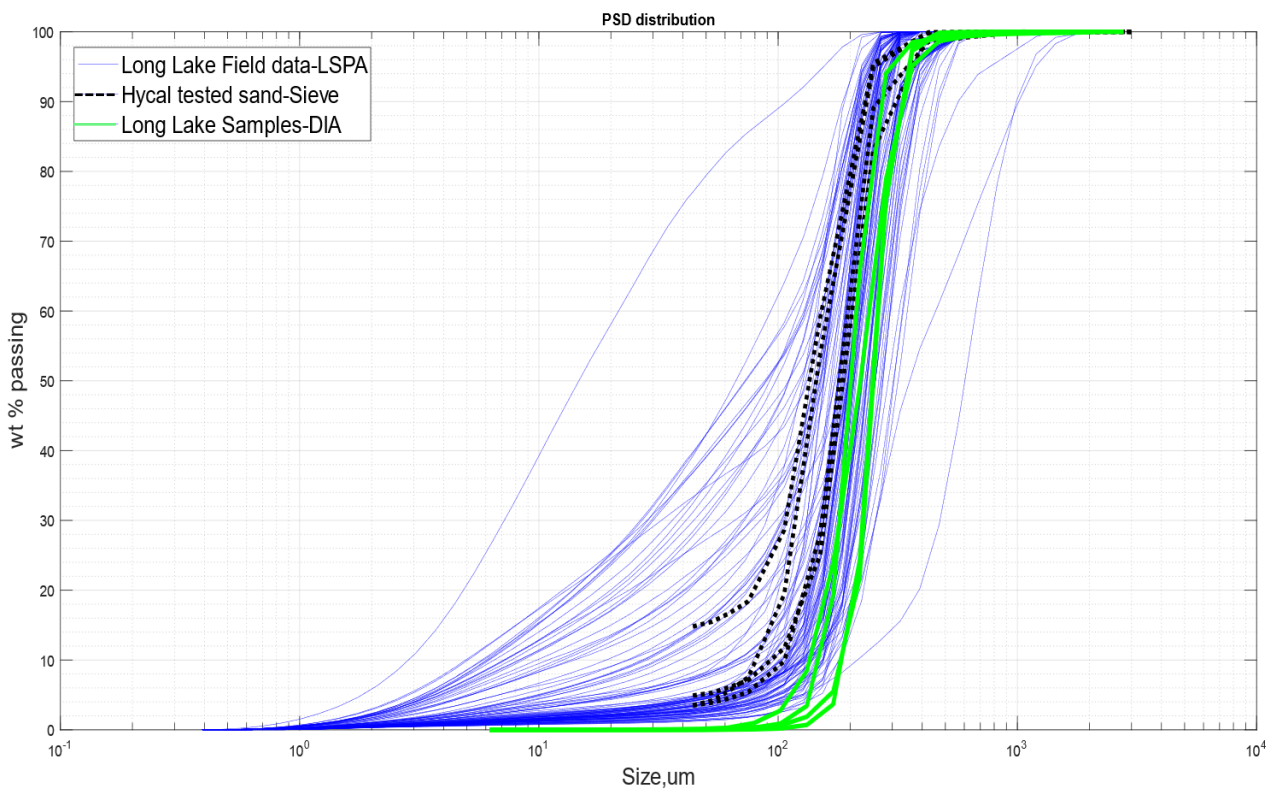


Figure 3-4. PSD of sands from the formation of interest analyzed by Hycal compared to the analysis conducted herein

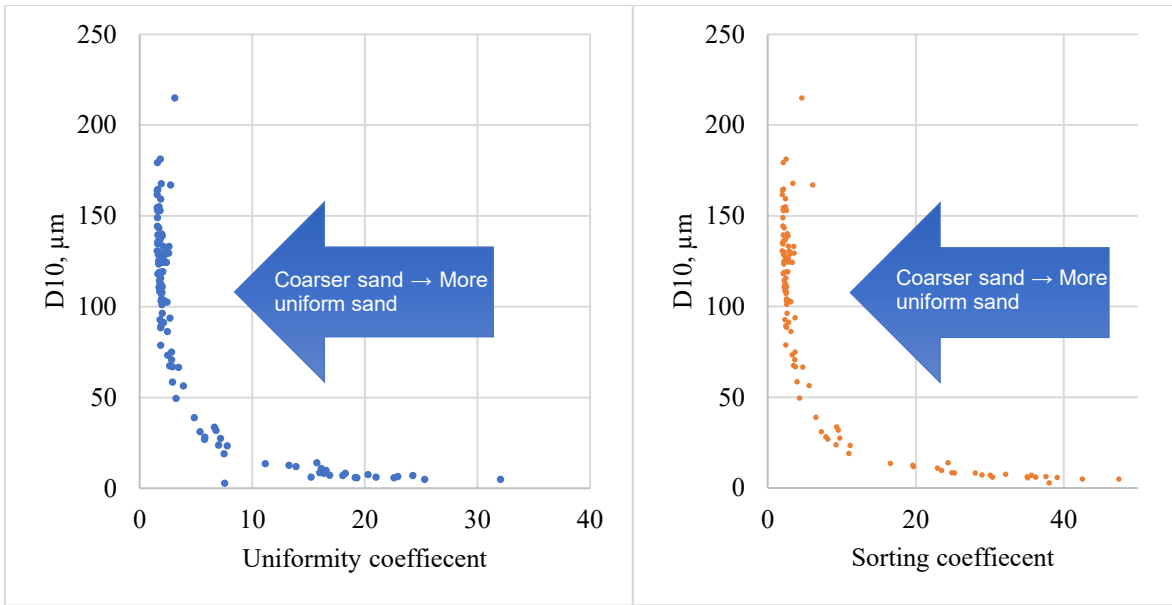


Figure 3-5. Uniformity and sorting coefficients versus D10 of the sand samples from the formation of interest acquired from different wells

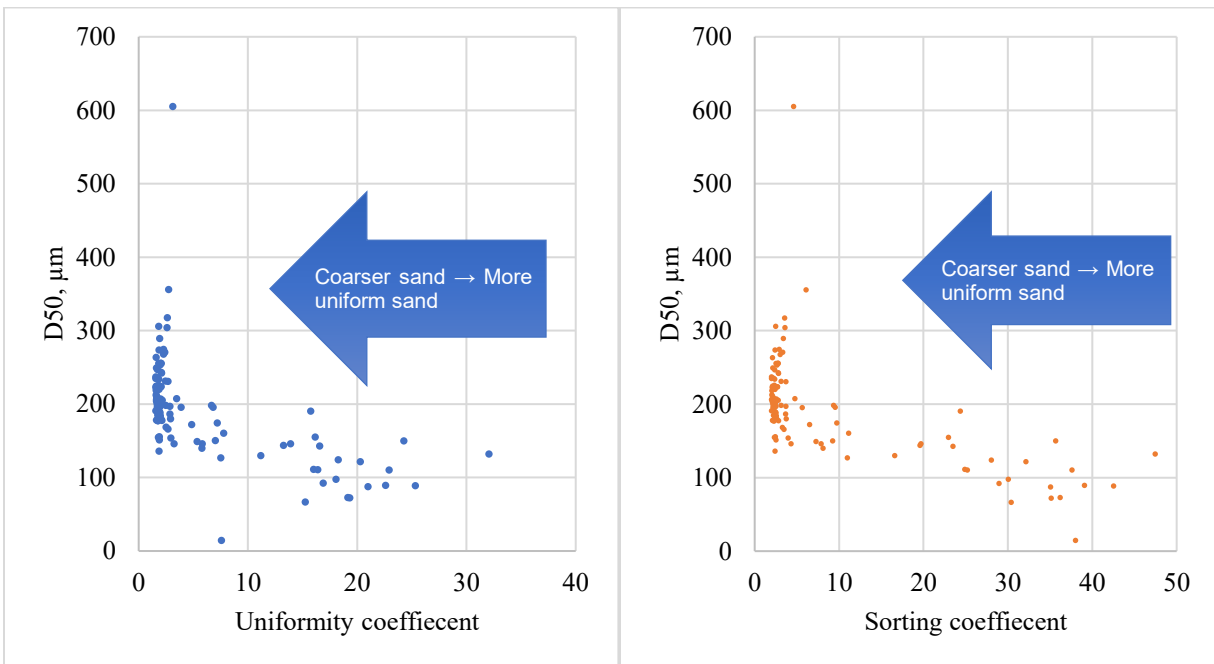


Figure 3-6. Uniformity and sorting coefficients versus D50 of the sand samples from the formation of interest acquired from different wells

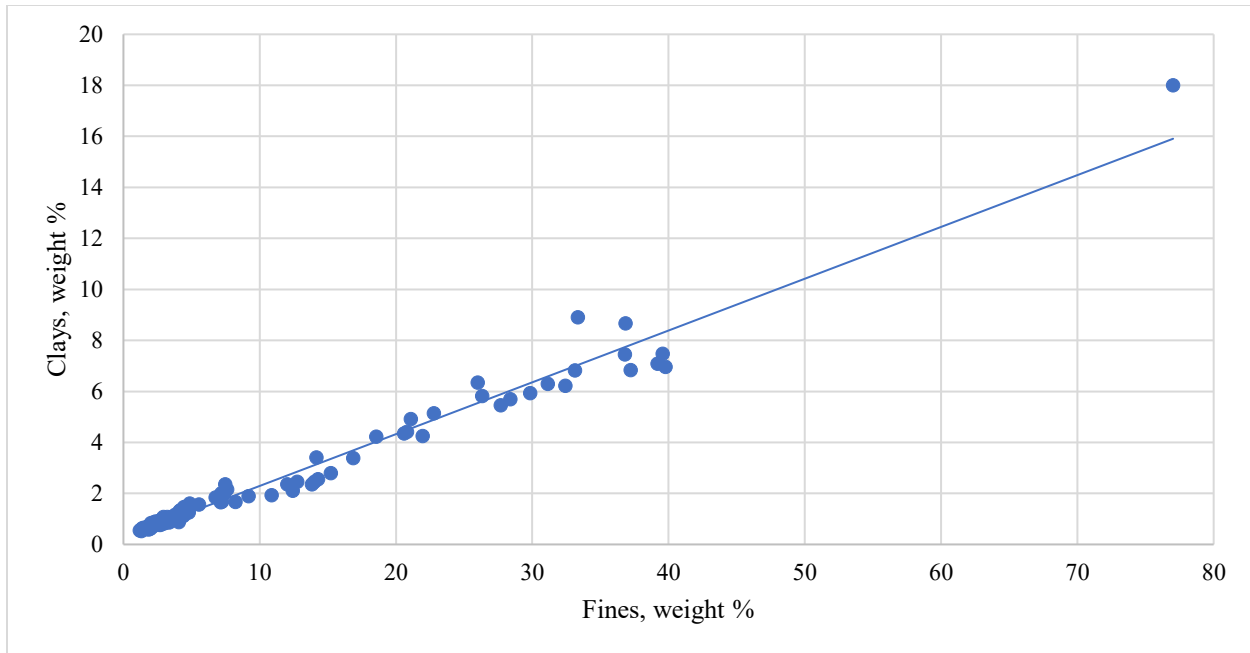


Figure 3-7. The relationship between fines and clay content in gathered oil sand samples from McMurray Formation in Long Lake

3.4.3 Replication based on PSD

Commercial sands were acquired for replicating oil sands. The PSD of commercial sands was measured by the DIA technique using a Sympatec QICPIC analyzer and then, compared with the PSD of oil sand gathered from different sources in Figure 3-8. Based on this figure, it is clear that the available PSDs of the commercial sands cover the range PSDs of the oil sands in the field of interest. Therefore, replication is feasible through mixing the commercial sands in proper proportions. The fines portion of the target oil sands can be replicated by combining commercial fines by matching the compositional analysis.

A methodology was introduced to replicate the target sand PSD as outlined in Figure 3-9. The method involves first fitting the target and the commercial sand PSDs by a piecewise fitting function. Then, D1 to D100 is extracted for every commercial sand PSD and, then the target PSD is placed in a series of linear simultaneous equations. The simultaneous equations are solved for the optimal commercial PSD weight percentages that would give the least sum squared difference between the replicated sand and the target sand. The methodology outlined was implemented using MATLAB R2017a.

For testing purposes, Hycal's oil sand Batch 3 was chosen for replication as it will be used to compare Hycal testing with the testing presented herein. The PSD replication is shown in Figure 3-10 along with the target PSD. PSD parameters describing the PSD is presented in Table 3-1. Based on the figure, the target sand and commercial sand replica produced by the MATLAB algorithm are in close agreement. The replica shows a maximum deviation 50 μm (0.0020 inch) respectively from the original sands. This deviation is acceptable since it is within the ± 0.002 -inch manufacturing tolerance of slotted liner (Penberthy, and Shaughnessy, 1992).

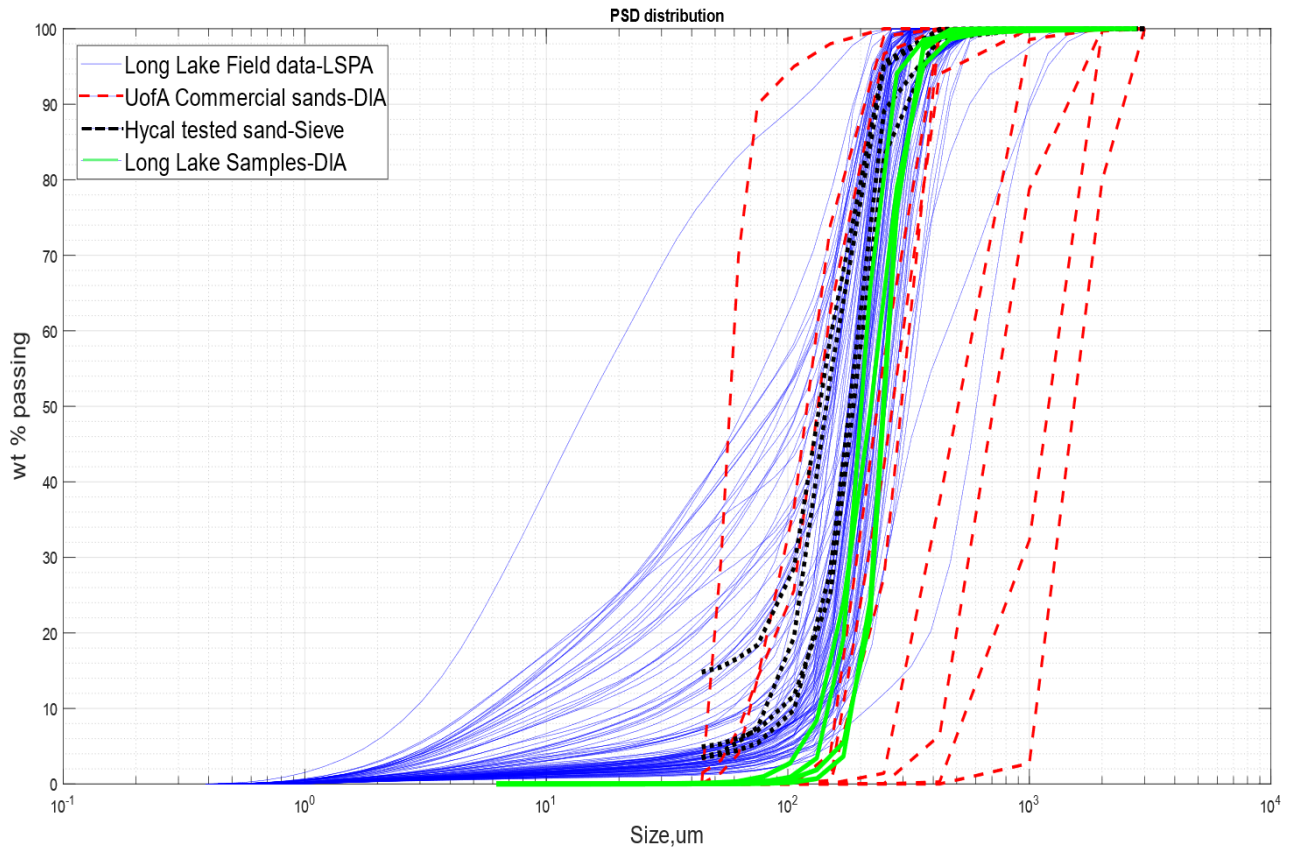


Figure 3-8. PSD curves of oil sands analyzed by Hycal by LPSA (blue), oil sands used in Hycal testing (black), Long Lake samples characterized in the University (green), and commercial sands available (red)

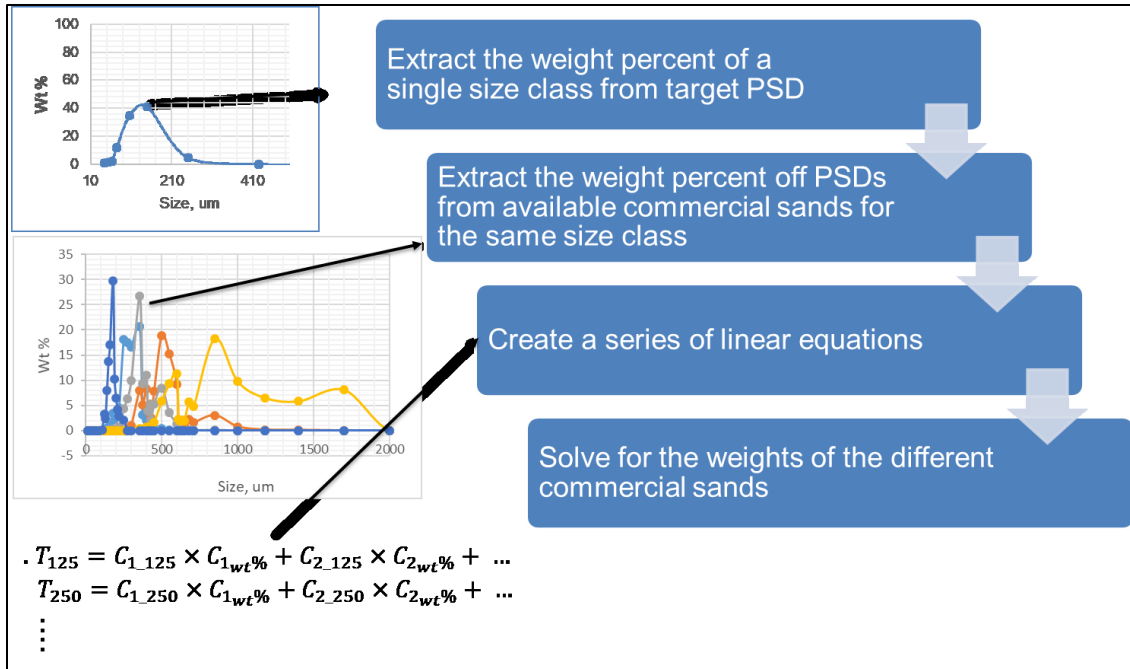


Figure 3-9. Diagram of the PSD replication technique

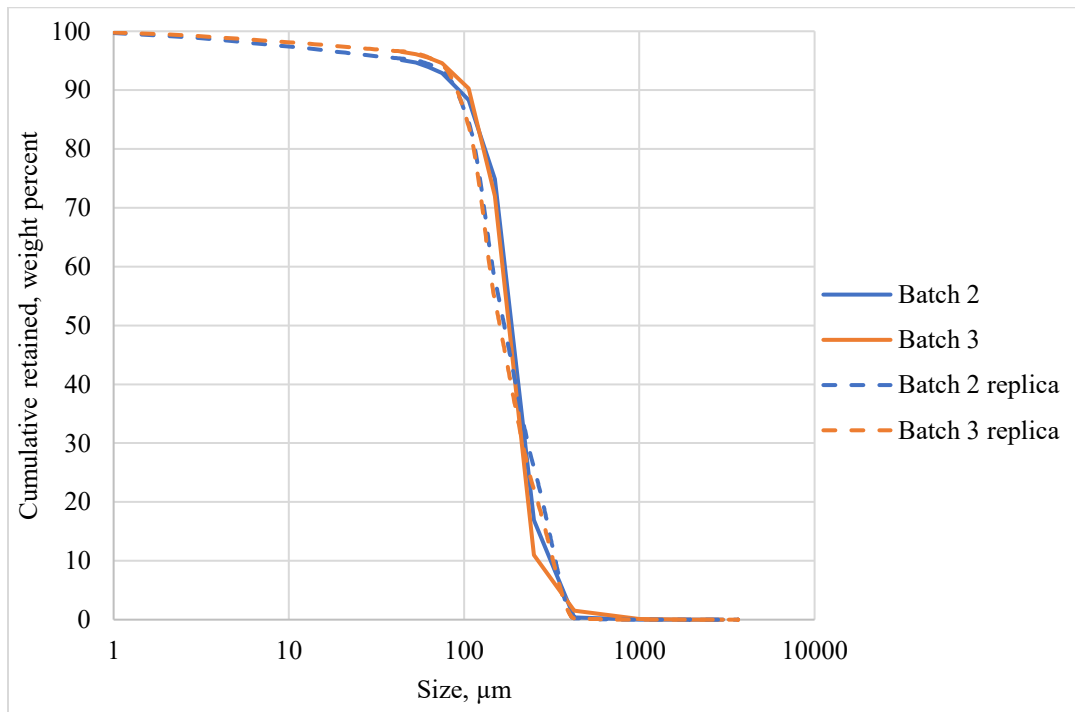


Figure 3-10. A comparison between the target (Batch 3) and replica PSD from the replication process

Table 3-1. PSD descriptors of sands used in testing

Sand print	D90, μm	D50, μm	D10, μm	Fines content (<44 μm), %	Uniformity Coefficient
Batch 2	93	189	318	4.9	2.2
Batch 3	107	183	267	3.5	1.8
Batch 2 replica	90	171	331	4.9	2.2
Batch 3 replica	91	161	317	3.5	2.0

3.5 Shape Factor Characterization and Replication

In the literature, shape description of sand grains is usually based on a qualitative approach, such as classifying grains as rounded or angular based on the picture-based diagram in Figure 3-11 (Powers 1953). The shape description may be quantitative by assigning values using charts as shown in Figure 3-12 (Krumbein and Sloss 1951). Recently, charts have been introduced based on geometric shape descriptors (Blott and Pye 2008). However, there are various definitions of the geometric descriptors and the measurement techniques in the literature (Rodríguez et al. 2013).

Recently, reliable laboratory size and shape analyzers based on dynamic image analysis has been introduced. Examples include QICPIC by Sympatec, and Camsizer by HORIBA Scientific, which provide the size and shape of particles using image analysis of free-falling particles captured by multiple cameras. This technique allows a larger sample size to be examined in a shorter period compared to the conventional techniques. Besides, image analysis of free-falling particles eliminates the orientation bias of particles analyzed under a microscope. Due to these advantages, this research utilizes the dynamic image analysis for the shape characterization of the commercial sands and oil sands samples.

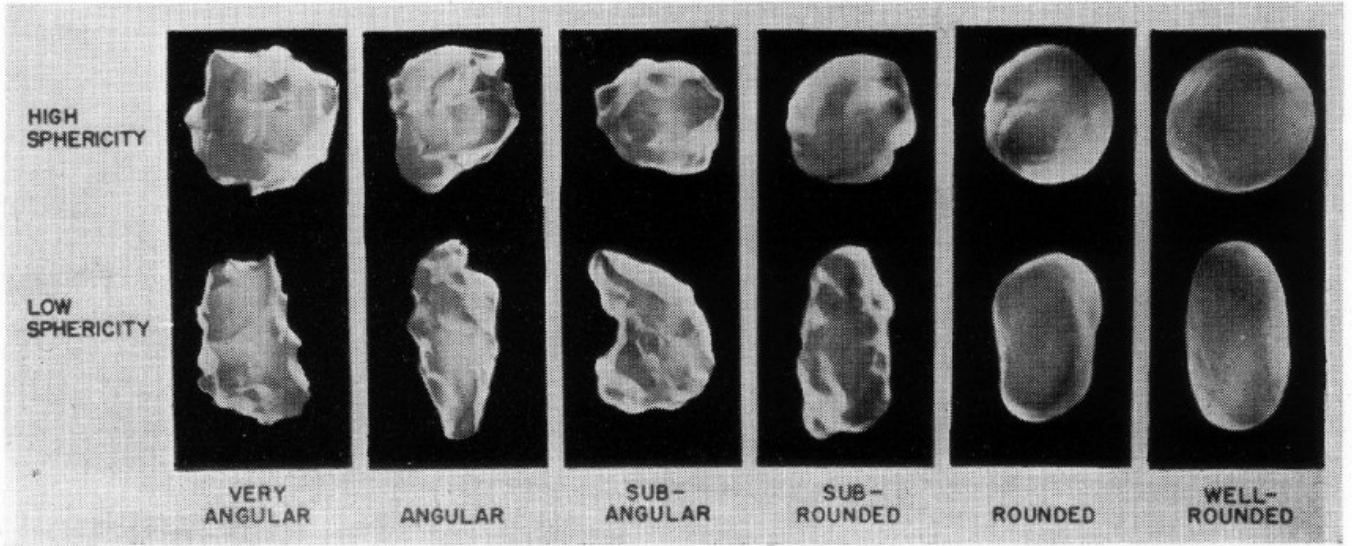


Figure 3-11. A qualitative measurement of shape (Powers 1953)

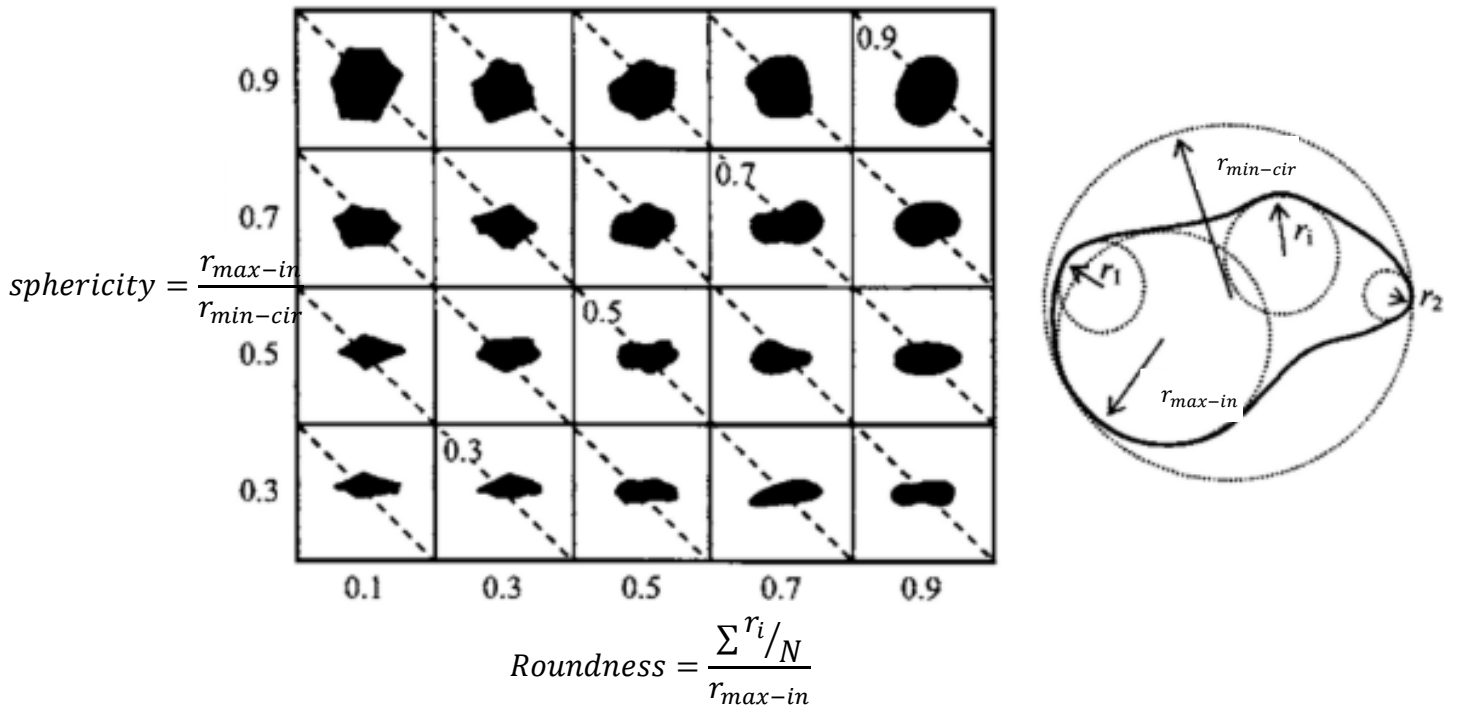


Figure 3-12. A guide for assigning roundness and sphericity values to a particle (Krumbein and Sloss 1951)

3.5.1 Shape factors description

Multiple forms of quantitative shape descriptors have been proposed in the literature to describe particle shapes. Such includes roundness (Wadell 1932), angularity (Lees 1964), circularity (Riley 1941), and irregularity (Blott and Pye 2008). A comprehensive review of different shape descriptors in the literature is provided by (Smart 2013). This work employs the grain shape factors to describe the shapes of oil sands and commercial sands regarding sphericity, convexity, and aspect ratio as defined by Sympatec (2018).

Sphericity

Sphericity (S) is defined as the ratio of the perimeter of a circle with the equivalent area as the 2D projection of a particle to the actual particle perimeter (Sympatec 2018).

$$S = \frac{P_{EQPC}}{P_{real}} = \frac{2\sqrt{A \cdot \pi}}{P_{real}} \quad (3.1)$$

Sphericity is a measure that describes how a given particle shape resembles a sphere. Sphericity is chosen as a relevant shape characterization parameter for sand control purposes as it assesses the surface shape and thus, correlates with the number of intergranular contact points in the porous media. The frictional strength between particles is influenced by the sphericity, impacting the arch stability around the slots. One can hypothesize that lower sphericity causes better bridge stability and therefore, less sanding.

Sphericity values vary from 0 to 1 where the larger the number, the closer the shape of the particle to a sphere. An irregular shape produces a larger perimeter to area ratio compared to a perfect circle.

Aspect ratio

Aspect Ratio (AR) in this context is defined as the ratio of two sizes observed on a projection of a 3D sand grain. The two sizes are the minimum and maximum Feret diameters as shown in Figure 3-13. The Feret diameter is the distance between two parallel tangents to the particle boundaries. A perfect sphere will have an AR value of 1. However, the value decreases as the overall shape deviates from a sphere.

For sand control purposes, the aspect ratio can be an indication of the ease of the particle rotation. The lower the AR, the higher the particle tendency to rotate under stress. Higher values of AR results in higher resistance to rotation (Fonseca et al. 2012). One can hypothesize that sand with a high aspect ratio produces a more stable sand bridge and is less prone to production.

$$\text{Aspect ratio} = \frac{\text{Feret min}}{\text{Feret max}} \quad (3.2)$$

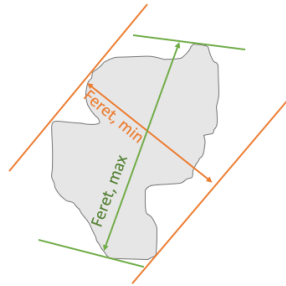


Figure 3-13. Schematic illustrating maximum and minimum feret diameters of a sand grain

Convexity

Convexity Ratio (CR) is a shape factor describing the irregularity of the surface of the particle. The CR is the ratio between the 2D area projection of the grain (A) to the area of the convex region (A+B) (Sympatec 2018) as shown in in Figure 3-14. The CR has a maximum value of 1 when there are no concave features. Convexity correlates with the prominence of shape corners of a particle, which in turn, dictates the number of contact points between particles. Thus, convexity can affect the intergranular friction and therefore, sand production.

$$\text{Convexity} = \frac{A}{A+B} = 1 - \frac{B}{A+B} \quad (3.3)$$

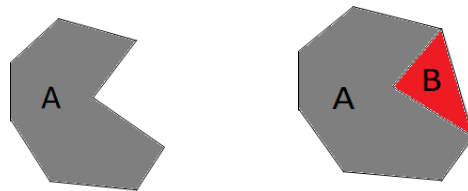


Figure 3-14. Schematic illustrating concept of convexity

3.5.2 Characterization of particle shape

The five oil sands samples acquired at different depth in the McMurry formation were analyzed by dynamic image analysis using the QICPIC image analyzer. Figure 3-15 shows the convexity, sphericity, and aspect ratio of the sands with depth. Based on this figure, the sands in this well in the McMurray Formation appear almost homogenous in shape at different depths. Thus, the formation sands can be replicated by using commercial sands that match in particle shape factors with those of the oil sands samples.

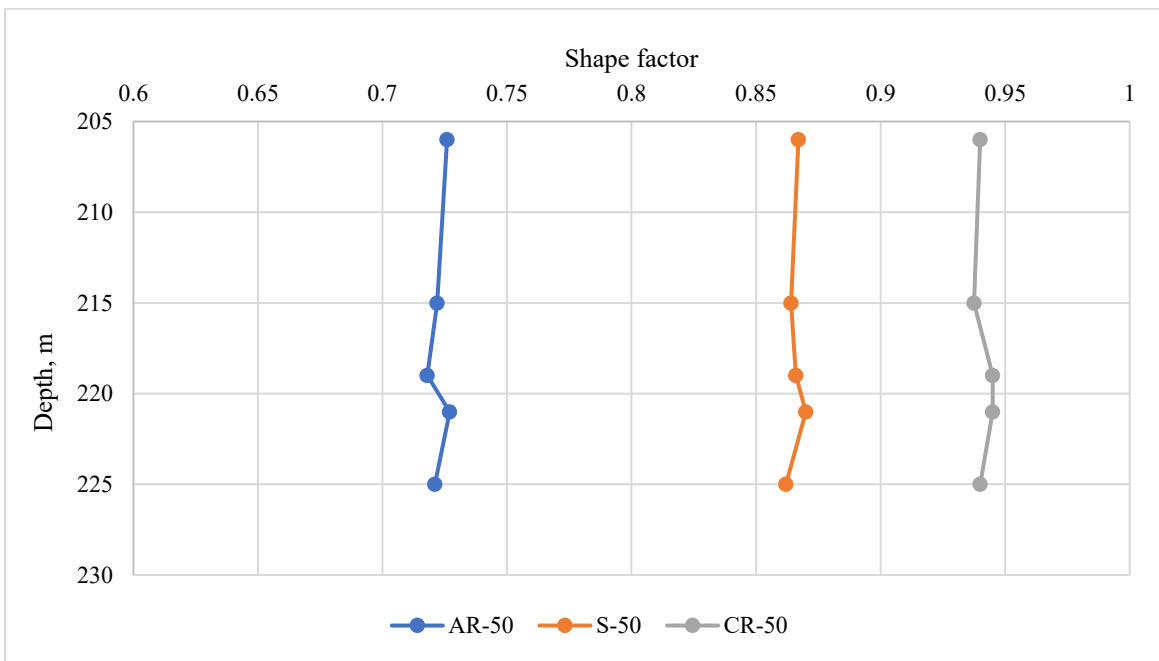
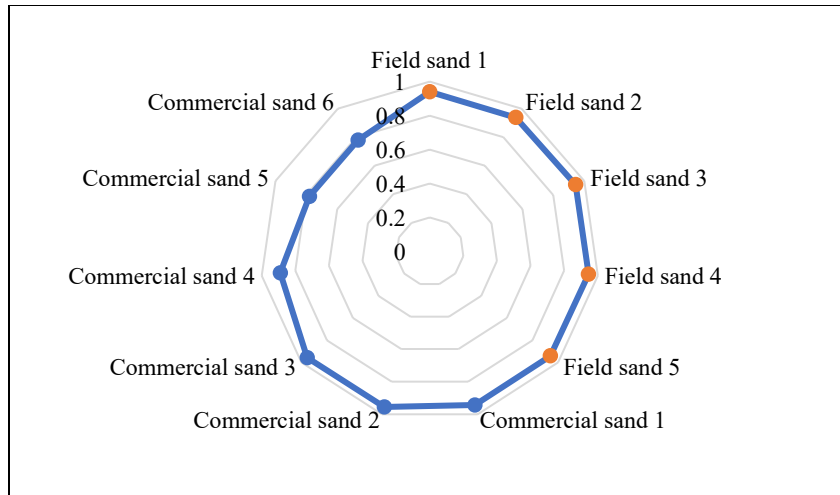


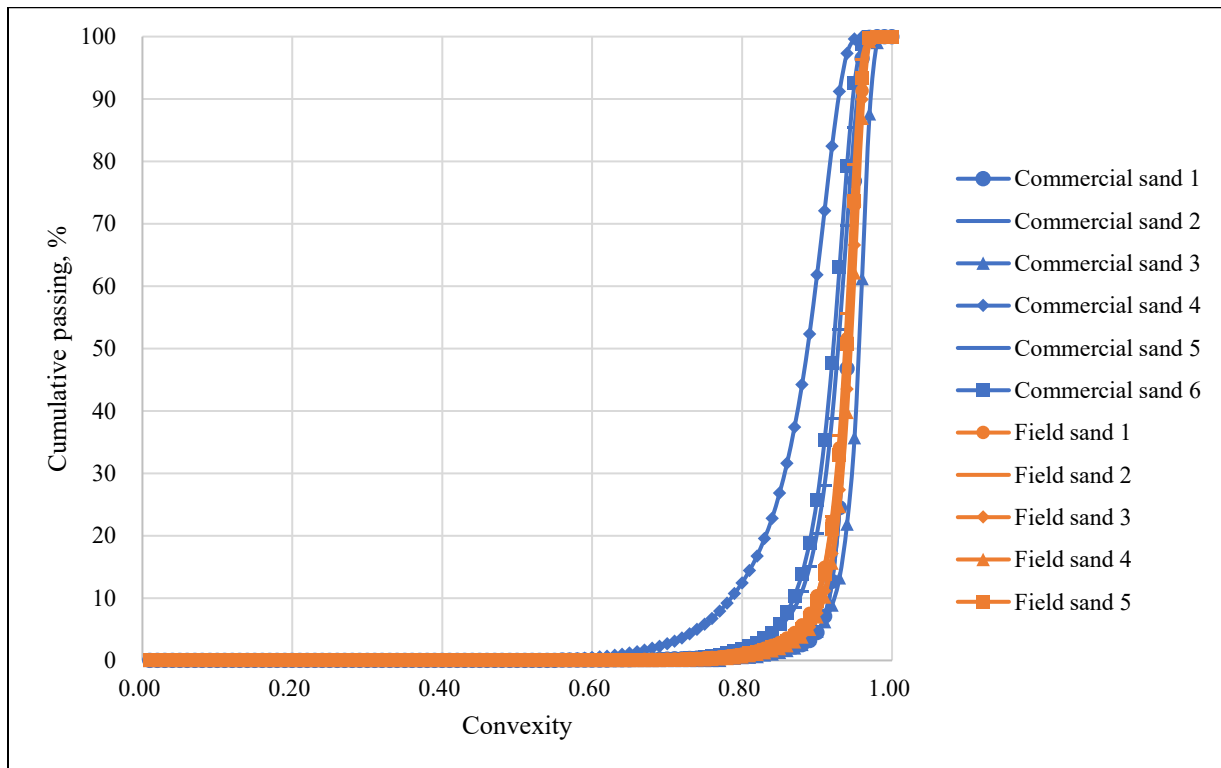
Figure 3-15. From left to right aspect ratio, sphericity, and convexity of oil sand samples versus depth

3.5.3 Matching grain shape

A variety of commercial sands were analyzed by dynamic image analysis for comparison with oil sand samples. Figure 3-16 through 3-18 compare the sands based on sphericity, aspect ratio, and convexity. By comparing convexity of commercial sands and oil sands, one can identify commercial sands 1, 2, 3, and 4 are consistent with oil sands. However, when sphericity and aspect ratio are considered, it becomes clear that the commercial sand 4 is not consistent. Thus, commercial sands 1, 2 and 3 shape factors match those of oil sands samples and can be used in the oil sands replication.

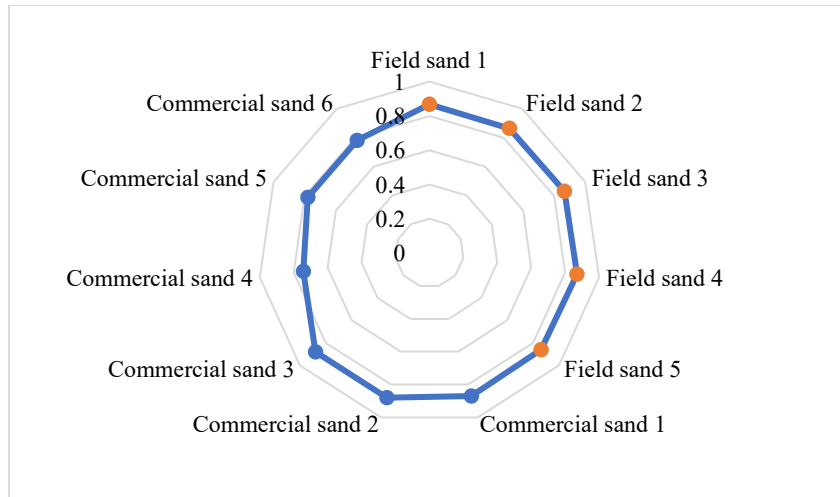


(a)

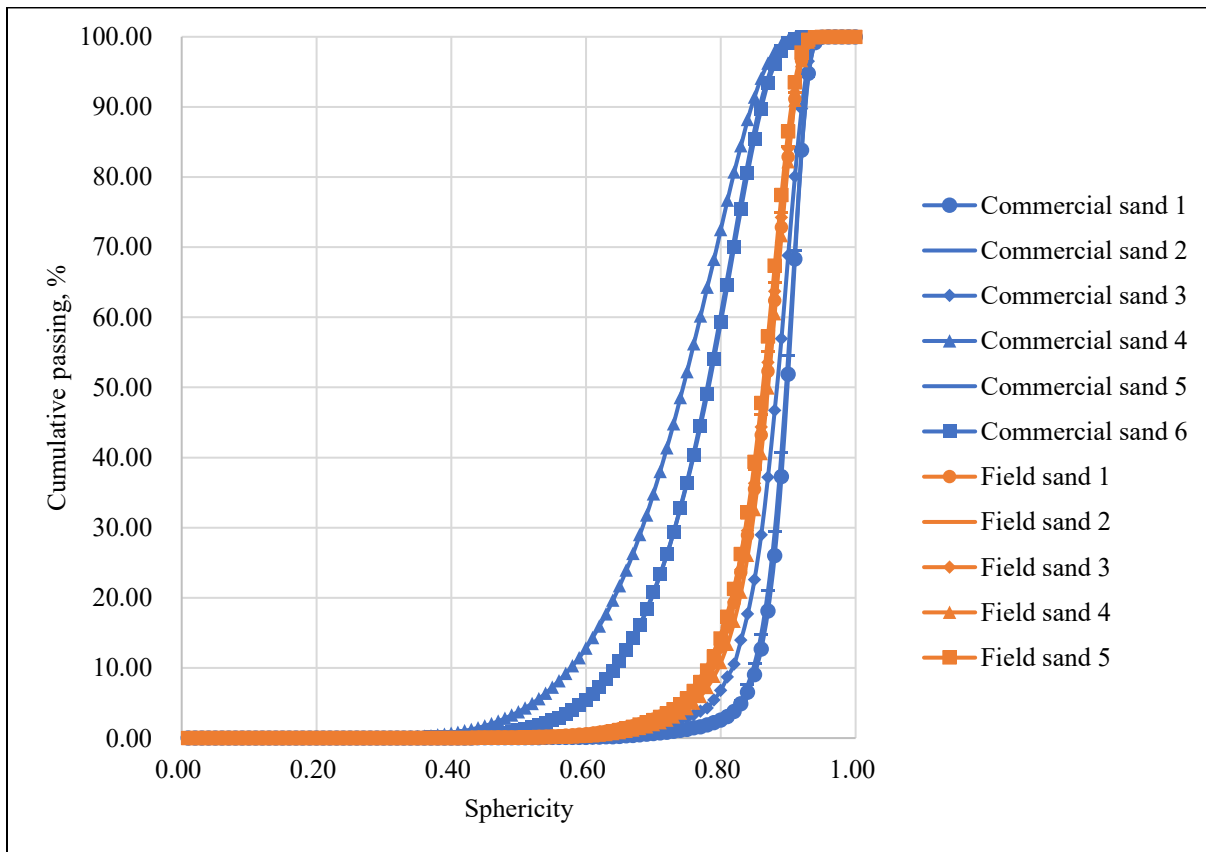


(b)

Figure 3-16. Oil sands and commercial sand convexity (a) and cumulative distribution (b) of convexity with the available commercial sands

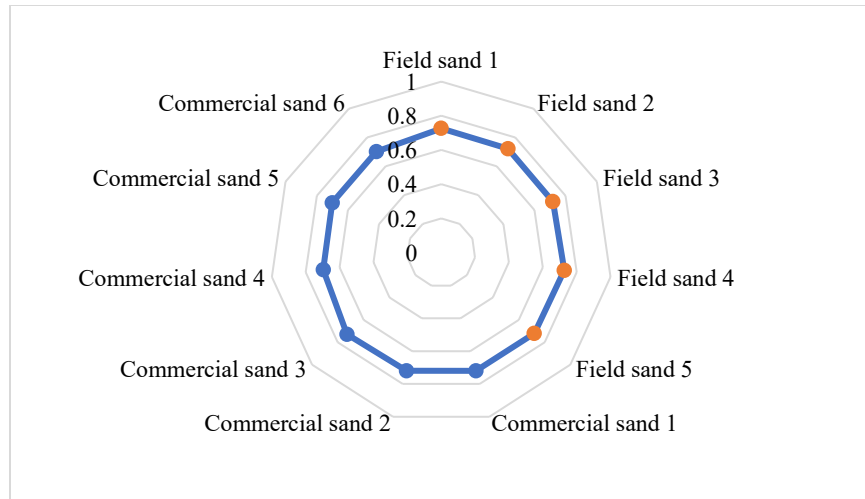


(a)

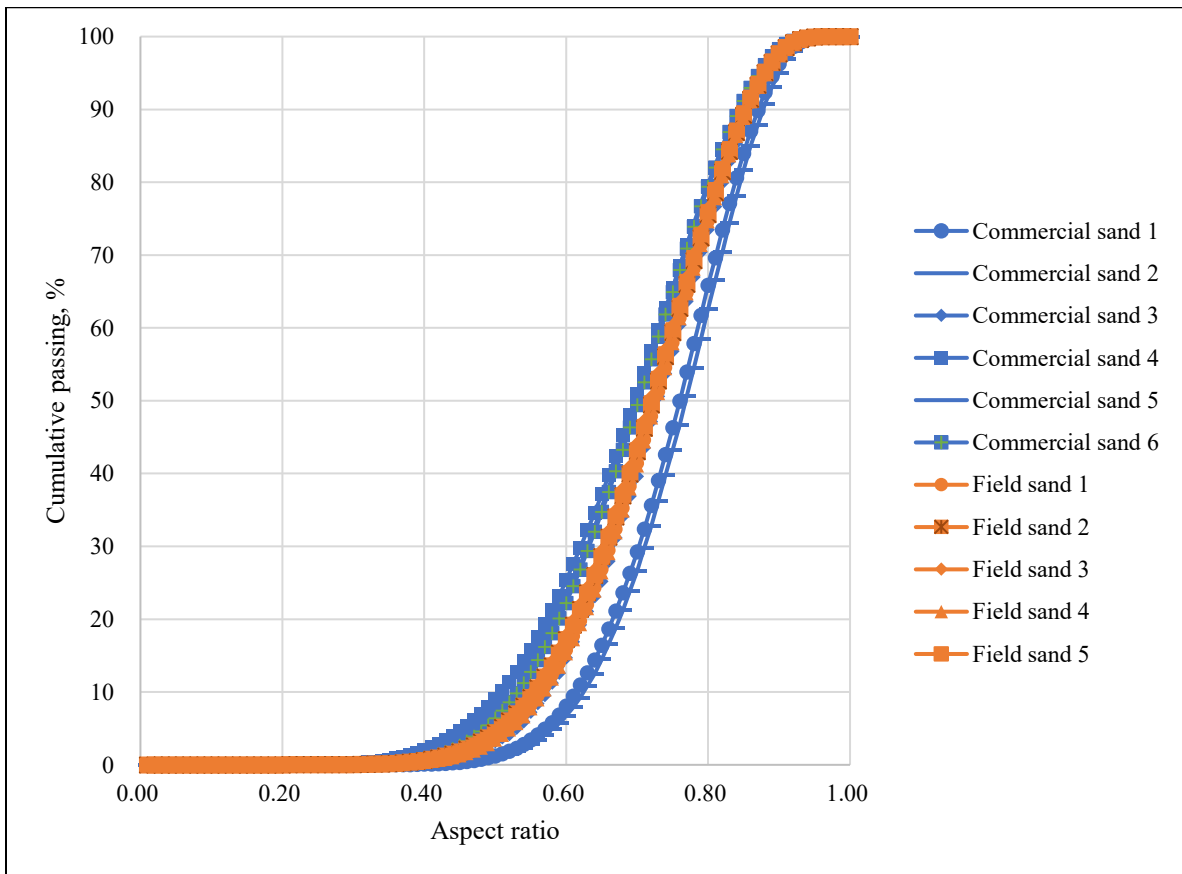


(b)

Figure 3-17. Oil sands and commercial sand sphericity (a) and cumulative distribution (b) of sphericity with the available commercial sands



(a)



(b)

Figure 3-18. Oil sands and commercial sand aspect ratios (a) and cumulative distribution (b) of aspect ratio with the available commercial sands

3.6 Compositional Analysis

Compositional analysis of fines (particles with diameter < 44 μm) is the focus of this section. Fines composition is important because fines migration is affected by parameters such as salinity, pH, and electronegativity of the fines in the matrix (Khilar and Fogler 1998). Since fines migration alters the near-coupon matrix and slot plugging, the composition of the fines must be replicated to allow for representative testing.

3.6.1 Oil sands fines compositional analysis

The oil sands compositional analysis was conducted using a combination of X-Ray Diffraction (XRD), Energy-Dispersive X-Ray Spectroscopy (EDS), and Scanning Electron Microscope (SEM). The combination of these techniques allows a better understanding of the samples of interest and provides more confidence in the results. I should be noted that the XRD interpretation was done by myself through self-learning and not by an experience personnel which may cast some uncertainty on the results.

The XRD was conducted using the Bruker D8 Discover diffraction system, which is equipped with Cu-source and high throughput LynxEYE one-dimensional detector with high intensity and speed compared to point detectors. The XRD analysis was conducted by the Rietveld method using the commercial software TOPAS and Freeware MAUD. The Rietveld method was chosen as it is widely accepted and is the most commonly used technique (Zhou et al. 2018). Rietveld method matches the calibrated crystallographic data to the full pattern response of XRD measurement using least square refinement and thus, quantifying constituent minerals. SEM imaging and EDS measurement were conducted using ZEISS sigma 300 VP SEM. The SEM images were acquired in backscatter mode with the samples not coated.

The results of the XRD analysis of oil sand samples are presented in Table 3-1. Based on the XRD analysis, the primary constituents of the fines are quartz and kaolinite. The results were confirmed by elemental analysis through EDS measurements shown in Figures 3-19 to 3-22. The measurements indicate that silicon, oxygen, and aluminum are the main elements in the oil sand samples. These three elements make up most of the quartz and kaolinite minerals. In addition, SEM analysis was used to confirm the trace mineral presence. Figure 3-23 shows the presence of

calcite, mica, and pyrite in the oil sands samples, which is in line with XRD results and thus, providing more confidence in the results.

Table 3-2. XRD Rietveld analysis results of the oil sands samples

Oil Sand Sample ID	Quartz	Calcite	Pyrite	Kaolinite	Illite	Augite
206	62.9	0.4	0	28.3	2.1	0.6
215	72.6	3.5	0	23.1	1.1	0
219	58.9	3.2	0.4	33.8	3.5	0
221	84.9	7.2	0	6.9	0	0
225	71.6	3.6	0	21.6	3.9	0
Average	70.2	3.6	Traces	22.7	2.1	Traces

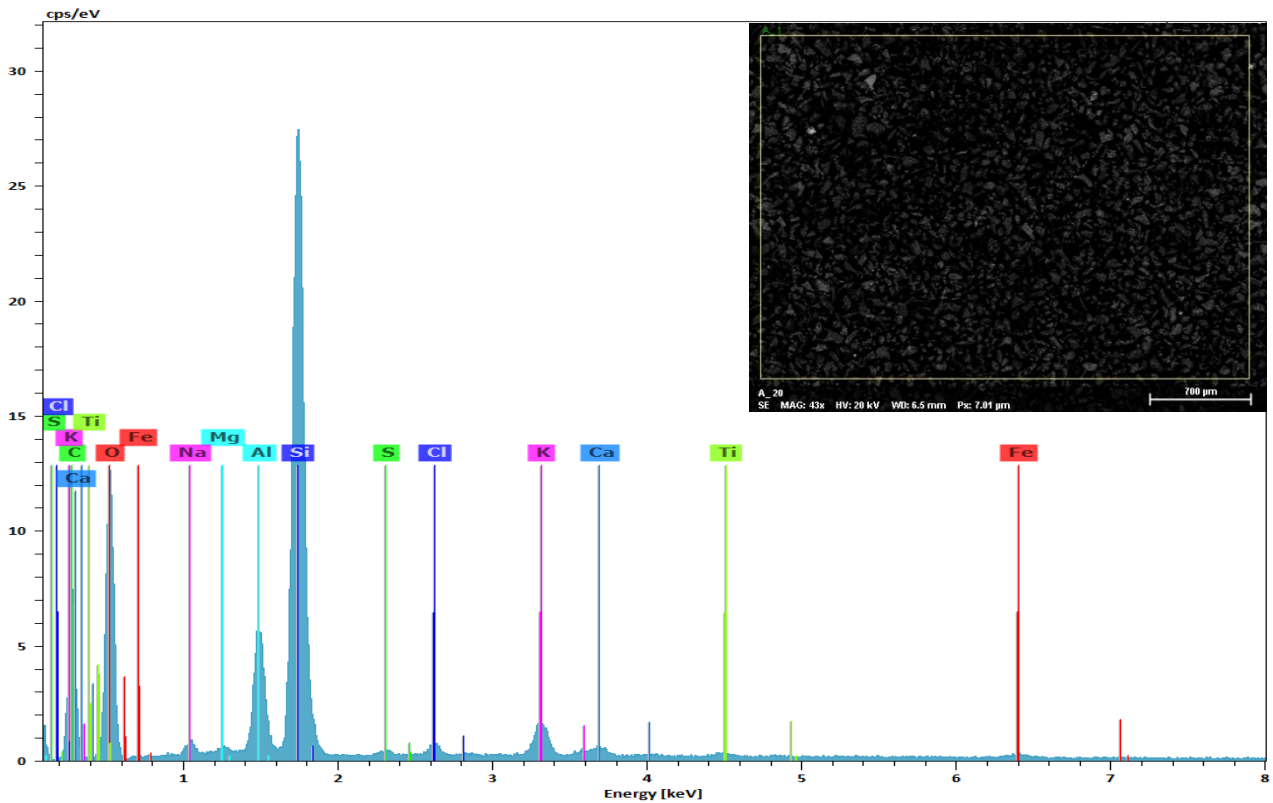


Figure 3-19. SEM image and EDS analysis of oil sands sample at a depth of 225 m

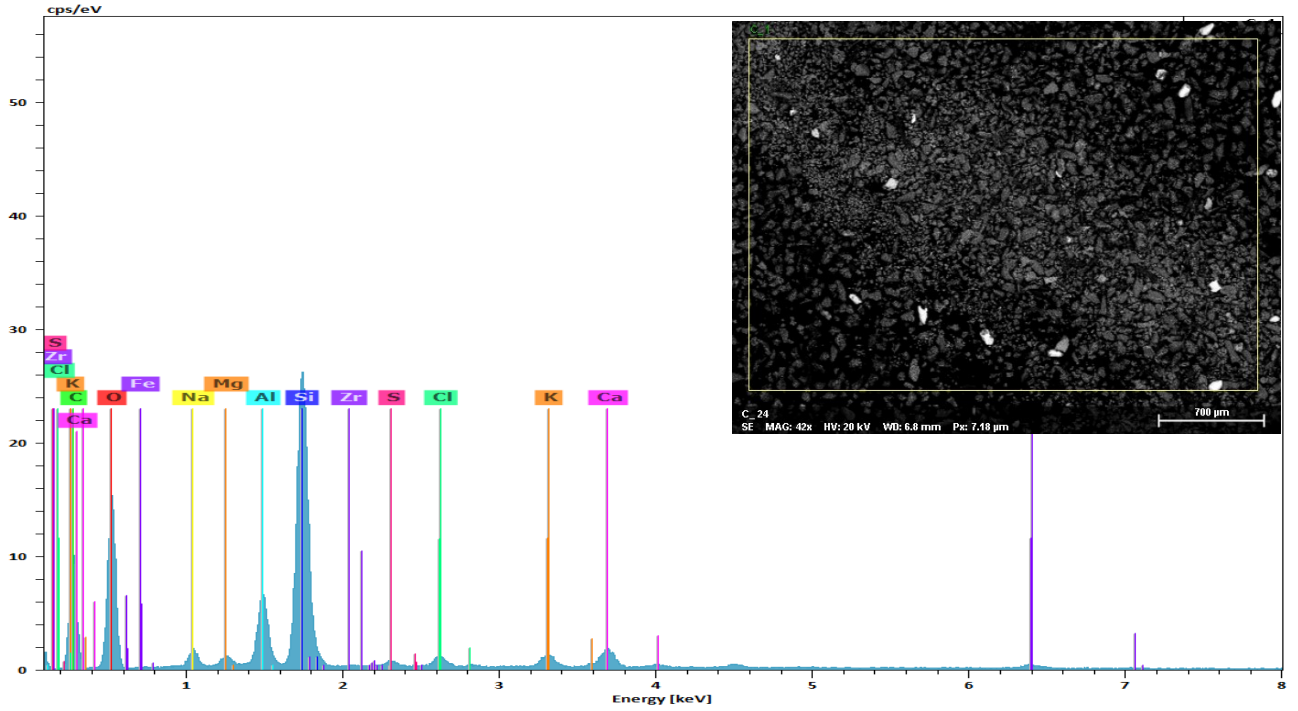


Figure 3-20. SEM image and EDS analysis of oil sands sample at a depth of 215 m

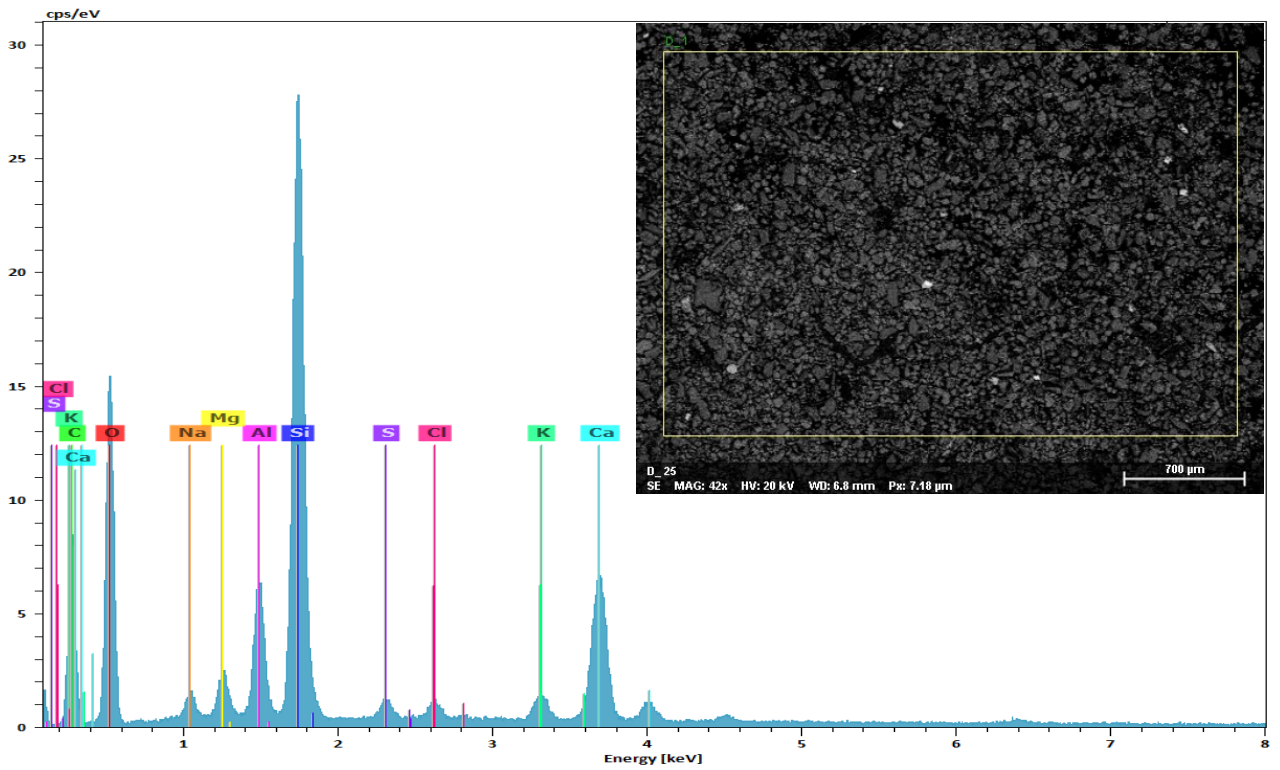


Figure 3-21. SEM image and EDS analysis of oil sands sample at a depth of 219 m

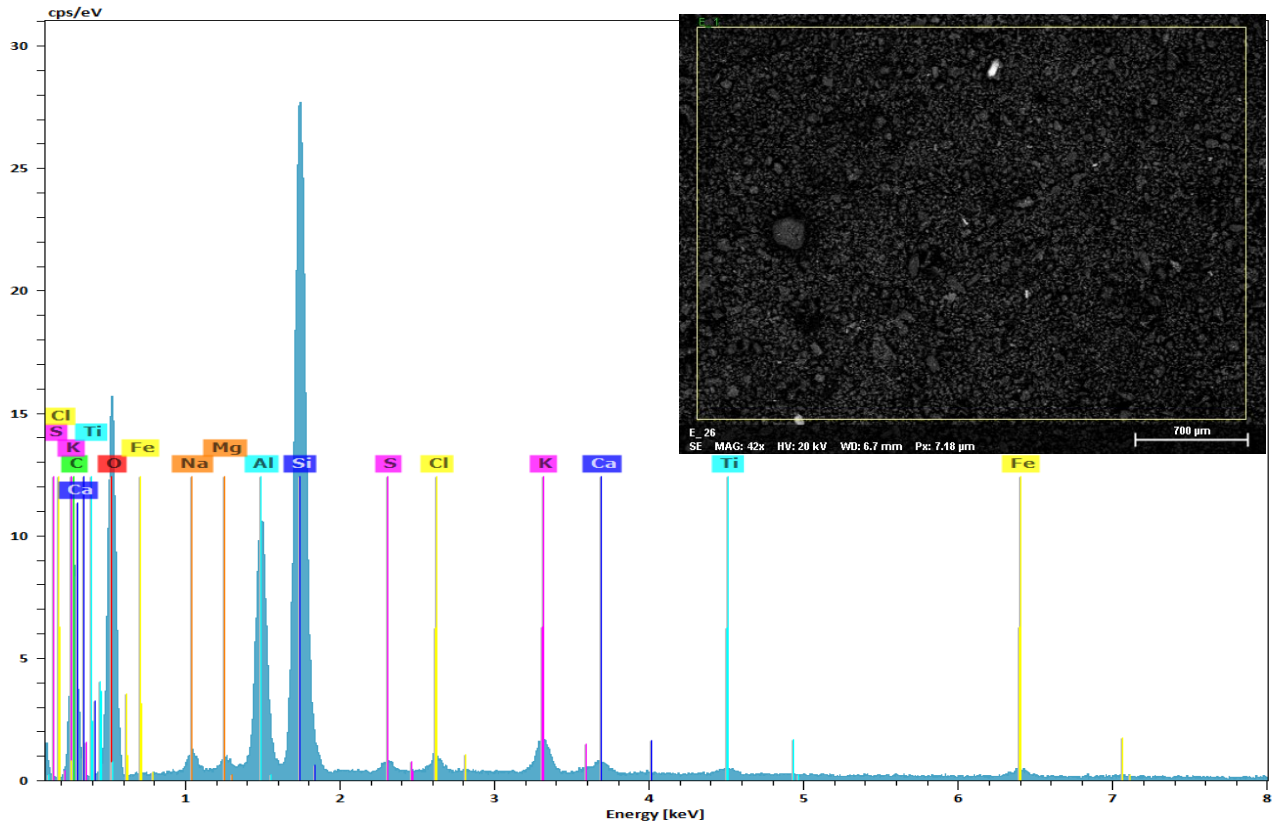


Figure 3-22. SEM image and EDS analysis of oil sands sample at a depth of 206 m

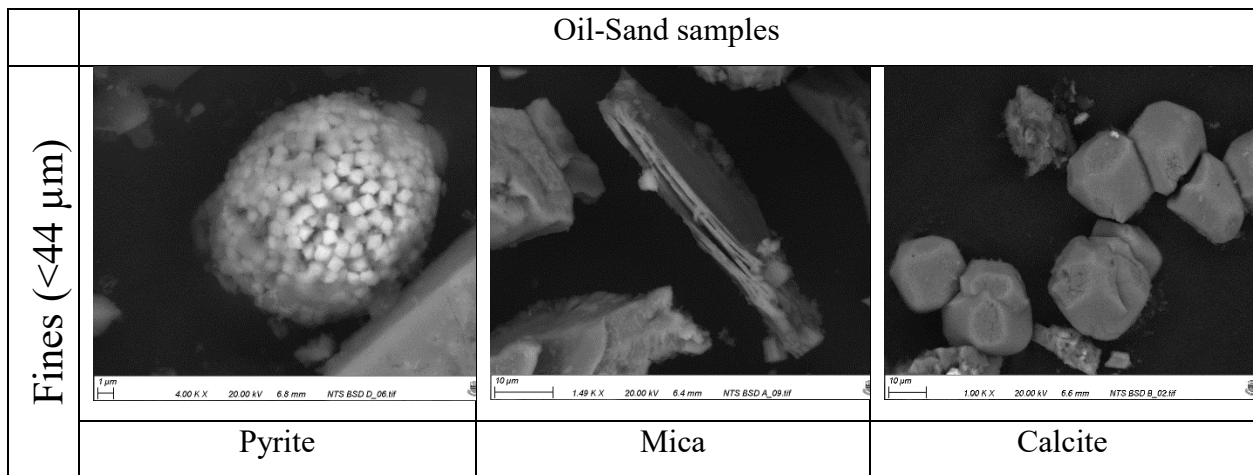


Figure 3-23. Close up SEM images of trace minerals in the fines of oil sands samples

3.6.2 Replication of fines based on compositional analysis

Compositional analysis of four commercial fines (CF1-CF4) was conducted by XRD to identify suitable candidates to be used in replication. The XRD results are presented in Table 3-2. Looking at the results, one can notice that CF2 and CF3 are predominantly quartz and kaolinite, respectively. Since the oil sands samples fines are made up primarily of quartz and kaolinite, a mixture of CF2 and CF3 was chosen to replicate the oil sand fines.

Table 3-3. XRD Rietveld analysis results of the commercial fines samples

Commercial Clay Name	Quartz	Kaolinite	Illite	Anorthite	Muscovite	Calcite
CF1	23.62	73.7	2.3	0	0	0
CF2	95.9	0	0	3.34	0	0
CF3	7.06	81.5	6.5	0	4.1	0
CF4	25	0	0	0	0	72

3.7 Conclusion

In this chapter, characterization of the PSD, grains shape, and mineral composition of commercial and field samples from the McMurray Formation were conducted and compared. In addition, a new methodology for replicating the field samples based on PSD, size, and mineral composition using commercial sands was implemented. Characterization of grains shape by DIA helped in eliminating the commercial sands with shapes incompatible with the formation sands. The recipe for commercial sand mix to replicate Batch 3 used by Hycal labs will be as follows:

Commercial Sand or Clay	Weight. %
CS1	52.9
CS2	43.6
CF2	2.58
CF3	0.92

Chapter 4: Experimental Setup and Testing Procedure

4.1 Introduction

A representative, economical, and practically feasible experimental setup and procedure is pivotal in recreating and capturing the sand production phenomenon under SAGD multiphase flow conditions. This chapter will focus on the design of the main components of the experimental setup and testing procedures. Justifications will be provided as to why the testing components are suitable to stimulate the near-wellbore conditions resulting in sand production and slot plugging of sand control devices in SAGD multiphase flow conditions.

4.2 Experimental Setup

The SRT setup is made up of six major units as shown in Figure 4-1, namely: (1) sand-pack and SCD holder, (2) fluid injection unit, (3) load frame, (4) data acquisition and monitoring unit, (5) sand and fines production measurement unit, and (6) Back-pressure unit. The following sections provide further details on the testing setup.

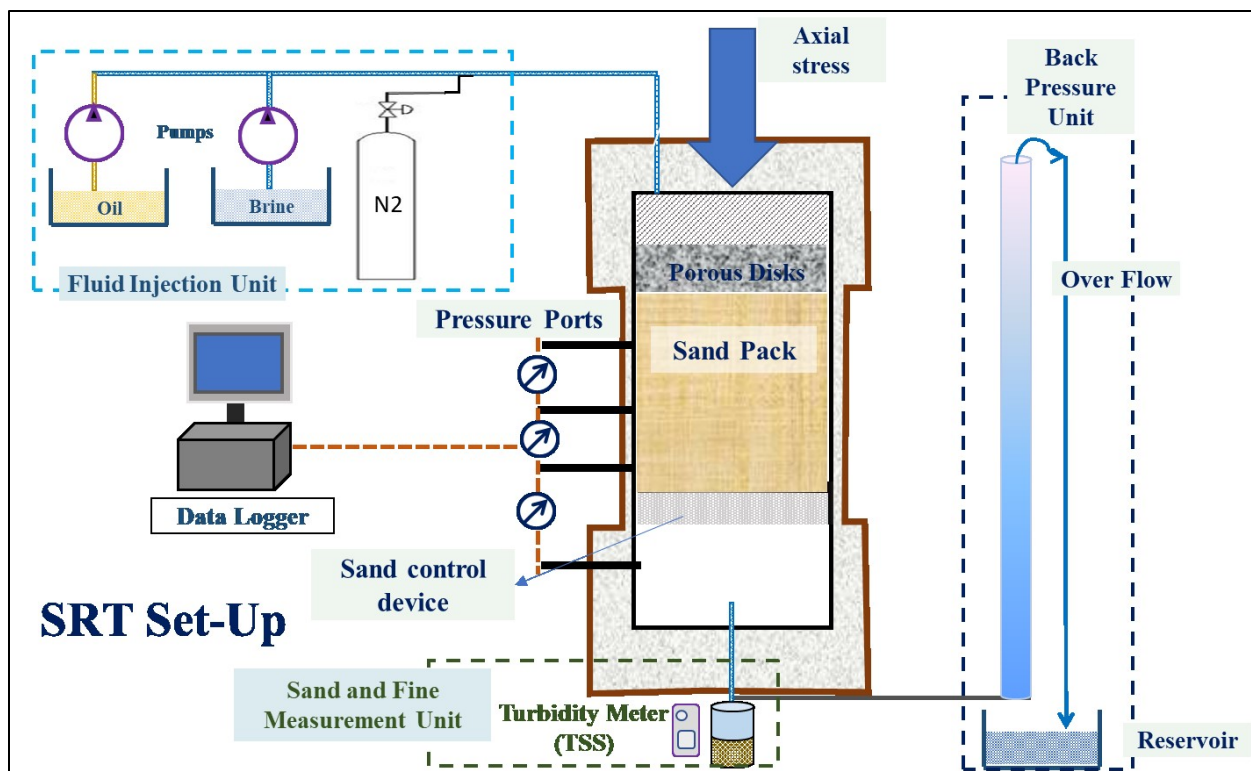


Figure 4-1. Schematic of the SRT setup

4.2.1 Fluid injection unit

The fluid injection unit consists of two mechanically actuated triplex diaphragm pumps manufactured by LEWA. Both pumps are capable of injecting brine and mineral oil at rates up to 18 liters per hour with an adjustment range of 1:50 and flow rate adjustment of $\pm 1\%$. The flow rate output is controlled by adjusting the stroke length manually in combination with adjusting the pump frequency through a variable frequency drive (VFD). The triplex design coupled with a pulse damper allows pulsation free fluid flow into the cell.

Before testing, each pump is calibrated so that appropriate setting can be chosen to achieve the desired rate. During testing, the flow rates are measured and verified by a mass balance reading at each flow rate change for test quality control purposes. The pumps are fed using two 25-liter tanks positioned above the pumps. The discharge of the core holder is not recirculated back as it may contain fines and thus, is disposed off based on the University of Alberta regulations.

Gas is delivered through nitrogen-filled high-pressure tank connected to a pressure regulator and gas rotameter with a choke. Three rotameters with different ranges are used in parallel to output the desired rate of gas to the cell. The low-rate rotameter has a range from 30 up to 300 cm³/min. The intermediate rate rotameter has a range from 200 up to 5000 cm³/min while the high rate rotameter has a range from 500 up to 10,000 cm³/min. All the rotameters are manufactured by Omega and have an accuracy of $\pm 2\%$ of full-scale accuracy. During testing, the upstream pressure is kept at 551 kPa (80 psi) as the downstream cell pressure during testing is never above 138 kPa (20 psi). This ensures critical flow for nitrogen since the downstream/upstream pressure ratio below 0.53 (Green 2008). Using critical flow minimizes rate variations resulting from downstream pressure variations.

4.2.2 Sand-pack cell and SCD holder

The SRT cell is composed of a core-holder, top platen, and base plate. The core holder is where the sand is packed and is made of aluminum with a burst pressure rating up to 690 kPa (100 psi) at 20 °C. The inner diameter of the core-holder is 17.1 cm with a length of 47 cm.

The larger cell compared to Hycal's cell allows the proper investigation of SL coupons with different slot densities. Larger cell sizes allow a closer representation of the field conditions but have to be limited due to the size of the setup, materials availability, test operation, and cost.

Along the walls of the core holder, there are three 0.635 cm (0.25 inch) NPT connection ports on the sides of the cell at 5 cm, 17.7 cm, and 30.4 cm from the bottom of the core holder, which allows for differential pressure measurement across the sand-pack. The first bottom ports from the sand control coupon are used to capture the pressure loss due to flow convergence, slot plugging, and fine migration. The second and third ports serve two purposes. The first is that they allow quality control to be performed on the packing technique and the second is for capturing pressure loss due to fines migration.

The base plate is a 5-cm aluminum slab cut out in the middle to allow easy interchangeability of the sand control liner coupons. A Viton gasket is used to seal the area between the core-holder and the base plate hydraulically. The top platen is used to transfer loads from the load frame to the sand-pack and hydraulically seal the core holder from the top using O-rings. In conjunction with a porous disk, the top platen provides the conduit for fluid injection, mixing, and distribution into the sand-pack.

4.2.3 Load frame

Stress is created in the sand-pack by applying force through the load frame on the top platen. The load frame can generate a maximum force output of 8 metric tonnes. The hydraulic system of the load frame was modified by reconnecting the pressure supply of the hydraulic oil to an ISCO pump, instead of a hand pump, to ensure a constant stress level during the test.

4.2.4 Data acquisition and monitoring unit

The data acquisition and monitoring system include three Yokogawa EJA110A differential transducers with a maximum range of 100 kPa (14.4 psi) and accuracy of $\pm 0.022\%$ of the full range. The transducers are connected to the National Instruments data acquisition system Model USB-6002 and recorded using National instruments Data Acquisition (DAQ) express software. Further, a camera is installed below the coupon that allows monitoring of the sand production at every stage of testing.

4.2.5 Sand and fines production measurement unit

The sand and fines production quantification unit consists of a sand trap that is specifically designed to retain the produced sands and fines. The sand trap is a flanged cylinder with a blind

flange at the bottom to allow collecting the produced sand. The sand trap has a 0.635 cm (0.25-inch) NPT connection and a ball valve, which has a tube that reaches just below the coupon slots. The unit allows the collection of fluids in 100-ml sample bottles to measure the mass of produced fines. The produced fines are quantified using a turbidity meter, which is calibrated using standard bottles of known fines concentrations. The relation between turbidity meter readings and fines concentration is linear. The total produced fines per stage are calculated by multiplying the concentration of produced fines per stage by the fluid volume produced per stage.

4.2.6 Backpressure unit

The back-pressure unit consists of a 185-centimeter pipe with a diameter of 5 cm. Its primary purpose is to ensure the full liquid saturation of the cell throughout the test, except when gas is injected. Moreover, the unit allows a small flow of brine during the saturation phase so to minimize the channeling and fingering phenomena.

4.3 Testing Material and Components

4.3.1 Representative sand

Hycal Batch 2 & 3 sand was replicated based on the PSD, shape factors, and fines mineralogy. Further details are found in Chapter 3. The suitability of the using the replication process for sand retention testing will be investigated by comparing an original replication test.

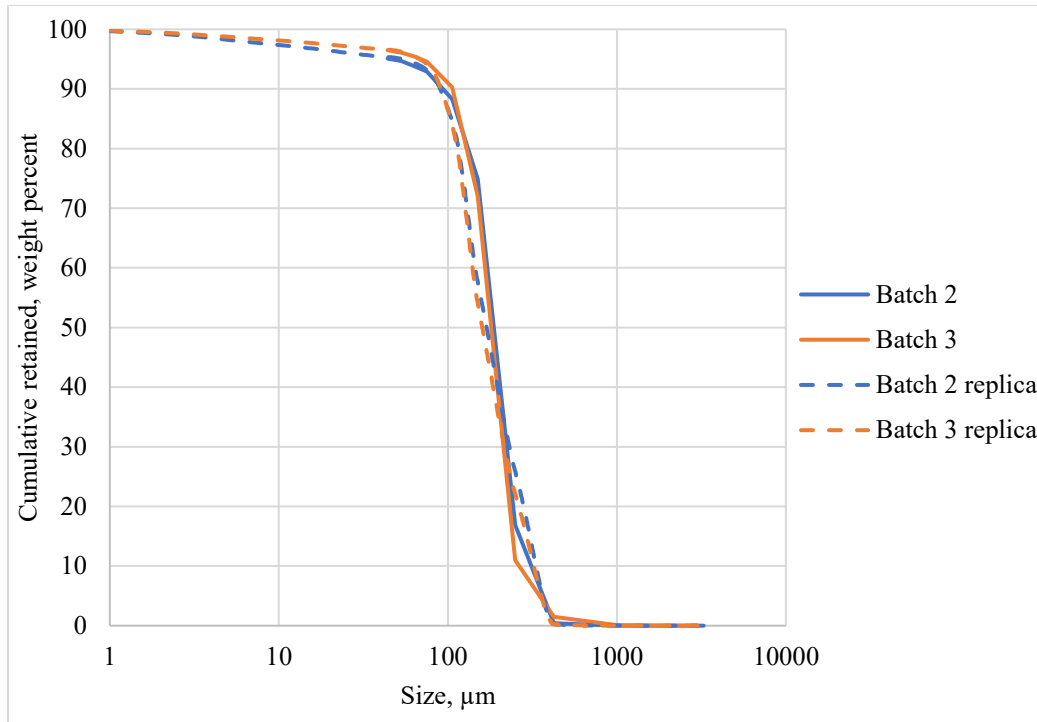


Figure 4-2. Target sand (Batch 2 & 3 of Hycal testing) and the sand replica

4.3.2 Representative fluids

Brine

In a SAGD reservoir, formation water mixes continuously with condensed water, and flows towards the SCD in the producer well. This mixing reduces the salinity of the produced water over time from an initial formation salinity ranging from less than 4000 -100,000 ppm (Cowie 2013) to around 1500- 5000 ppm at the producer (Peterson 2007). Also, initially acidic gases such as carbon dioxide, hydrogen sulfide, and methane reduce the pH of the formation waters. However, as condensed steam mixes with formation water, the pH increases to become slightly alkaline (Bennion et al. 2008).

Brine salinity and pH have significant impacts on the clay mobilization in porous media (Khilar and Fogler 1998; Mahmoudi 2016). Brine used in Hycal tests had a salinity of 10,000 ppm by adding sodium chloride to deionized water. However, the measured composition in Table 4.1 indicates this level of salinity does not represent the reservoir of interest. Figure 4-3 is a STIFF diagram that compares the brine composition from the analysis of field produced water and the

brine employed in sand control testing by Hycal. The figure shows that Hycal brine cations and anions are not representative of the well-produced brine composition.

In this investigation, field water compositional analysis provided by the operator is used to recreate field representative testing brine (Table 4.1). The representative brine was achieved by matching the total cation concentrations of the field brine sample with sodium bicarbonate. Only the cation concentration was matched since cations are the ions predominantly affecting clay deflocculating phenomena (Khilar and Fogler 1998). In other words, only cations influence fines migration and thus, pore and slot plugging.

Table 4-1. Ionic composition of brine in field and lab

Description		Unit	Field Sample *	Hycal Brine Composition
pH		-	8.04	Not known
Cations	Sodium (Na)	mg/L	194	3935
	Potassium (K)	mg/L	3.6	-
	Calcium (Ca)	mg/L	56.7	-
	Magnesium (Mg)	mg/L	21.4	-
Anions	Bicarbonate (HCO ₃)	mg/L	708	-
	Carbonate (CO ₃)	mg/L	0.5	-
	Hydroxide (OH)	mg/L	0.5	-
	Chloride (Cl)	mg/L	40.4	6065
	Sulfate (SO ₄)	mg/L	46.1	-

* Data Provided by Nexen CNOOC

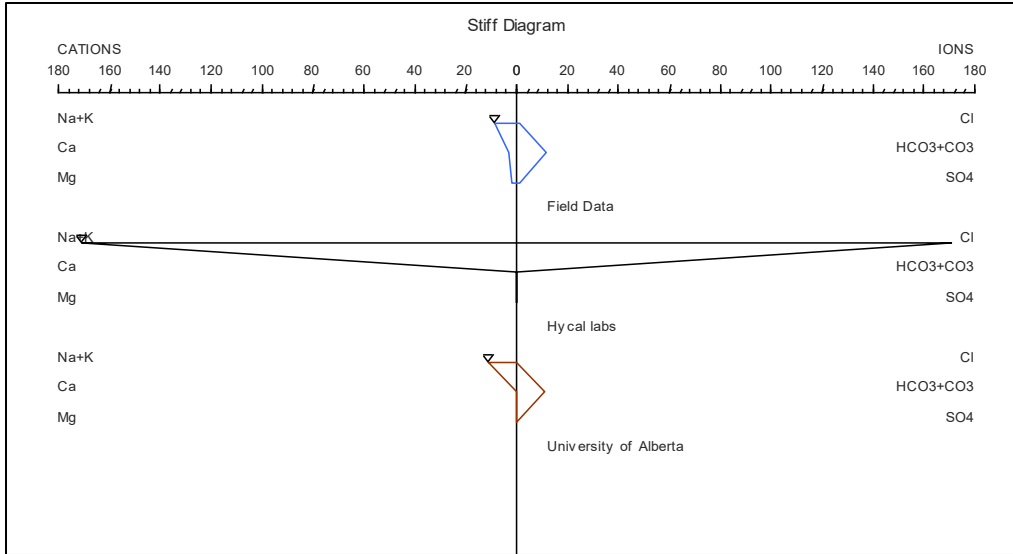


Figure 4-3. STIFF diagram comparing field samples to brine used to testing by Hycal labs and University of Alberta

Oil

Bitumen viscosity exponentially decreases with increasing temperatures. Figure 4-4 depicts the viscosity reduction of two oil samples from the field of interest. The operating temperature of a SAGD well ranges from 150 °C to 270 °C (Irani 2013). Since this setup is not capable of operating under high temperatures and pressures, mineral oil with a viscosity of 15 cp was used to match the drag force on sand grains caused by oil production.

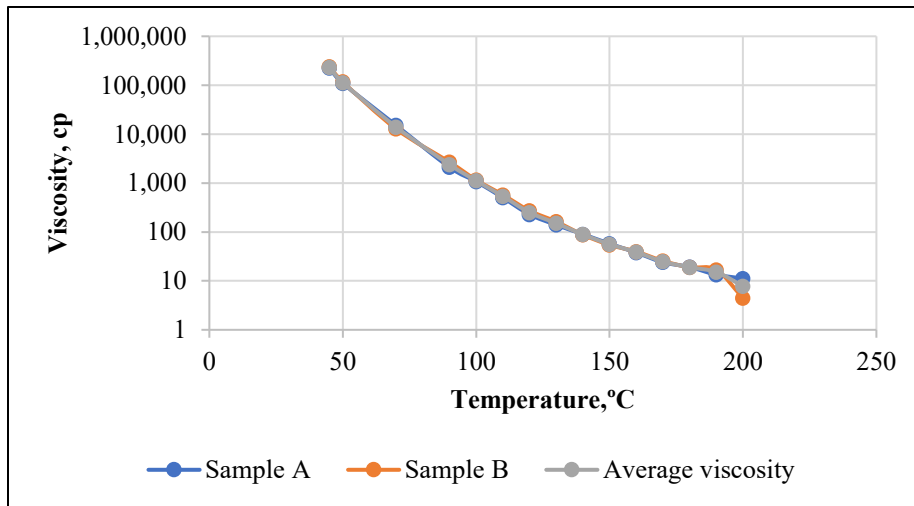


Figure 4-4. Measured oil viscosity for Long Lake field as a function of temperature

Gas

In a SAGD production well, a steam breakthrough can occur due to a low sub-cool (Gates and Leskiw 2010), which can result in sand production (Mahmoudi et al. 2018). Therefore, simulating steam breakthrough in the testing is essential to evaluate sand control devices under SAGD conditions. However, due to practical and safety concerns, testing with steam was not feasible with the current core-holder. Steam viscosity in a typical SAGD production well operating conditions at temperatures and pressures between 190 to 210 °C and 1600 to 1800 kPa, respectively, would be approximately 0.016 cp. Since nitrogen, at room temperature and pressure, has a viscosity of 0.0176 cp, it was chosen to simulate the drag force on sand grains by the steam breakthrough.

4.3.3 Liner coupons

The sand control liner coupons used in the experiments are actual cut-outs of manufactured liners acquired from RGL Reservoir Management as shown in Figure 4-5. Testing using multi-slot coupons allows capturing the inter-slot interactions, which was a significant limitation with pre-pack SRTs reported in the literature.

The replication test in this research was conducted using a 152 μm (0.006-inch) WWS as was used by Hycal. The WWS was chosen for replication instead of a slotted liner as all Hycal slotted liner SRTs employed single-slot liners, making the test difficult to replicate with a larger setup as the open-to-flow-area ratio cannot be matched. Following the replication test, all the tests were performed using the 406-508 μm (0.016-0.020-inch) rolled top slotted liner as installed in the field of interest. Figure 4-6 shows an image and schematic cross-sectional view of the coupons used in the testing.

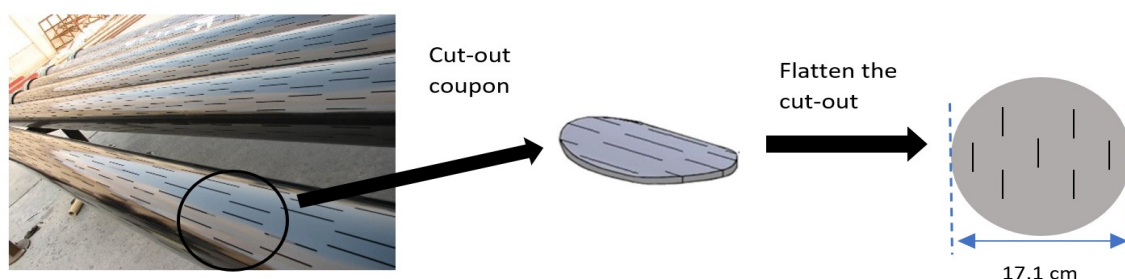


Figure 4-5. Multi-slot coupon as a cut-out of a slotted liner

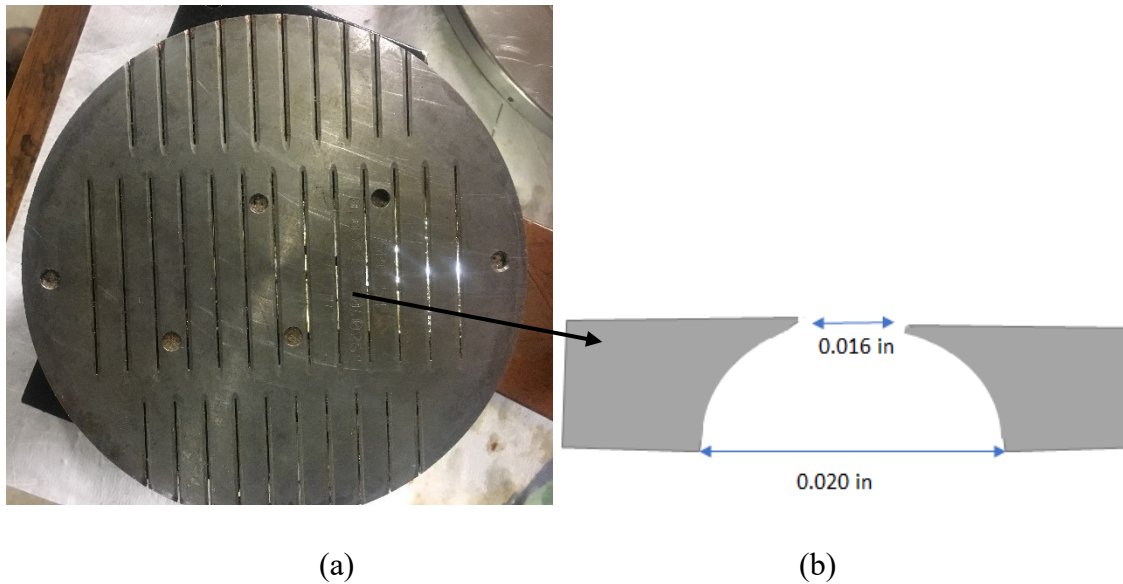


Figure 4-6. (a) An image of a multi-slot 0.016-to-0.020 coupon, (b) schematic cross section of a rolled top slot

4.4 Testing Plan

The objective of the work is to assess the effect of varying experimental parameters and procedures of prepack SRT on sand and fines production under multiphase flow conditions. Therefore, the work will start by attempting to replicate Hycal testing procedure for sand control testing under multiphase conditions, as introduced in Chapter 2. Subsequently, one testing parameter at a time will be changed to investigate its effect on test results until an improved procedure is achieved. The testing plan is presented in Table 4-2.

Table 4-2. Test matrix

Test #	Coupon	Flow rates			Packing	Water composition	Stress	Objective
		Water	Oil	N ₂				
1	WWS 152 μm	Hycal rates	Hycal rates	Hycal rates	Dry packing	1% NaCl	2413 kPa (350 psi)	Replication
2	Multi-slot Rolled top OFA 2.33%, 406 μm	Hycal rates	Hycal rates	Hycal rates	Dry packing	1% NaCl	2413 kPa (350 psi)	The base case for SL testing
3	Multi-slot Rolled top OFA 2.33%, 406 μm	Hycal rates	Hycal rates	Hycal rates	Moist Tamping	1% NaCl	2413 kPa (350 psi)	Effect of the packing procedure
4	Multi-slot Rolled top OFA 2.33%, 406 μm	Hycal rates	Hycal rates	Hycal rates	Moist Tamping	1% NaCl	413 kPa (60 psi)	Effect of stress
5	Multi slot Rolled top OFA 2.33%, 406 μm	Rep. rates	Rep. rates	Rep. rates	Moist Tamping	1% NaCl	413 kPa (60 psi)	Effect of flow rates
6	Multi-slot Rolled top OFA 2.33%, 406 μm	Hycal rates	Hycal rates	Rep. rates	Moist Tamping	Rep. ions	413 kPa (60 psi)	Effect of water composition

4.5.2 Sand-pack packing

If the dry packing technique of Hycal is used in the test, the dry mix is poured into the core-holder using a funnel so that the final height of the sand-pack is 40 cm. Next, the mix is compacted by applying 2413 kPa (350 psi) of axial stress. However, packing in this manner can result in undesired effects. Packing the sand column in one attempt results in non-uniform stress along the sand column. This effect is caused by the friction between the sand and the core holder. The second

deficiency is the likely segregation of particles along the core of the sample where the finer particles will settle at the bottom and the coarser at the top by percolation of fine particles or vice versa due to elutriation segregation (Rhodes 2008). Also, applying high levels of stress on sand can produce excess fines due to crushing, especially for angular sands (Wang and Coop 2016). However, dry sands show more resistance to crushing due to the decreased pack compressibility compared to wet sand (Ovalle et al. 2014).

For the moist tamping technique, the sand-pack is prepared by packing twelve layers using a modified version of the moist tamping technique presented by Mahmoudi (2016). The packing technique for the mix used in the testing program resulted in a sand-pack of 40-cm height, a diameter of 17.1 cm, and a porosity of 35%.

The modified version of the moist tamping technique involves preparing 3.3 cm layers using a certain amount (mass) of the mix. Next is compacting each layer uniformly so that each packed layer has equal height and, thus, equal porosity. The compaction is done using a packing rod designed to achieve uniform compaction. Each layer's weight is around 935 g and is predetermined based on the target porosity and sand mixture grain density. Packing with wetted sand layer by layer should help achieve a uniform porosity and permeability (Ladd 1978).

4.5.3 Sand-pack saturation

In both Hycal and proposed procedures, the sand-pack was saturated by injecting brine from the bottom of the core holder through the coupon into the sand-pack. Hycal did not specify the flow rates they used for saturation. In the proposed procedure, the fluid flow rate was chosen at a practical rate of 1000 cm³/hr. Once one liter of brine is produced from the top, the sand-pack is assumed fully-saturated. Stress levels applied over the sand-pack during the saturation were adapted to ensure no fluidization will occur. Details of calculation of the stress required to prevent fluidization are in Appendix A

4.5.4. Representative stress conditions

Stress has been proven to reduce sand production due to increased inter-particle friction forces (Guo 2018). In lab testing, it is desired to simulate worst-case scenarios for liner design and selection purposes. In a SAGD well, low-stress conditions are expected in the early well life (Penberthy and Shaughnessy 1992; Fattahpour et al. 2016). Therefore, to simulate the early SAGD

well conditions, a low value of stress is applied to the sand-pack. The amount of axial stress around a collapsed horizontal slotted liner has been simulated to be less than 555 KPa (80 psi) (Diaz 2008). An amount of 414 kPa (60 psi) was concluded to be a reasonable value, with the details of the stress calculation given in Appendix A. The stress value was calculated based on the Eugen fluidization theory that allows estimation of the minimum stress required to prevent fluidization in a sand-pack and be representative of early SAGD stress conditions.

4.5.5 Fluid injection rates

Fluid injection is the primary component of the test in which brine, oil, and gas are injected in a step-rate manner downward through the sand-pack and toward the multi-slot coupon. A porous disc is placed on the top of the sand-pack to provide a uniform fluid injection during the test. Each fluid rate was varied depending on whether the test was conducted by Hycal- based rates or the new rate-setting methodology. During the injection stages, the pressure differential is continuously monitored at different sand-pack locations to evaluate fines migration and flow convergence. The produced fluids are sampled at each stage to quantify fines migrated and produced.

Hycal rates

Hycal labs used brine, oil, and nitrogen flow rates as shown in Figure 4-7. The Hycal fluid flow rates were scaled up according to the coupon size ratio for the replication tests since the coupon size in the Hycal and University setups are different. The upscaled rates as calculated using Eq. 4.1 are shown in Figure 4-8.

$$Q_{UofA} = Q_{Hycal} \times \frac{Area_{UofA}}{Area_{Hycal}} \quad (4.1)$$

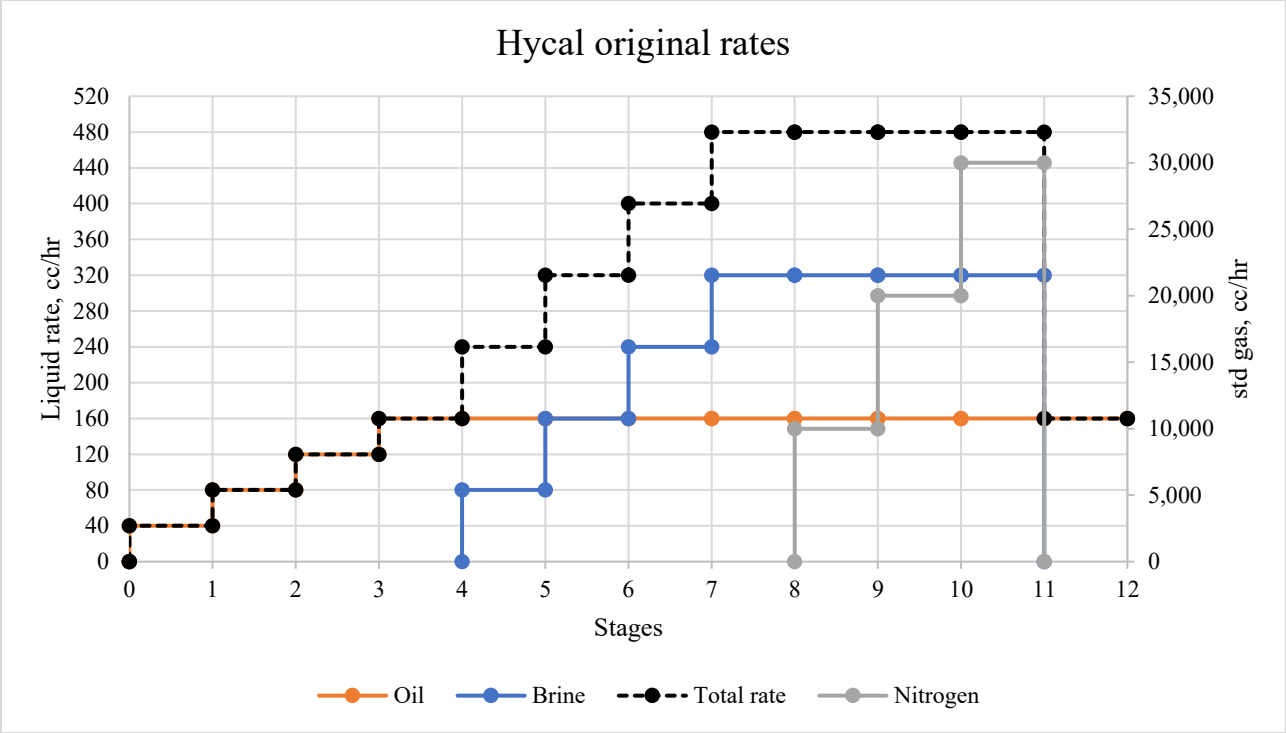


Figure 4-7. Hycal original rates used with their setup

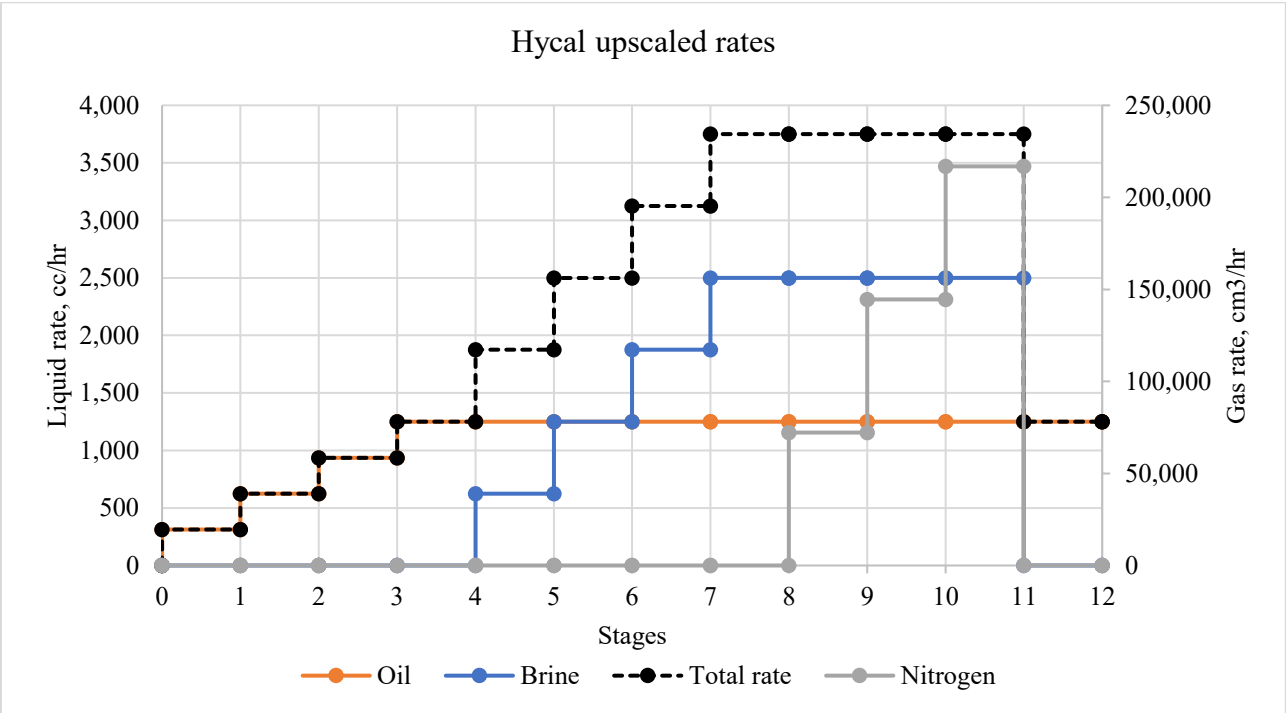


Figure 4-8. Hycal upscaled rates used with the University of Alberta setup

University rates

The rates used at the University of Alberta do not match those of Hycal. First, the order of phase injection was rearranged so that the water phase is injected first before the two-phase flow regime. This practice allows the measurement of absolute permeability at the beginning of each test. Hence, it enables the verification of the sand packing consistency among the tests. Also, the rates for each phase were revised based on typical field production rates for each phase.

The new flow rate-setting methodology is summarized in Figures 4-9 to 4-12. The actual wellbore production rates provided by Nexen CNOOC is scaled down from the total wellbore liner surface area to the coupon area. In other words, the tests match the target field fluids flux. Several effective flow factors are used to account for the potential flow non-uniformity along the wells, slot plugging, and blank liner segments.

Figure 4-9 illustrates schematically how variations of sub-cool in a SAGD well can result in fluid flow variations along the well. The non-uniformity of production along the wellbore could stem from multiple reasons including non-uniform steam chamber growth due to reservoir heterogeneity (Ravalec et al. 2009), the absence of flow control devices (Stone and Bailey 2014), and undulations in wellbore trajectory (Sidahmed 2018). In a case study presented by Beshry et al. (2006), 50% of the non-uniformity in a SAGD production well reached 50%

The calculated flux also accounts for the liner segments not contributing to production due to blank pipes and packers and tubing connections (Figure 4-10). Based on communication with RGL engineers, a value of 20% was considered for the non-contributing length of the completion.

Plugging of slots during the SAGD well life must also be considered when setting the effective flow factor. Plugging of sand control devices can be a result of scale deposition (Brand 2010), corrosion products, and fouling by fines deposition (Romanova and Ma 2013). These factors can cause plugging that can reach as many as 90% of the slots.

For representing two-phase flow, water-cuts ranging from 50% to 100% were chosen as the values representing typical SAGD water-cuts which are around 75% (Anderson 2017) up to 90% (Nexen CNOOC 2017). The water-cut values for the University testing practice are higher than Hycal levels ranging from 0% to 67%. The water-cut influences the capillary pressure in the near-liner

region. High water saturations decrease the capillary pressure and the bonding between the sand particles, resulting in higher sand production (Han and Dusseault 2002; Vaziri et al. 2002).

Table 4-3 contains the effective flow factors for different potential scenarios for the testing rate calculations. The approaches for calculating the test liquid injection rates and gas injection rates for steam breakthrough simulation are presented in Figure 4-11 and 4-12. Figure 4-13 presents the University rates for the sand control tests. Details of the flow rate calculations are presented in Appendix B.

Table 4-3. Effective flow factors to calculate testing flow rates

Effective flow factor calculation				
Scenarios	Non-uniform effect	Plugging factor	Non-contributing liner sections	Effective flow
Favorable conditions scenario	0.8	0.5	0.8	0.32
Non-uniform flow scenario	0.5	0.5	0.8	0.2
Plugged and non-uniform flow scenario	0.5	0.3	0.8	0.12

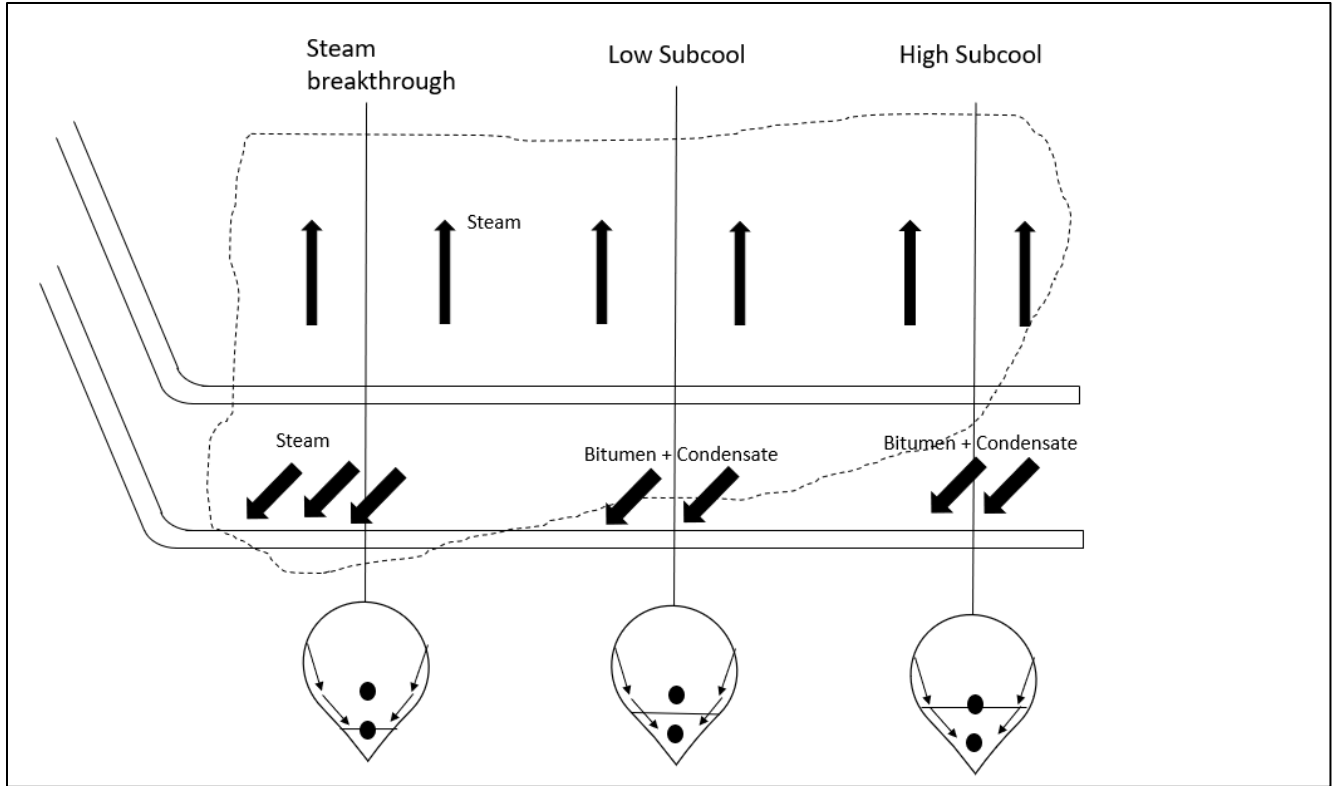


Figure 4-9. Schematic view to illustrate how variations of sub-cool in a SAGD well can result in fluid flow variations along the length of the well

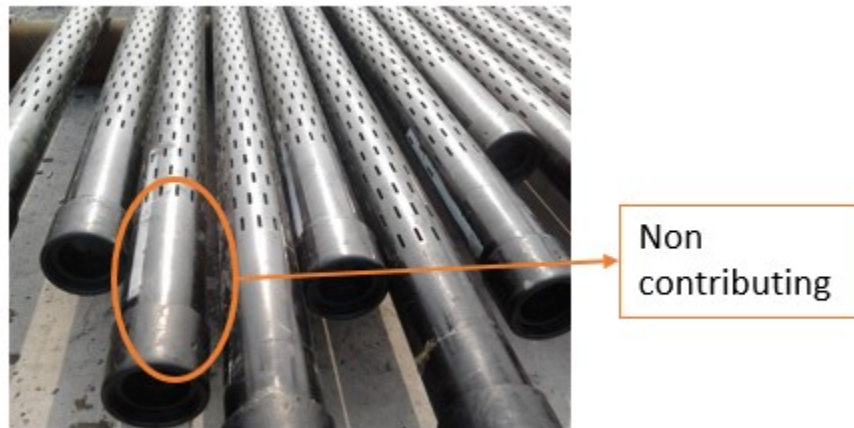


Figure 4-10. Non-contributing sections of a slotted liner

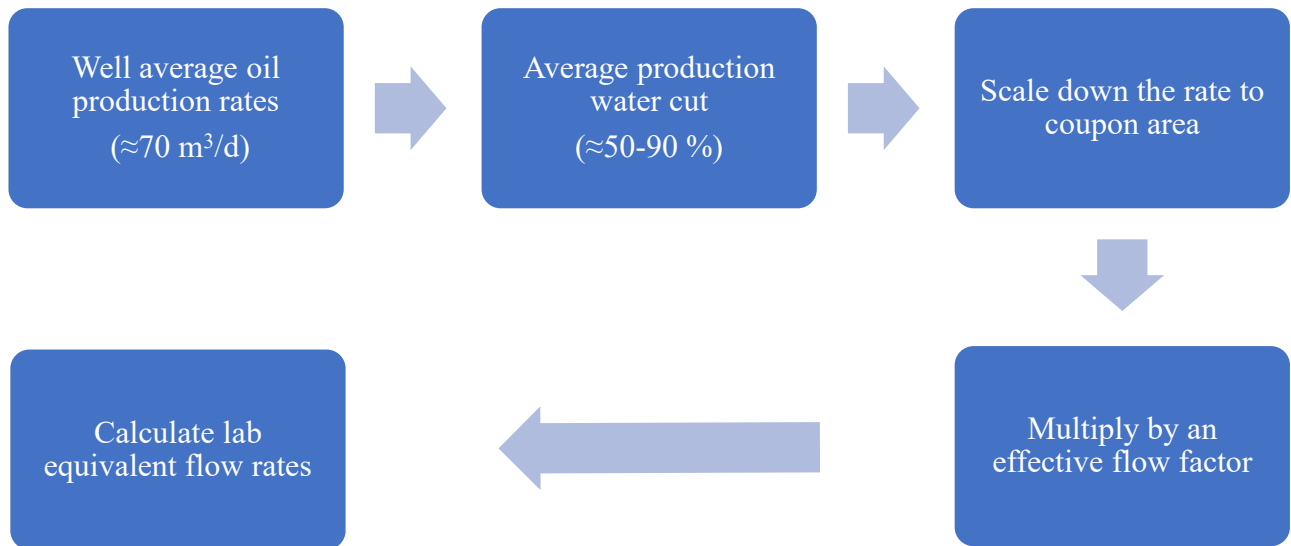


Figure 4-11. The methodology for setting representative liquid flow rates

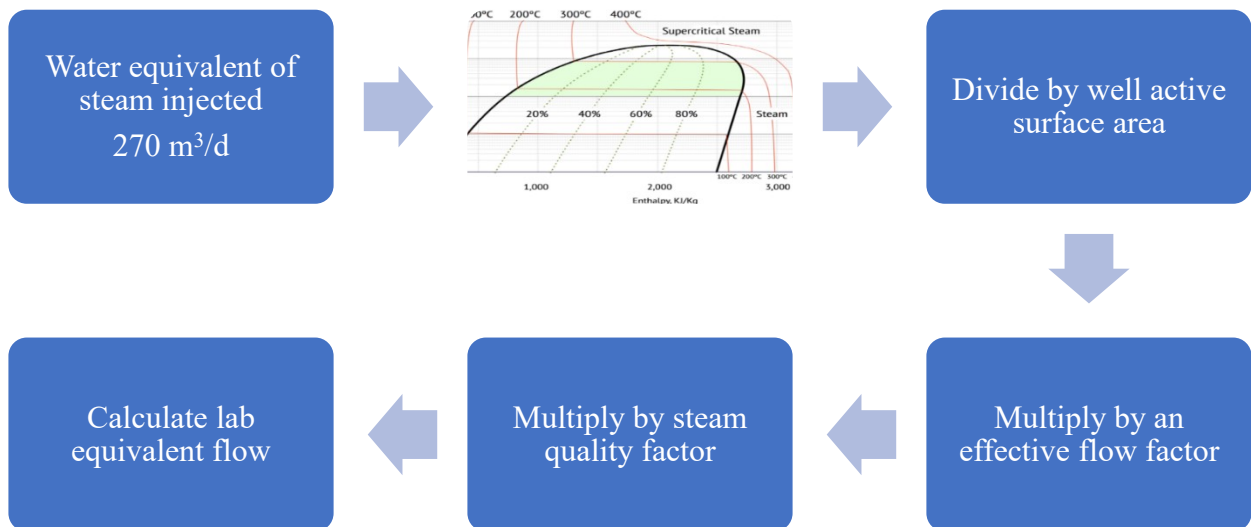


Figure 4-12. A diagram illustrating the new methodology for setting representative gas flow rates

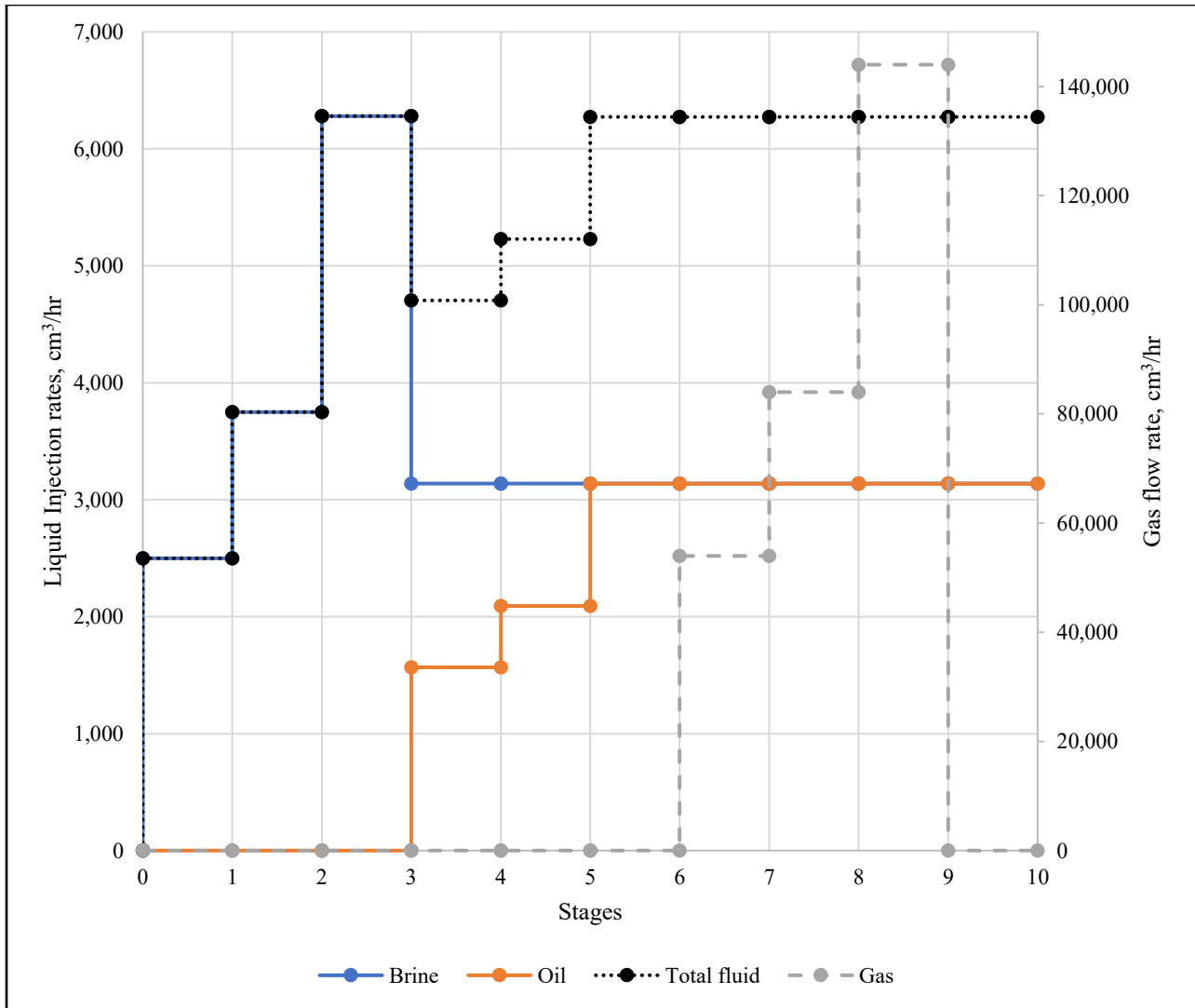


Figure 4-13. Liquid and gas rates for the University testing procedure

4.6 Test Measurements and Uncertainty Analysis

The sand production is quantified and compared based on the cumulative produced sand mass at the end of each test. The pressure gradient is defined as the pressure loss across a specified length divided by the length (Figure 4-14).

$$\text{Pressure gradient} = P_{\text{gradient}} = \frac{\text{Measured Pressure drop (dP)}}{\text{Sand core length between ports (L)}} \quad (4.2)$$

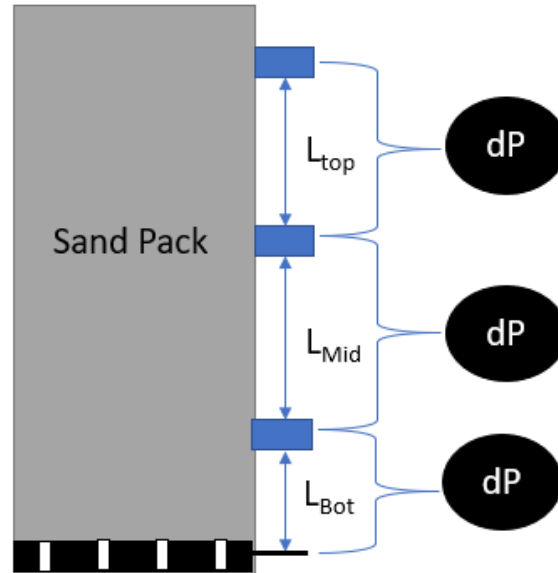


Figure 4-14. Concept of the pressure gradient in the context of testing setup presented herein

The uncertainty analysis is also performed for each measurement. The sand measurement produced by a mass balance in grams and is converted to lb/ft² by normalizing it with the coupon area by multiplying by a constant (c). The equivalent uncertainty ΔW can be calculated by Equation 4.3 where Δw is the from the mass balance (± 0.01 g).

$$\Delta W = c * \Delta w \quad (4.3)$$

The pressure gradient is a function of length and corresponding pressure drop across the sand pack. The uncertainty of pressure gradient is the function of pressure measurement uncertainty, uncertainties of pressure gradient which can be calculated using Equation 4.4. $\Delta P_{\text{gradient}}$ is the absolute uncertainty of pressure gradient while ΔP is the uncertainty of pressure measurement. The confidence intervals are incorporated for each measurement in all figures showing the results.

$$\Delta P_{\text{gradient}} = \sqrt{\left(\frac{dP_{\text{gradient}}}{dP}\right)^2 (\Delta P)^2} \quad (4.4)$$

4.7 Test Repeatability

To test for repeatability, the replication test with testing parameter presented in Table 4-4 was carried out twice. Figure 4-15 and 4-16 show the sand production and pressure gradient responses

for these tests, respectively, indicating a reasonable agreement. The sand produced values are within 12 % and the pressure gradients are within 15 %, confirming repeatability.

During each test, the absolute permeability is measured and compared at the top and middle regions under single-phase flow conditions. If the permeability difference reaches above 5%, the test is terminated, and the sand is repacked. For the repeatability tests, the top and middle permeabilities for the first test are 1920 md and 1869 md respectively while for the second test they are 1845 md and 1764 md respectively which are within the 5 % limit. All absolute permeability data will be provided in Appendix C.

Table 4-4. Testing parameters of the replication test

Test #	Coupon	Flow rates			Packing	Water composition	Stress
		Water	Oil	N ₂			
Replication test	Multi-slot Rolled top OFA 2.33%, 406 μm (0.016 inch)	Hycal rates	Hycal rates	Hycal rates	Dry packing	1% NaCl	2413 kPa (350 psi)

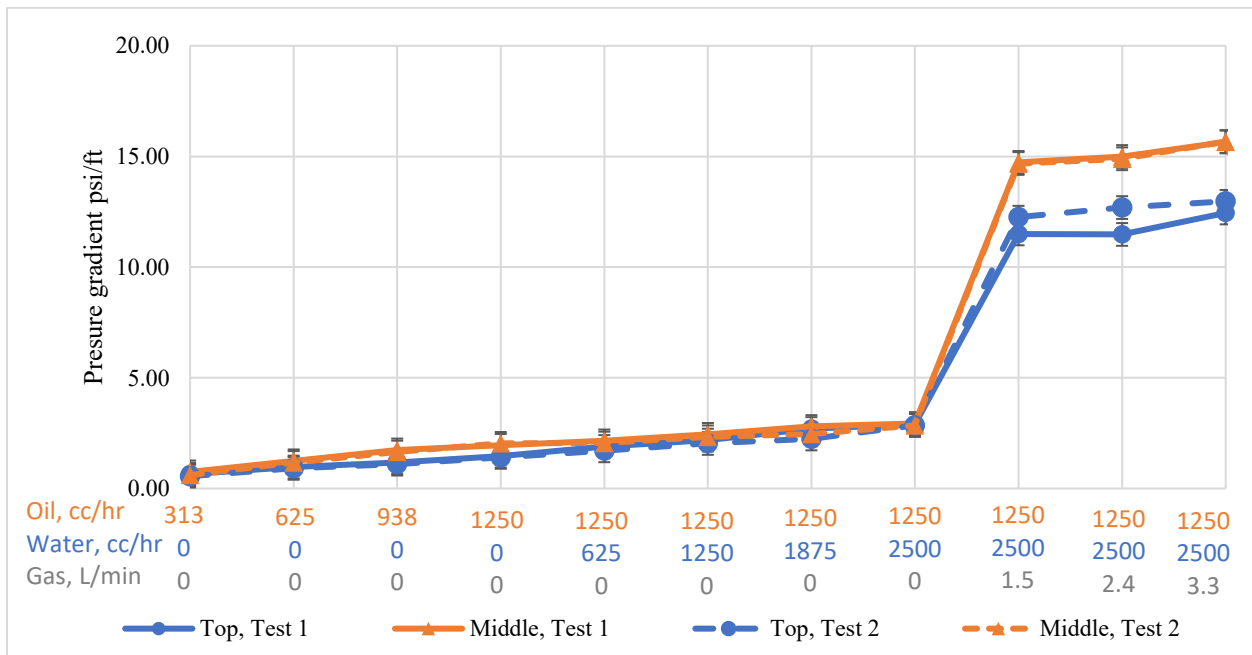


Figure 4-15. Pressure gradients for repeatability tests

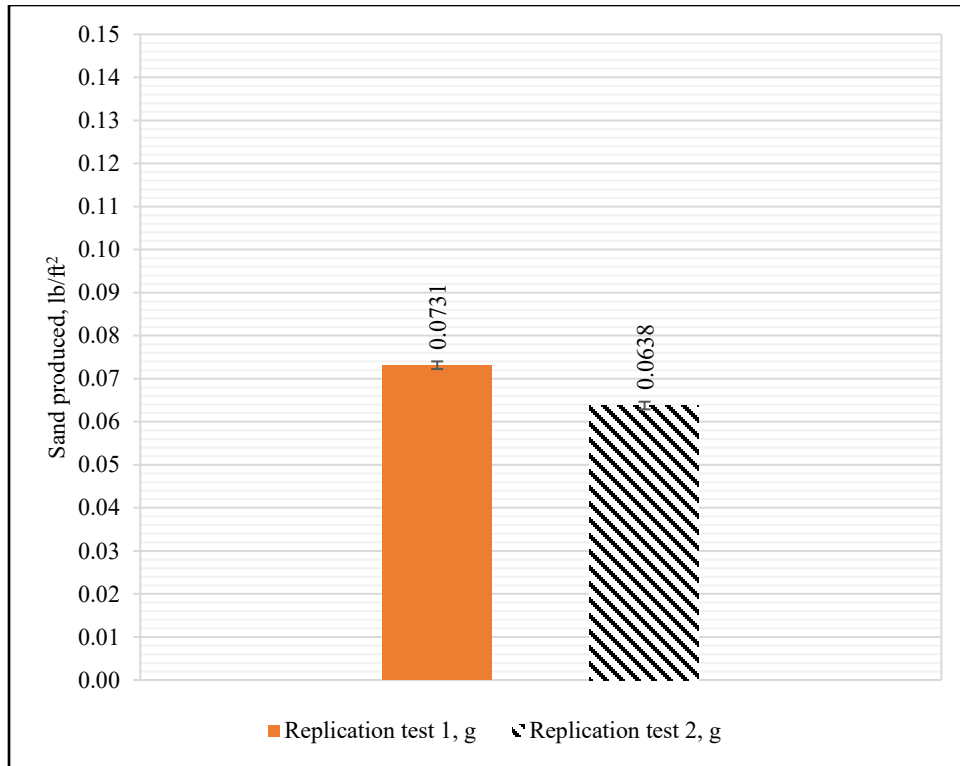


Figure 4-16. Normalized sand production in repeatability tests

4.7 Conclusion

This chapter detailed and justified the testing parameters employed in a new sand control prepack testing methodology and illustrated how the new methodology is an improvement over conventional sand control prepack testing methodology. The suggested improvements concern the packing technique to improve the pack homogeneity, the brine salinity to better represent field conditions causing fines migration, lower stress conditions during testing to describe the early life of the well, and methodology of setting the different phases fluid rates to represent the actual fluid rates expected in the well. Furthermore, a testing plan was presented that aims to quantify the effect of each improved testing parameter, in the new procedure, on sand control testing results through gradually applying the improvements. Finally, the repeatability of the new testing setup was established through conducting two tests giving comparable sand production and pressure response.

Chapter 5: Effect of SRT Testing Procedure and Parameters on Sand Production and Fines Migration

5.1 Introduction

Multiple variations of the prepack SRT setup have been introduced in the literature as discussed in Chapter 2. Each study focuses on investigating the effect of one or two testing parameters. However, due to the variation in experimental setup design and testing procedure, identifying the most critical parameters affecting sand production becomes subjective and dependant on how reliable and representative the testing is deemed to be.

This chapter firstly introduces replication results of a multiphase prepack SRT setup used by Hycal Energy Research Laboratories Ltd. (hereafter called Hycal labs) to simulate SAGD conditions (Bennion et al. 2008, 2009; Romanova et al. 2014; Devere-Bennett 2015). Hycal labs have used a specific procedure for the sand-pack preparation and testing and have used certain values for sand-pack stress, flow rates of phases, and injected brine salinity. In this work, each testing parameter is changed one at a time to gradually vary the testing design from that of Hycal's to the way which is believed to be more representative of SAGD condition as discussed in Chapter 4. The effect of change of each parameter is quantified in terms of sand production and pressure responses.

The sand production is quantified and compared based on the cumulative produced sand mass at the end of each test. The pressure gradient is defined as the pressure loss across a specified length divided by the length (Figure 4-15). The pressure response is analyzed and compared based on the pressure gradient across the setup to allow a comparison between different setups.

5.2 Replication Test

5.2.1 Introduction

Although there are references to multiple setups in the literature, it is seldom to find replication and comparison works with other setups. The setup size can influence the test results and also the level of test resemblance to downhole conditions (Hara 2015). One aim of this research is to evaluate the size effect on the test results through comparing the results of the testing in smaller-sized Hycal tests to the results of the same test conducted using a larger setup. Testing with a larger

setup allows the use of multi-slotted coupons with different slot densities. Such testing has the advantage of considering the inter-slot interactions in an actual slotted liner, which had proven to be significant as was illustrated by Mahmoudi et al. (2016).

5.2.2 Testing program

Hycal labs conducted tests for Nexen CNOOC in which they evaluated the performance of WWS and SL with different apertures through prepack SRT testing on actual oil sands of varying PSDs. One of the tests used a 152 μm (0.006-inch) WWS with a sand PSD named Batch 2 (Devere-Bennett 2015). This test was chosen to be replicated as its sand PSD was best replicated by the available commercial sands. In addition, it used WWS, which eliminates the problem of ignoring the inter-slot interaction resulting from upscaling the single-slot SL coupons. The rates of the aforementioned test were scaled up to the larger SRT setup as outlined in Chapter 4, while the sand was replicated using the methodology discussed in Chapter 3. Applied stress during the replication test was set at 2413 kPa (350 psi) instead of the 3500 kPa (500-psi) used by Hycal labs due to practical constraints in the load frame of the SRT setup. All other Hycal testing parameters such as packing technique, the order of phase injection, the viscosity of fluids injected, the salinity of brine were reproduced in the new test setup.

5.2.3 Results and discussion

Sand production

Figure 5-1 plots the produced sand from Hycal and replication test. The normalized produced sand by Hycal was calculated by first normalizing the sand produced by the coupon area.

The replication test produced 25% less sand which can be attributed Hycal reporting that produced sand includes both produced sands and fines, while the produced sands and fines are separated in the results of the replication test. It is to be noted that although sanding in SAGD is usually considered a problematic phenomenon and is avoided, fines production is regarded as a desirable phenomenon that should be encouraged as the production of fines reduces wellbore plugging. Hence, it is desirable to separate the measurements of sand production and fines production in the sand control testing.

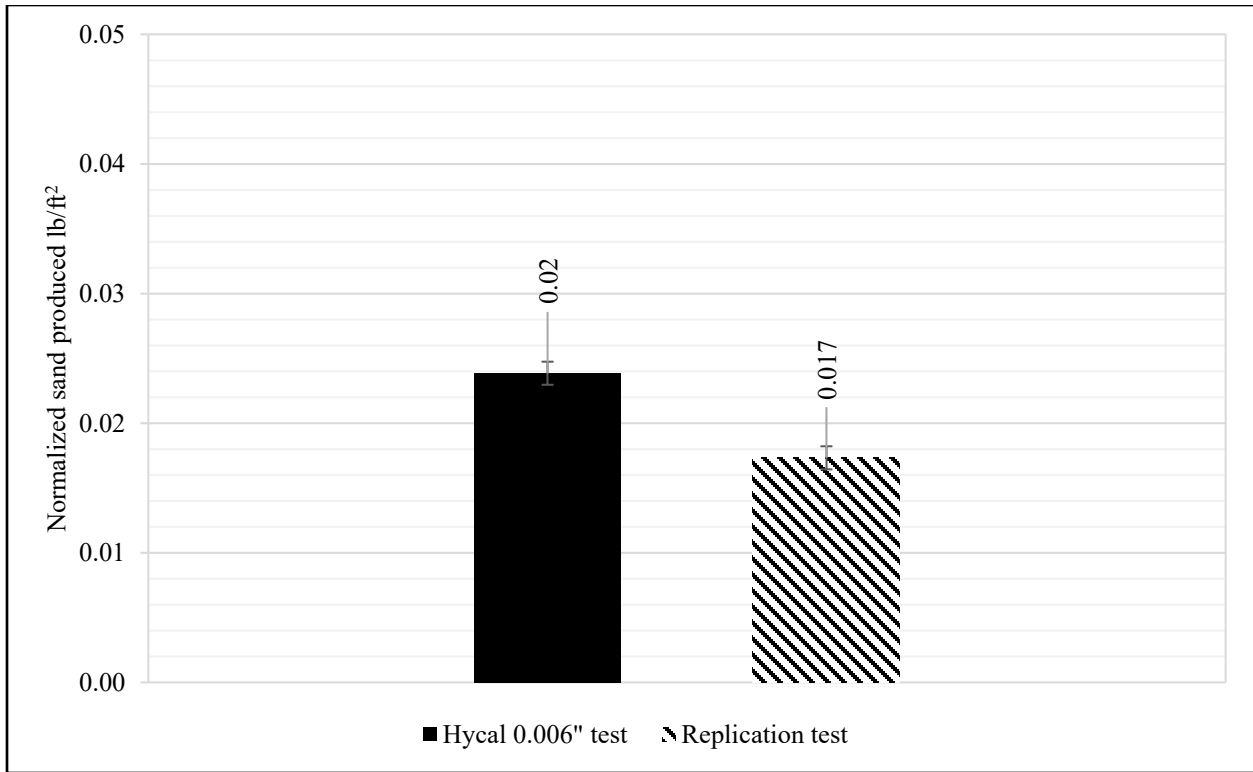


Figure 5-1. Normalized produced sand of replication test with sand produced by Hycal testing

Pressure response

The near-coupon region of Hycal is 2 cm (0.8 inch) while the near-coupon region in the university setup is 5.05 cm (2 inch). The near-coupon pressure gradient produced from the test using 0.006 inch WWS reported in Devere-Bennett (2015) does not follow the trend of the replication test as shown in Figure 5-3. However due to the difference in the length of the pressure differential measurement in the near-coupon zone, the effect of flow convergence is not comparable between the Hycal and the University setups. Moreover, the near-coupon pressure gradient trends of Hycal tests using Batch 2 with other SCD coupons does not have a consistent trend as shown in Figure 5-4. For instance, the 0.016 SC results show a significant reduction in pressure gradient after gas introduction which is not consistent with other tests. Also, the test with 0.012" WWS shows a sharp drop in pressure gradient when brine is introduced and continues to decrease with increasing water rate which is inconstant with Darcy's law.

The pressure gradient of Hycal SRT across the far from the coupon section of the sand pack is plotted in Figure 5-2. Hycal performed five tests with Batch 2 sand with different SCDs. The upper and lower bound in Figure 5-2 was plotted from data extracted from the five tests published in their report. The upper and lower bounds represent the pressure gradient variations across the sand pack section away from the coupon in Hycal tests. The replication test pressure gradient across the sand pack section far from the coupon (Top and Middle sections) throughout the test stages is within the pressure gradient variations reported by Hycal. The replication can thus be deemed success which validates the sand replication procedure and the setup capabilities of replicating previous results. The viability of using replicated sands in SRT is a significant improvement as it reduces the cost of SRT testing since core material is limited in quantity and expensive to obtain.

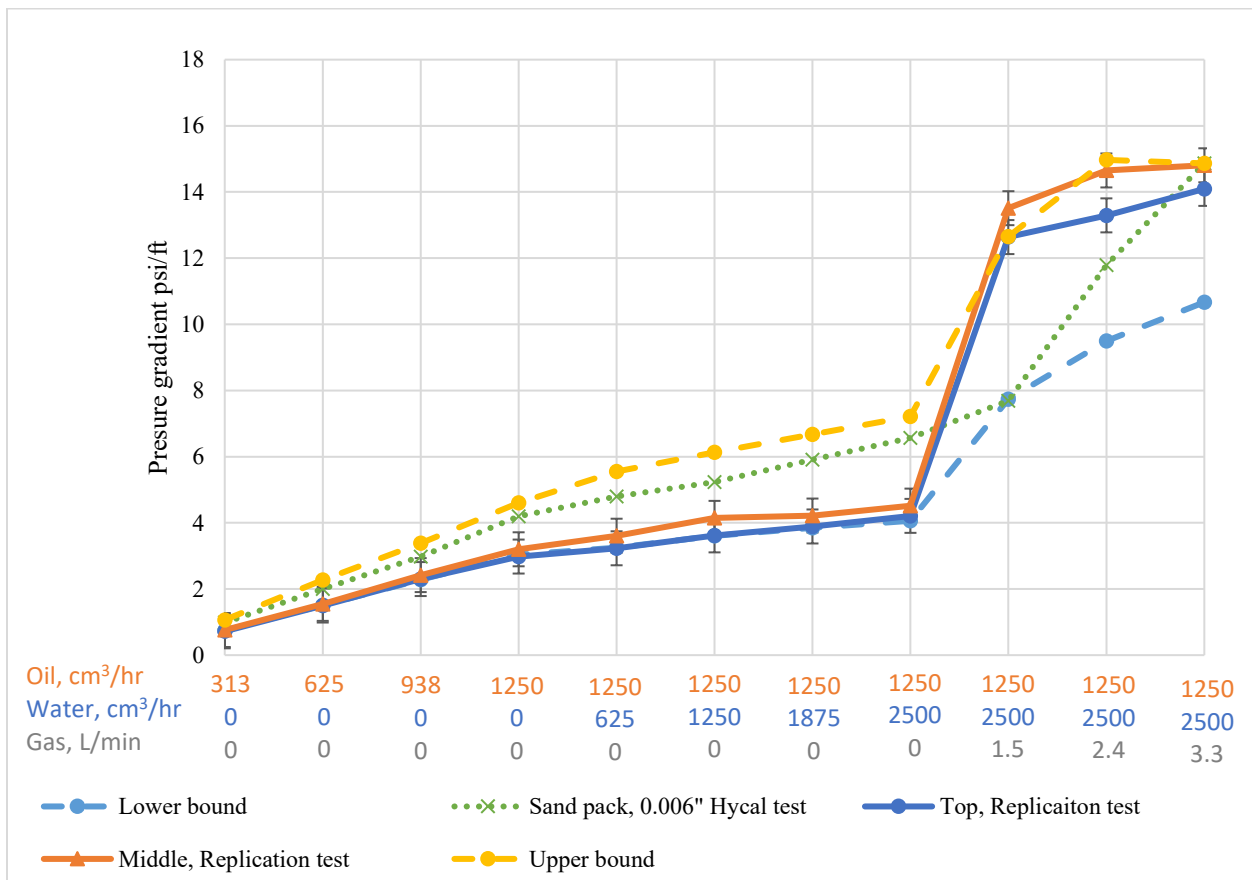


Figure 5-2. Compares the pressure gradients across the cell of Hycal tests employing sand-pack of Batch 2 with the pressure gradients of the replication test on the 153 μ m (0.006 inch) WWS

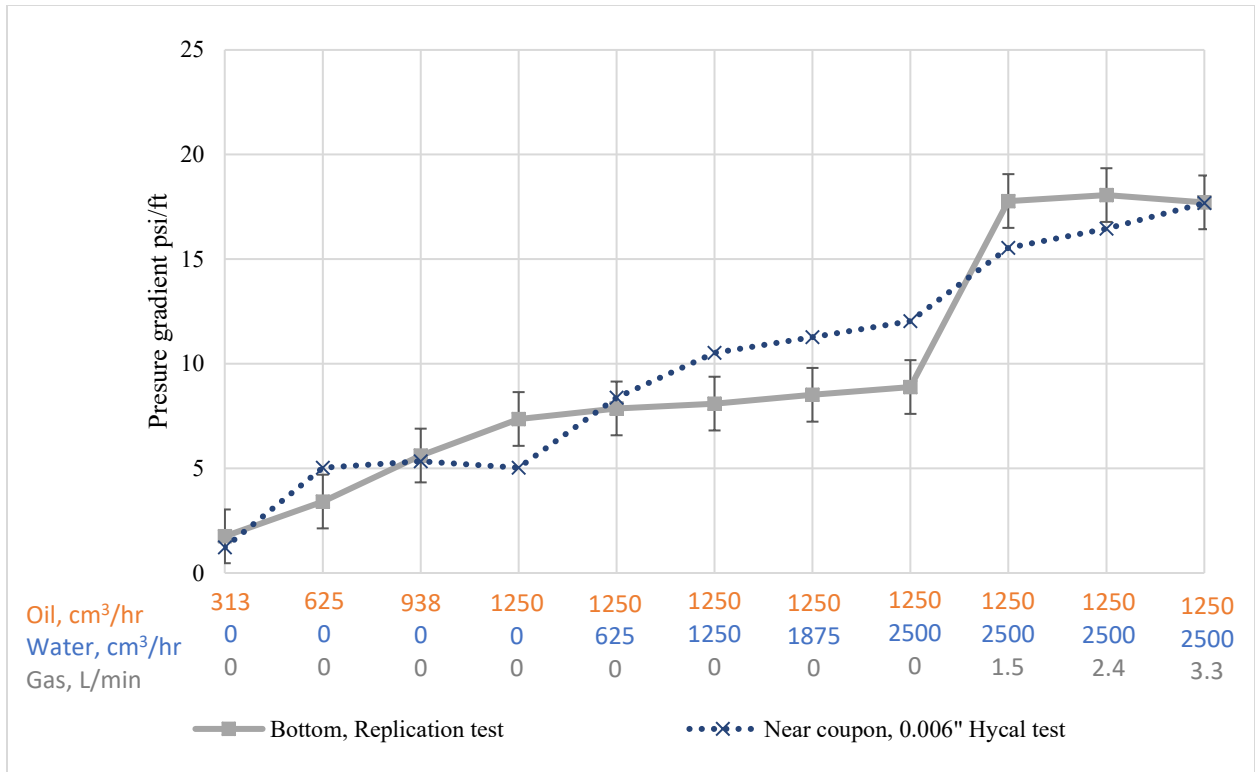


Figure 5-3. Near-coupon pressure gradients of Hycal's SRT using different SCDs reported in (Devere-Bennett 2015)

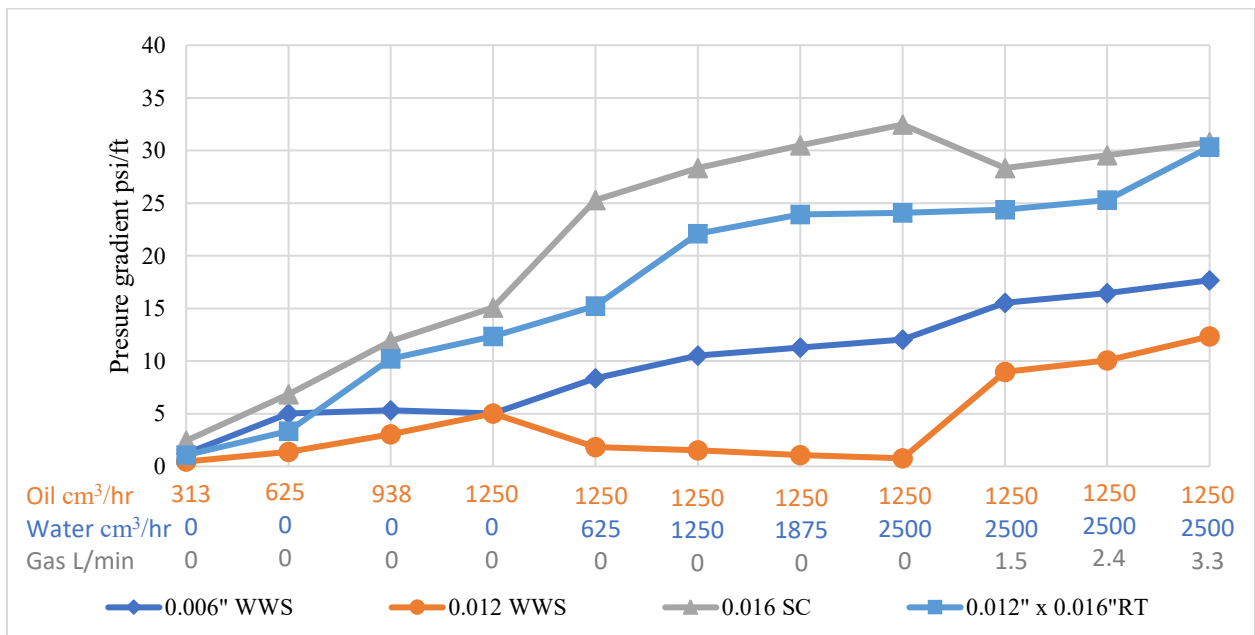


Figure 5-4. Near-coupon pressure gradients of Hycal's SRT using different SCDs reported in (Devere-Bennett 2015)

5.3 Effect of Using Moist Tamping Packing Technique

5.3.1 Introduction

The sand-pack preparation method has been found to have a significant impact on the stress-strain relationship (Oda 1972; Arthur and Menzies 1972; Vaid and Sivathayalan 2000) and liquefaction resistance of sands (Mulilis et al. 1977; Miura and Toki 1982; Tatsuoka et al. 1986; Yamamuro and Covert 2001; Yamamuro and Wood 2004). Multiple techniques have been proposed to pack sand cores aimed to produce homogenous sand-packs (Ladd 1978; Miura and Toki 1982; Kuerbis and Vaid 1988; Ueng et al. 2006; Huang et al. 2015). An investigation into packing techniques here aims to find an appropriate packing technique that practically produces a sand-pack that is adequately uniform for sand control tests.

Hycal labs packed their core by pouring dry sand into the core holder and then, applying stress from the top to compact it. Pouring dry sand is known to cause segregation in the deposition across the pack where finer particles will accumulate at the bottom (Rhodes 2008). Furthermore, when pouring dry sand with high fines content, a portion of the fines are lost (Kuerbis and Vaid 1988). Moreover, applying stress on the core from the top causes non-uniform compaction across the core length due to the friction between the sand grains with the core holder walls. The non-uniform compaction will cause higher porosities at the bottom of the sand-pack than the top. Estimations of the effect of friction on compaction are presented in Appendix D. This issue is exacerbated with a small diameter core in Hycal setup causing the ratio of the wall area to cross section area to be 30% higher than the same for the University cell, resulting in higher variability of stress across the core length.

5.3.2 Testing program

Two SRT tests using 0.016 inches, slotted liner coupon with slot density equivalent to 168 slots per foot (SPF) in a 7-inch liner (OFA: 2.33%) were conducted to evaluate the effect of packing technique on sand production and pressure differentials across the sand-pack. The sand-pack for the first test was prepared using moist tamping while for the second test the sand was packed using

the Hycal procedure. All other testing parameters were consistent with Hycal labs procedure that was scaled to the new setup. The packing uniformity of each technique was evaluated based on porosity distribution and pressure differentials across different sections of the core holder. Parameters of the tests are detailed in Table 5-1 extracted from Table 4-2.

Table 5-1. Testing program (Packing)

Test #	Coupon	Flow rates			Packing	Water composition	Stress
		Water	Oil	N ₂			
2	Multi-slot Rolled top OFA 2.33%, 406 μm (0.016 inch)	Hycal rates	Hycal rates	Hycal rates	Dry packing	1% NaCl	2413 kPa (350 psi)
3	Multi-slot Rolled top OFA 2.33%, 406 μm (0.016 inch)	Hycal rates	Hycal rates	Hycal rates	Moist Tamping	1% NaCl	2413 kPa (350 psi)

5.3.3 Results and discussion

Sand production

Figure 5-5 compares the sand produced in the SRT tests with the samples packed by moist tamping with the one packed by the Hycal technique. It can be noticed the produced sand for moist tamping is 45% less than that of Hycal packing. This phenomenon can be explained by the higher porosity, hence, lower interstitial velocities in the near-coupon region of the test packed by moist tamping (see next section). The lower interstitial velocities create lower drag forces on the sand grains and, thus, weaker destabilizing forces on the sand bridges compared to the lower-porosity sand-pack produced by the Hycal packing technique.

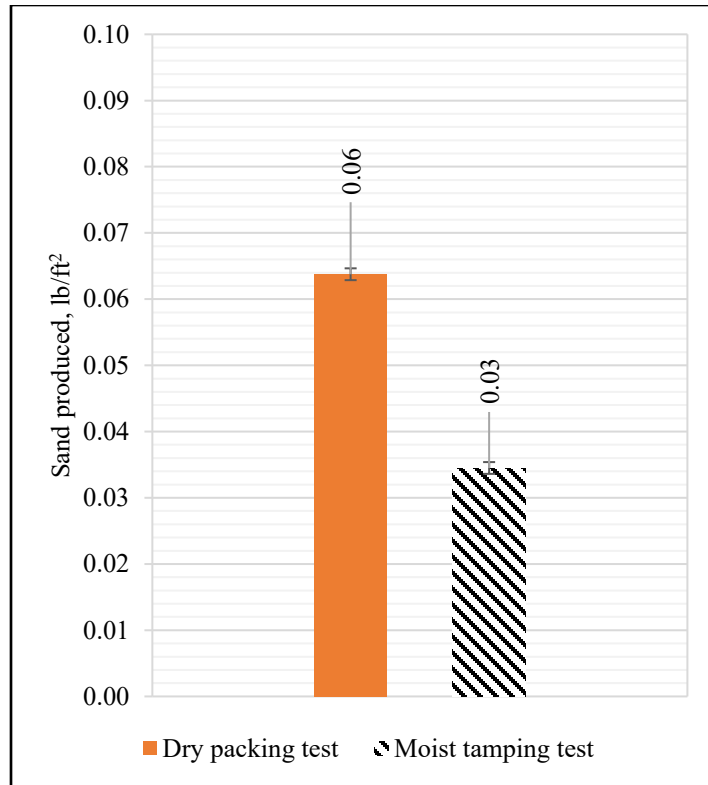


Figure 5-5. Normalized produced sand in testing on sand-packs by moist tamping and Hycal packing techniques

Porosity distribution

A core sample was extracted after the packing and saturation phases and cut into plugs of equal sizes of 2 inches to obtain porosity distribution. Each plug is weighed dry and wet. Then, the porosity is calculated.

Figure 5-6 compares the porosity distribution of the SRT tests packed by moist tamping with the one packed by Hycal technique. Section A to E represents the bottom to the top of the core, respectively. Looking at the bar chart, one can notice that the moist tamping has less variability in the porosity than the Hycal packing technique. The pack produced by dry had a standard deviation of 1.05 which is 74% higher than the standard deviation of pack produced by moist packing. Besides, dry packing produced a 4% denser pack than moist tamping, which aligns with the pressure response data in this next section. The higher porosity pack produced by moist packing more closely represents the high porosity of the collapsed region around the liner reported by a simulation study of the near wellbore region (Diaz, 2008).

Figure 5-7 shows the porosity distribution of the SRT tests packed by moist tamping with and without applying stress. The standard deviation in porosity distributions are 0.70 and 0.60, respectively; meaning that stress reduced the porosity variation in the sand-pack. Compared with dry packing, moist tamping produced more uniform pack even when the pack was not stressed.

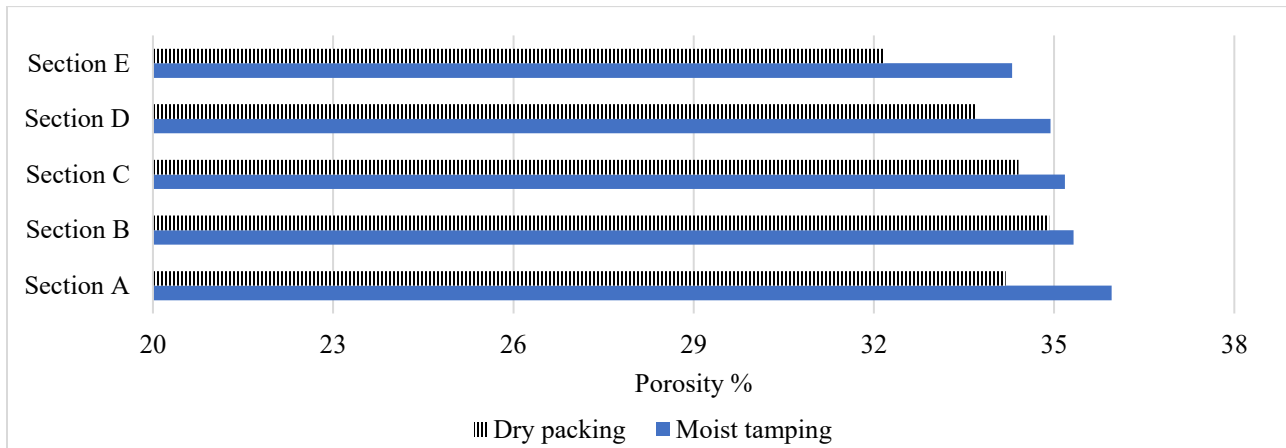


Figure 5-6. Porosity distribution across the sand-pack after stress was applied (A: Bottom and E: Top)

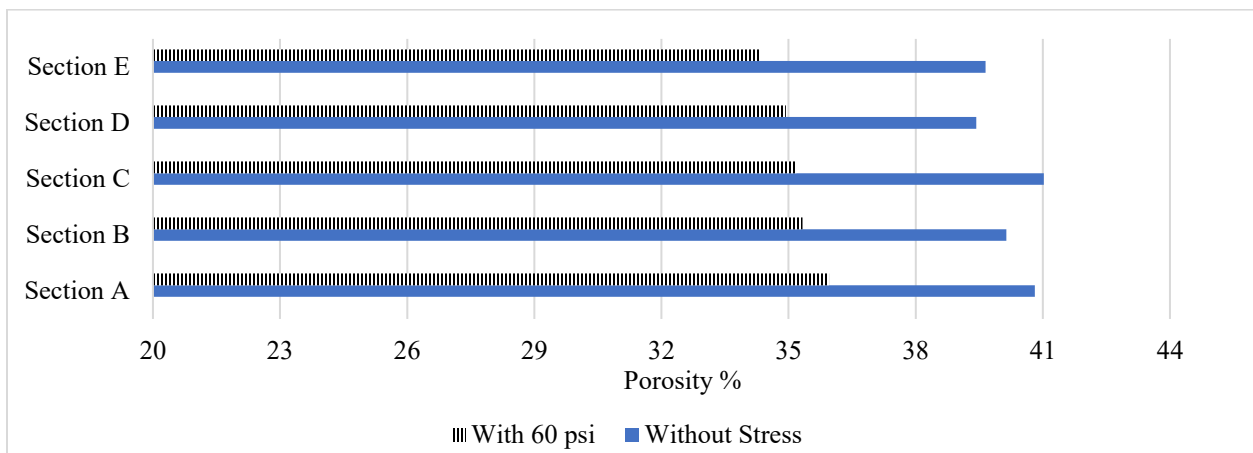


Figure 5-7. Porosity distribution across the sand-pack before stress was applied (A: Bottom and E: Top)

Pressure response

Figure 5-8 compares the pressure gradient of the SRT tests packed by moist tamping with the one packed by the Hycal technique. One can notice that the moist tamping results in a lower pressure

gradient, which can be attributed to the higher average porosity of the sand-pack. The pressure gradient across the near-coupon region is approximately two times higher than the rest of the pack in both tests. This can be attributed to flow convergence (Mahmoudi et al. 2017) and fines accumulation near the coupon.

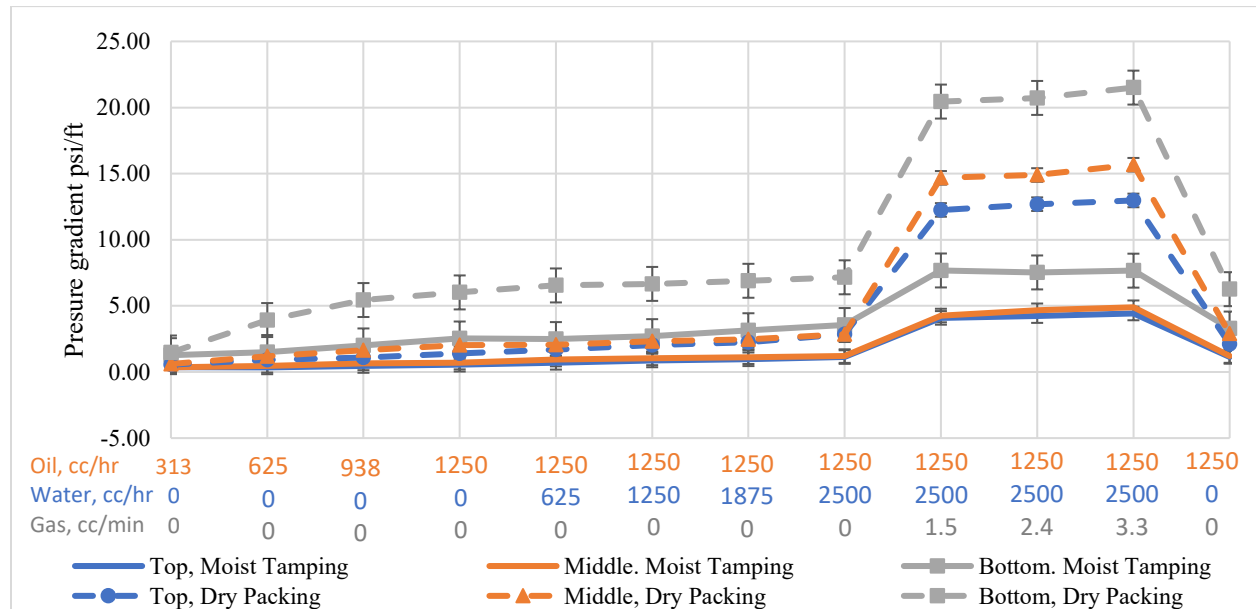


Figure 5-8. Pressure gradient across the sand-pack in SRT testing packed by moist tamping and Hycal’s packing technique

5.4 Effect of Using Representative Stress

5.4.1 Introduction

The effects of stress on sand control test performance have been acknowledged and investigated in recent literature (Guo 2018). However, the authors conducted the testing using a Scaled Completion Test (SCT) setup under isotropic stress conditions.

Here, the stress effect is investigated under axial stress conditions since it is more cost effective and practical. The aim is to replace the high stress applied in prepack SRT at Hycal labs to simulate SAGD conditions with a low-stress value that would represent the early stages of SAGD production well. The applied stress must be high enough to prevent sand-pack disruption through fluidization during the saturation phase. The comparison will quantify how the difference in the applied stress will affect testing results in terms of sand production, and pressure drops.

5.4.2 Testing program

For investigating the effect of stress, two tests were conducted. The first test involved applying 350 psi to simulate high-stress conditions of Hycal testing while the second test was conducted under 60 psi, which represents low-stress conditions expected in early SAGD well lifetime (Fattahpour et al. 2016). Low stress regimes are worse case conditions concerning the sand production in SAGD production wells (Guo, 2017). Performance comparison is evaluated based on the sand produced, and pressure gradients. Parameters of the tests are detailed in Table 5-2 extracted from Table 4-2.

Table 5-2. Testing program (Stress)

Test #	Coupon	Flow rates			Packing	Water composition	Stress
		Water	Oil	N ₂			
3	Multi-slot Rolled top OFA 2.33% 406 μm (0.016 inch)	Hycal rates	Hycal rates	Hycal rates	Moist Tamping	1% NaCl	2413 kPa (350 psi)
4	Multi-slot Rolled top OFA 2.33%, 406 μm (0.016 inch)	Hycal rates	Hycal rates	Hycal rates	Moist Tamping	1% NaCl	413 kPa (60 psi)

5.4.3 Results and discussion

Sand production

Figure 5-9 compares the produced sand under 350 and 60 psi stress levels. The produced sand under 60 psi of axial stress is higher by 33 % than that produced under 350 psi of applied stress. The lower produced sand at higher stress observed here is in line with previous observations from sand control testing in the literature (Fattahpour et al. 2016; Guo 2018). A physical explanation of the decrease in sand production is due to the mobilized friction coefficient at higher stress, resulting in higher strength at higher effective stresses (Jafarpour et al. 2012). The outcome is more stable sand bridges and thus, less produced sand.

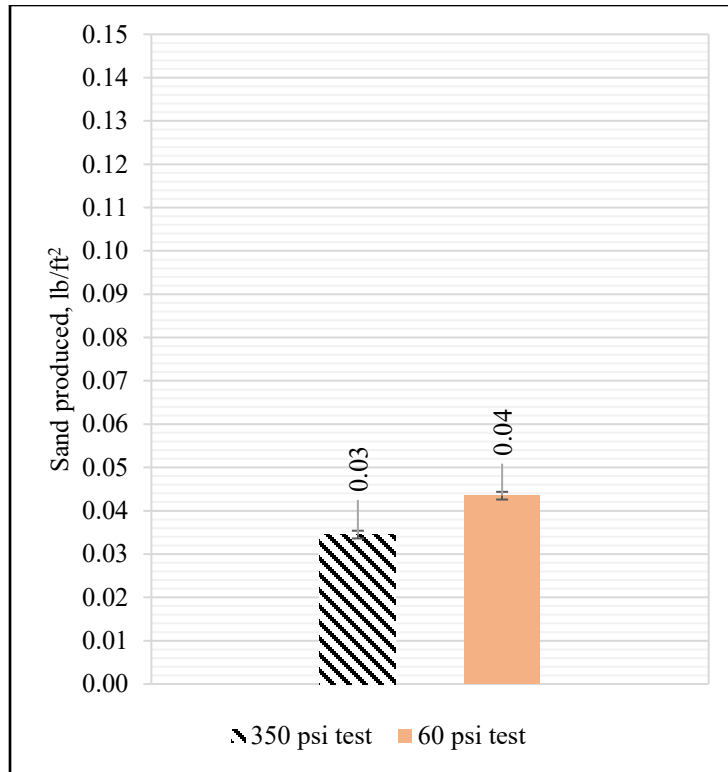


Figure 5-9. Normalized sand production under 60 and 350 psi axial stress

Pressure response

Figure 5-10 compares the pressure gradient at the top and the middle sections of the SRT tests under 350 and 60 psi. Results indicate slightly lower pressure gradients at the top compared to the middle segment of the sample. This is expected as the fines migration from the segment is more severe than the middle segment. Further, results indicate slightly higher pressure gradients for higher levels of stress, which can be attributed to the higher compaction and lower porosity and permeability at higher stresses. However, one can state that the reduction in porosity in the 60-350 psi stress range results in only a minor reduction in porosity and permeability, hence, did not affect the pressure readings significantly.

Figure 5-10 shows that the pressure gradient in the middle section is higher than the top section of the sand pack during gas injection. This phenomenon can be explained by the high gas injection pressures at the top of the cell causing higher saturations of gas at the top of the cell compared to the middle. The lower gas saturation at the middle can cause lower relative permeability to gas and thus higher pressure gradients.

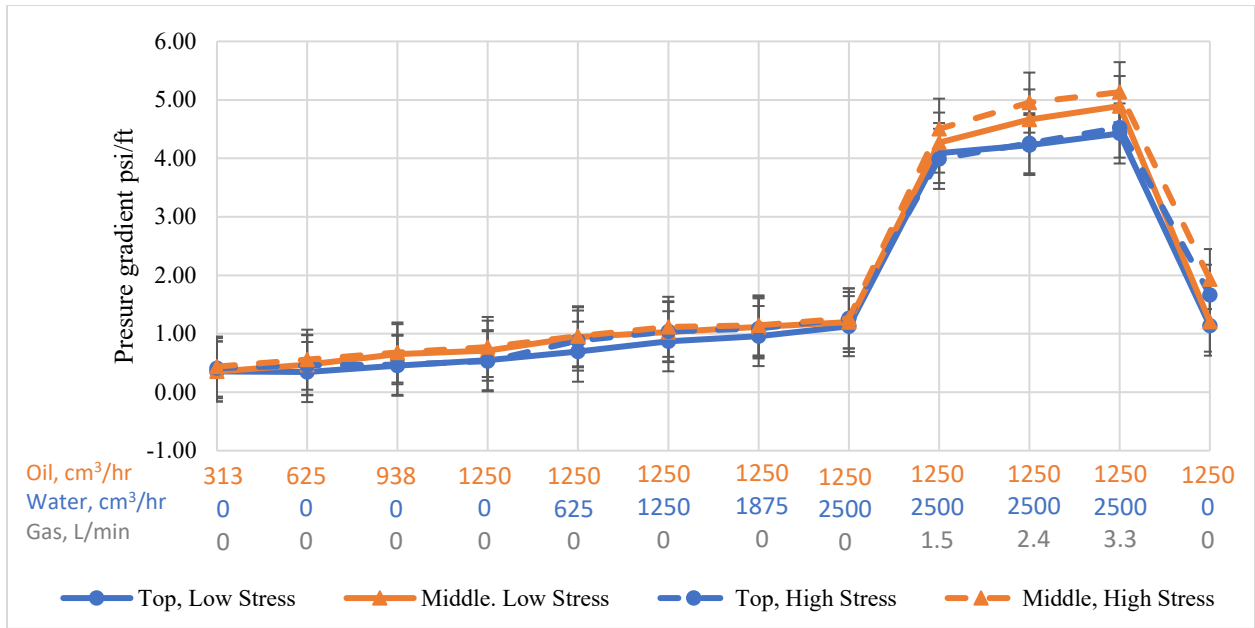


Figure 5-10. Effect of axial stress on pressure gradient across the top and middle segments of the sand-pack at 350 and 60 psi

Figure 5-11 compares the pressure gradient in the near-coupon segment under 350 and 60 psi. The near-coupon pressure gradient at 60 psi was on average 23% less than pressure gradient at 350 psi. The reason can be attributed to the lower porosity at higher stress, and higher levels of fines entrapment at lower porosities under higher stress levels.

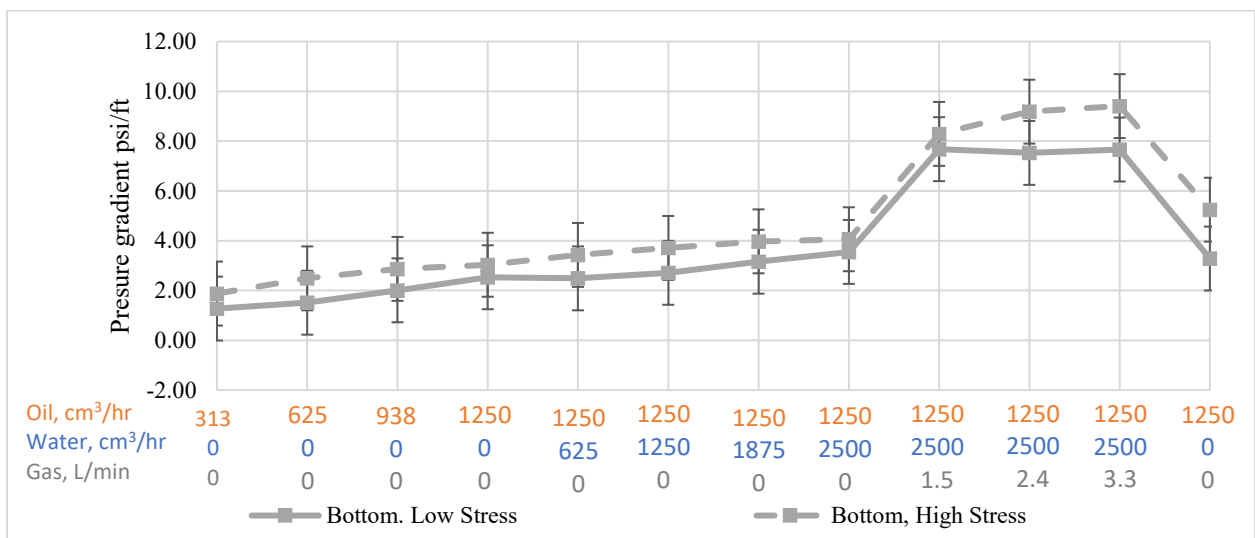


Figure 5-11. Effect of stress on pressure gradient across the near-coupon region of the sand-pack

5.5 Design of Flow Steps

5.5.1 Introduction

The significance of fluid flow rates as a contributing factor to sand production has been established in the literature.(Stein and Hilchie 1972; Veeken et al. 1991; Morita and Boyd 1991; Abass et al. 2002; Matanovic et al. 2012; Mahmoudi 2016). The general consensus is that sand production increases rapidly after a critical rate at which no stable sand bridges are formed.

Multiple authors have attempted to capture the effects of multiphase flow in sand control testing for SAGD wells (Bennion et al. 2007, 2008; Romanova et al. 2014; Hara 2015; Devere-Bennett 2015; Fattahpour et al 2018). Compared with single phase testing, multiphase flow testing can simulate the effects of capillarity and relative permeability on sand production. However, the success of the literature is limited due to the lack of consensus on water cut levels of SAGD producers and gas rates that simulate steam breakthrough in SAGD wells.

The effect of flow rate magnitude on fines migration has been proven by several researchers (Khilar and Fogler 1998; Mahmoudi 2016; Guo 2018). Fines migration has been proven to increase with an increase in the flow rate owing to the increased hydrodynamic forces on the fines particles. The effect is particularly notable above a critical flow rate.

As outlined in Chapter 4, a new rate-setting methodology was outlined based on the field production rates multiplied by the effective flow factor that accounts for non-uniform production along the well and slot plugging, among others. The new methodology will be compared with the constant flow rates used by Hycal lab's researchers (Bennion et al. 2007, 2008; Romanova et al. 2014; Devere-Bennett 2015).

5.5.2 Testing program

The flow rates used by Hycal lab were upscaled from their smaller sized setup to the University setup. Figure 4-8 and 4-13 present the flow rates exercised in the Hycal and University tests. Figure 5-12 compares the maximum flow rates used in the two testing programs. One can notice that the proposed normalized brine and oil rates here are 30% and 160% higher, respectively. However as illustrated in Figure 5-15, after normalizing liquid flow rates of SL of equal slot width by OFA, the maximum liquid flow rate used in this work is found to be approximately 65% lower than the

rates employed by Hycal. This indicates that the use of single-slot coupons causes excessively high flow velocities for SL testing compared to WWS. Thus, the testing procedure is biased against SL.

Figure 5-13 compares the water cuts used by both tests. The water cuts specified here (50-100%) are higher compared with Hycal’s water cuts (0-67%). The specified water cuts here are in line with water cuts observed in SAGD production wells since the average water cut of the field of interest (Long lake field) in 2017 was 79 % (Nexen CNOOC 2018).

Figure 5-14 compares the gas injected by Hycal compared with the new methodology. Unfortunately, the lack of field data and research quantifying the magnitude of steam breakthrough in SAGD wells makes determining the representative levels of steam rates unachievable. The proposed rates in this thesis attempt to simulate the worst-case scenario of gas production under the SAGD production. It assumes all steam injected breaks through and the steam properties are estimated under production well typical thermodynamic conditions using steam tables such as Dahm (2013).

Two tests were conducted with the first using the new rates while the second uses the upscaled values of Hycal labs. The coupon performances for both cases are compared in terms of sand production. Testing parameters are presented in Table 5-3 extracted from Table 4-2.

Table 5-3. Testing program (Fluid Flow Rate)

Test #	Coupon	Flow rates			Packing	Water composition	Stress
		Water	Oil	N ₂			
5	Multi-slot Rolled top OFA 2.33%, 406 μm (0.016 inch)	Rep. rates	Rep rates	Rep. rates	Moist Tamping	1% NaCl	413 kPa (60 psi)

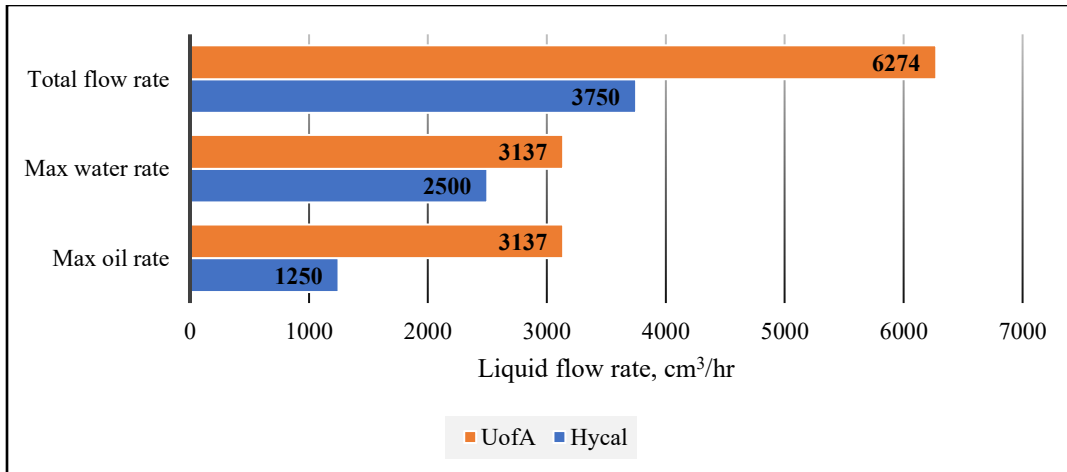


Figure 5-12. The maximum liquid flow rates used in testing stages of Hycal and the University

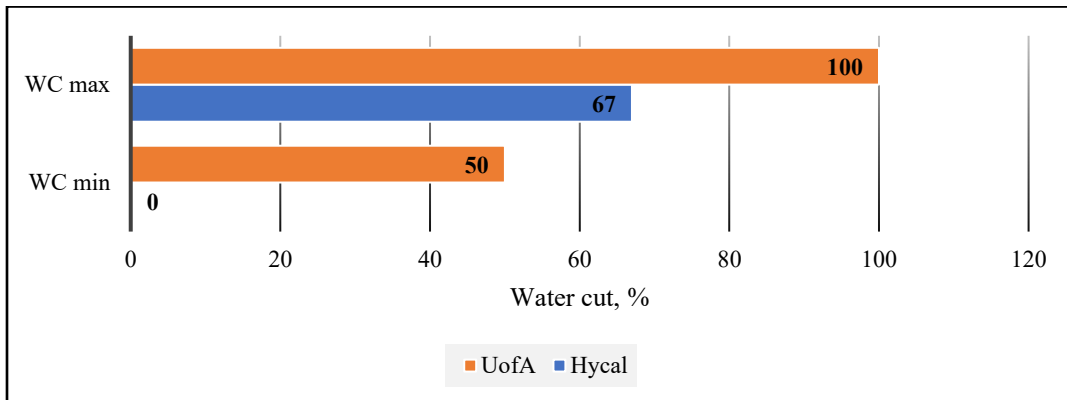


Figure 5-13. Water cuts used in testing stages of Hycal and the University

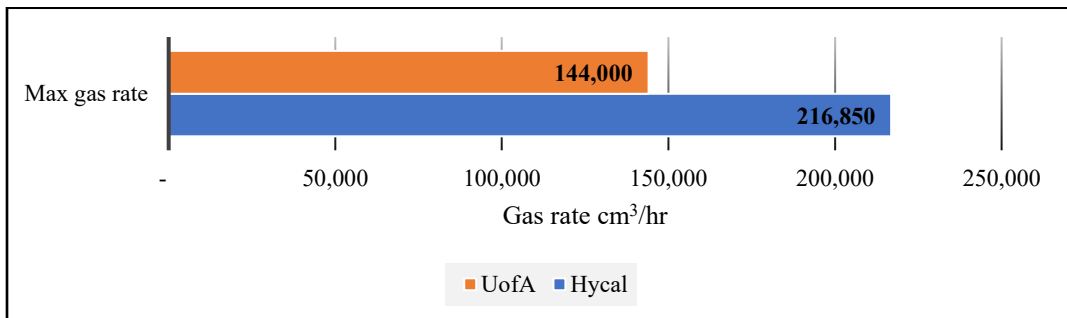


Figure 5-14. The maximum gas flow rates used in testing stages of Hycal and the University

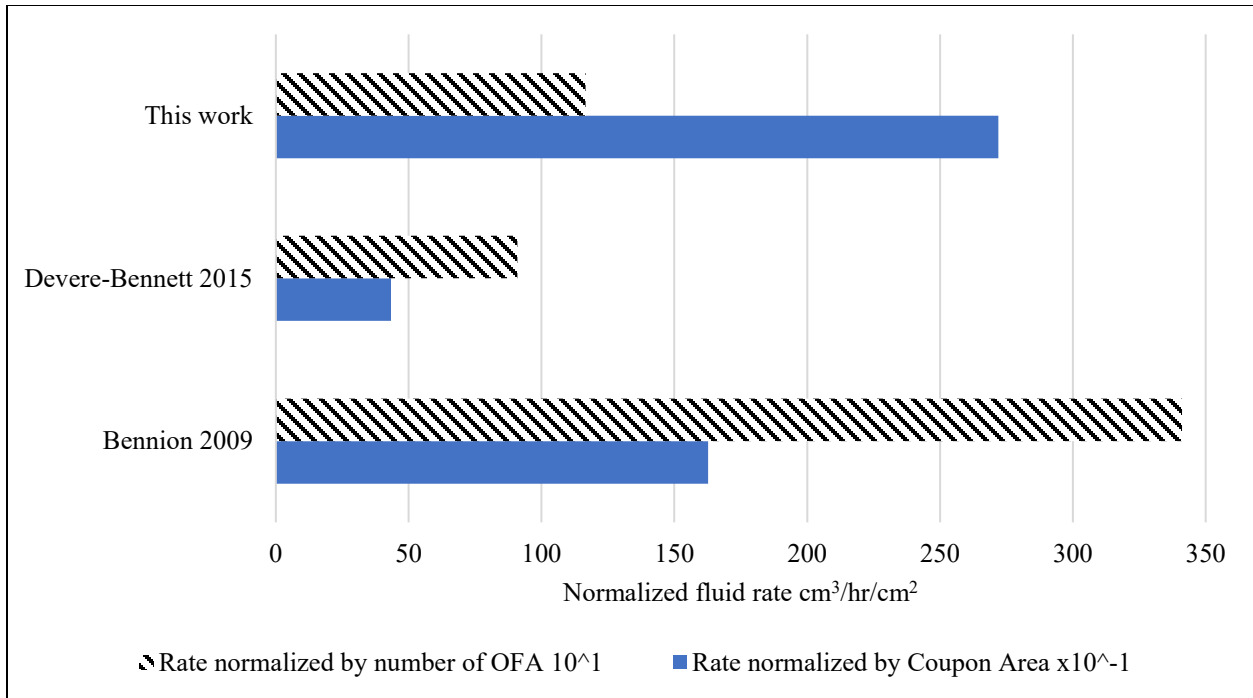


Figure 5-15. The maximum liquid flow rates employed by Hycal and the University for SL testing

5.5.3 Results and discussion

Sand production

Figure 5-16 shows the sand produced in the testing using the proposed rates and Hycal-equivalent flow rates. The sand produced by the developed technique is 153% higher than that produced by Hycal rates due to the higher new rates.

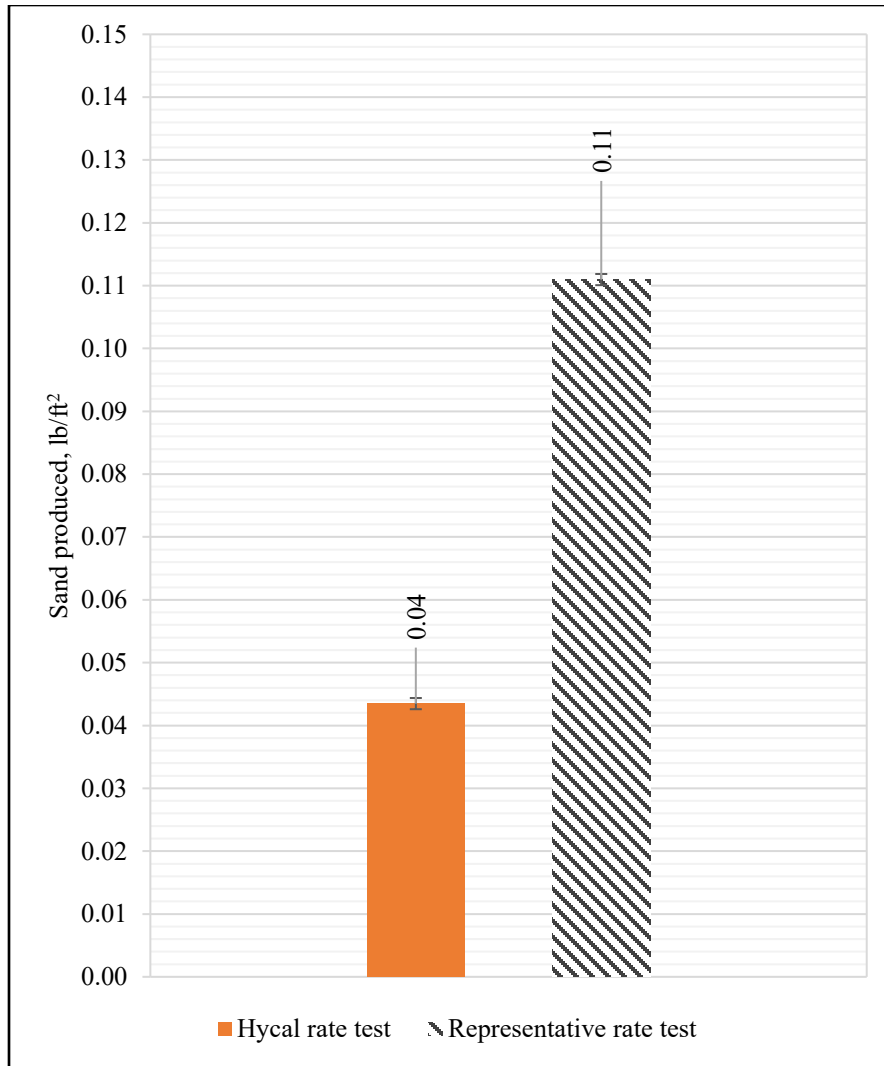


Figure 5-16. Normalized sand production by SRT testing at different flow rates

Pressure response

Figure 5-17 shows the pressure gradients using the new rates. The single-phase stages (Stage 1-3) show smaller pressure gradients compared to the two-phase stages (Stage 4-6). The higher-pressure gradients can be attributed to the relative permeability effects and the flow of oil which has higher viscosity compared to water. Stages 7-9 represent the introduction of gas, which results in higher pressure gradients at Stage 7 compared to Stages 8 and 9 that correspond to higher gas flow rates. A possible explanation for the decrease in pressure gradient with increase in gas rate is that with introduction of gas the pore pressure in the cell increases which reduces the effective stress thus increasing porosity and permeability. This combined with the low axial stress may have

disturbed the sample enough to create preferential paths of flow which lead to decrease in pressure gradient across some sections of the pack. However more investigation is needed to fully explain the observation.

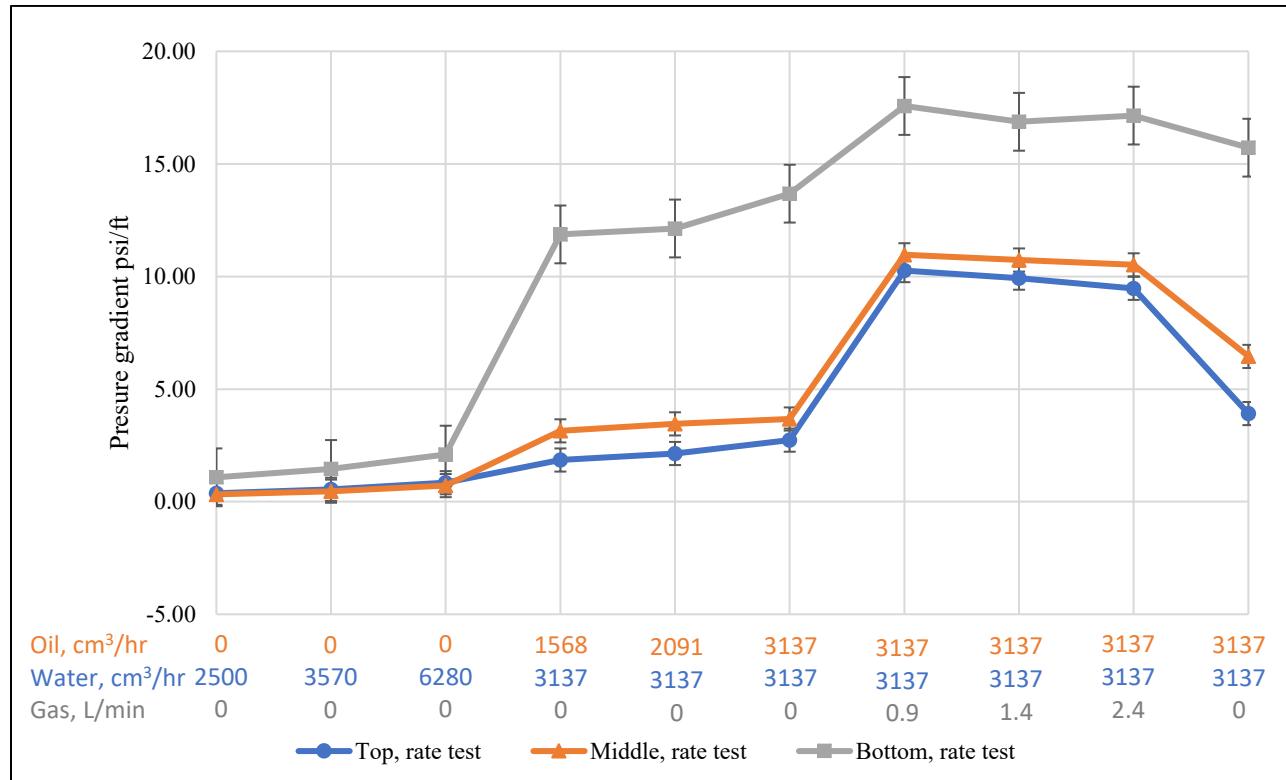


Figure 5-17. Pressure gradient associated with the new procedure

5.6 Effect of Using Representative Salinity

5.6.1 Introduction

Previous laboratory testing results (Khilar and Fogler 1998; Bennion et al. 2008; Mahmoudi et al. 2016b) determined that salinity and pH of brine flowing in water-wet sands plays a significant role in fines migration. The reason is electrochemical forces between fines and pore body are affected by the interaction between the surface electrical charges of clay particles and the water polar charges and ionic strength.

5.6.2 Testing program

Two tests were conducted to investigate the effect of salinity on test results. The first used a brine with a salinity of 10,000 ppm as was used by Hycal labs while the second test used a brine with

350 ppm to be representative of the reservoir of interest. Parameters of the tests are detailed in Table 5-4 extracted from Table 4-2.

Table 5-4. Testing program for salinity test

Test #	Coupon	Flow rates			Packing	Water composition	Stress
		Water	Oil	N ₂			
5	Multi-slot Rolled top OFA 2.33% 406 μm (0.016 inch)	Rep. rates	Rep rates	Rep. rates	Moist Tamping	1% NaCl	413 kPa (60 psi)
6	Multi-slot Rolled top OFA 2.33% 406 μm (0.016 inch)	High Hycal rates	High Hycal rates	Rep. rates	Moist Tamping	Rep. ions	413 kPa (60 psi)

5.6.3 Results and discussion

Sand production

Figure 5-18 compares sand produced by the test with 10,000 ppm salinity with the test using 350 ppm salinity. The 350-ppm salinity test produced 16% more sand than the high salinity test. A possible explanation for the slight increase in sand production could be deterioration of clay bonding between sands as the cementing clays are mobilized in the low-salinity environment.

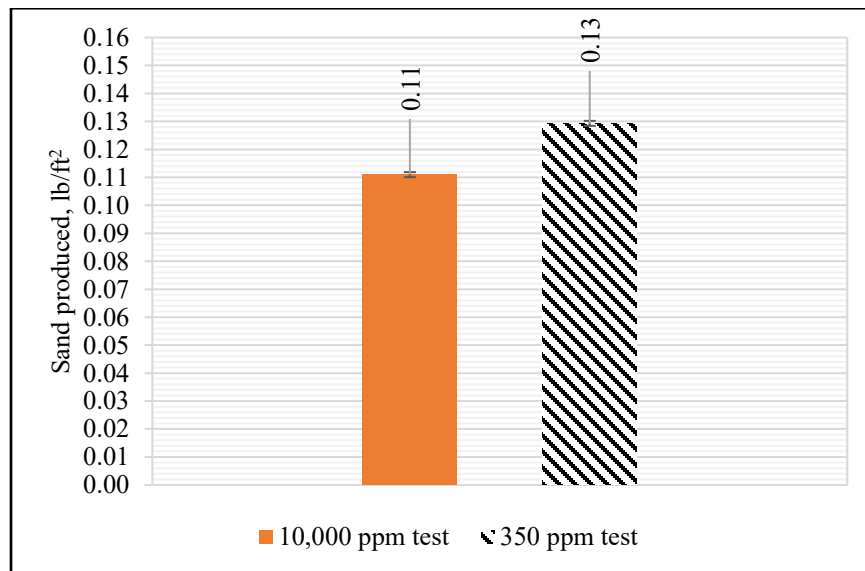


Figure 5-18. Normalized sand production by SRT testing with a brine of salinity of 350 ppm and 10,000 ppm

Pressure response

Figure 5-19 illustrates a schematic indicating where the brine sample is collected beneath the coupon. Figure 5-20 shows the concentration of fines beneath the coupon at Stages 1-3 for the high- and low-salinity SRT tests. It is evident from this figure that the low-salinity testing resulted in more severe fines migration than the high-salinity test. Besides, it appears that fines migration concentration increased in the second and third stages indicating that under these testing conditions, the critical flow rate for fines mobilization is between 2500 and 4000 cc/hr.

Figure 5-21 compares the pressure gradient of both the high- and low-salinity tests in the top and middle section of the sand-pack. It is evident that the low salinity test exhibited 45% higher pressure gradient, which can be attributed to the mobilization of fines causing plugging of pore throats and reducing the permeability. Figure 5-22 compares the pressure gradient across the near-coupon region of both the high- and low-salinity tests. Both tests show similar pressure gradients, which can be attributed to the lack of fines build up in the near-coupon region.

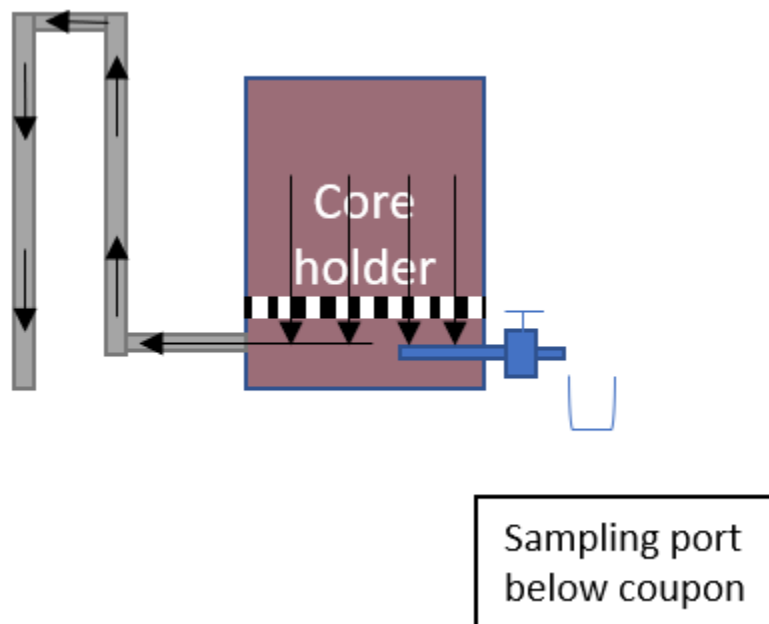


Figure 5-19. Location of the brine sampling port in the SRT setup

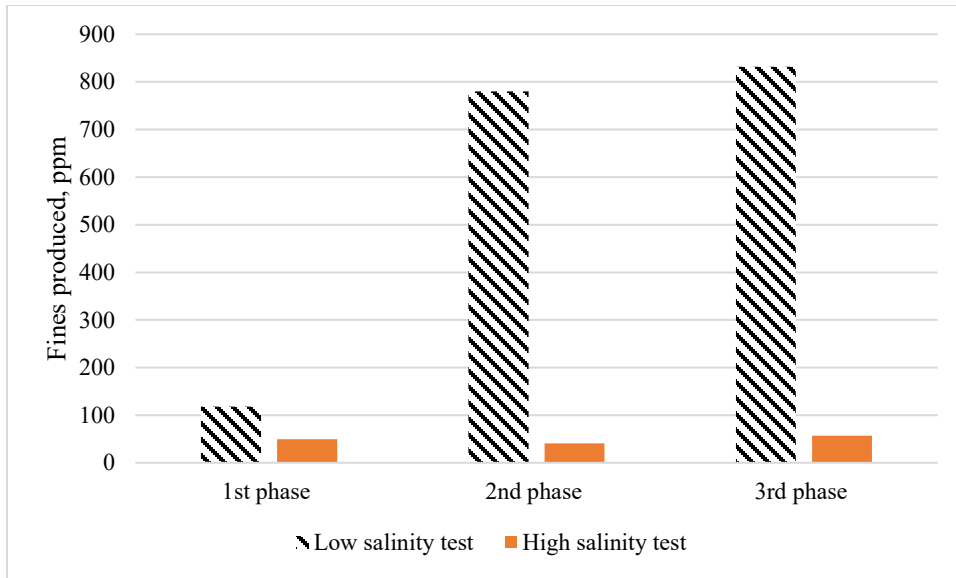


Figure 5-20. Solid concentration in brine under the coupon at different testing stages

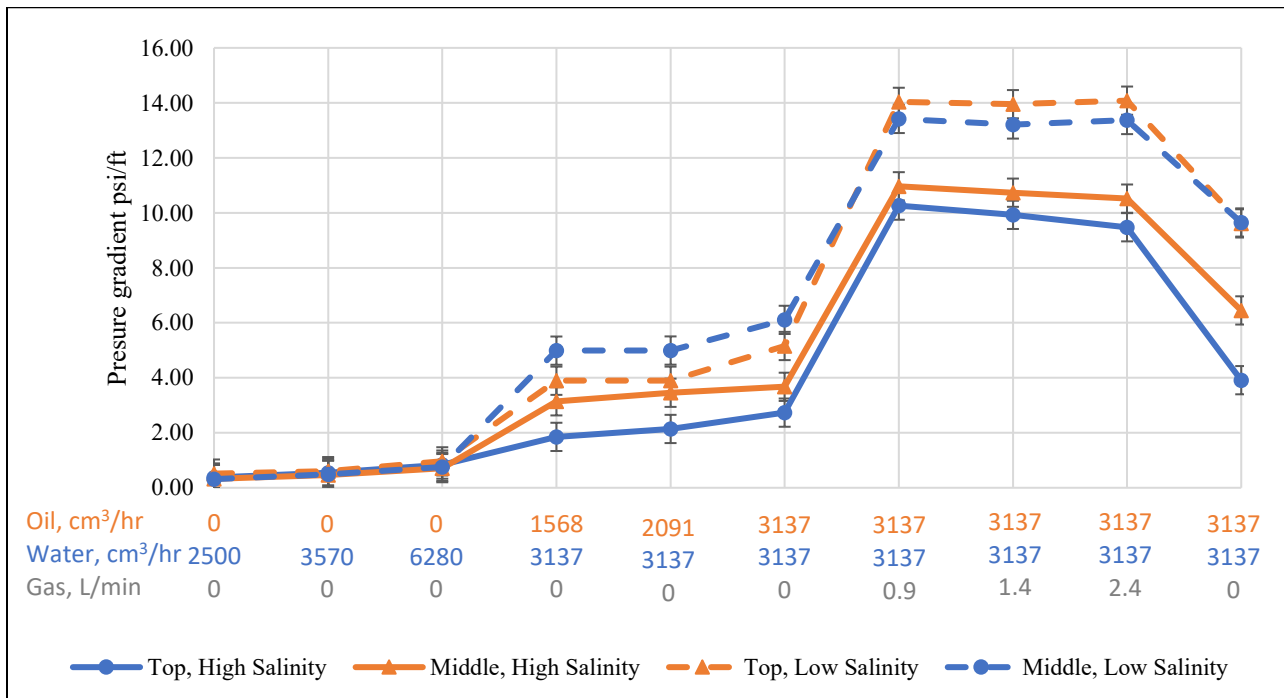


Figure 5-21. Pressure gradient of the top and middle sections of the SRT sand-pack while injecting with brine salinity of 350 and 10,000 ppm

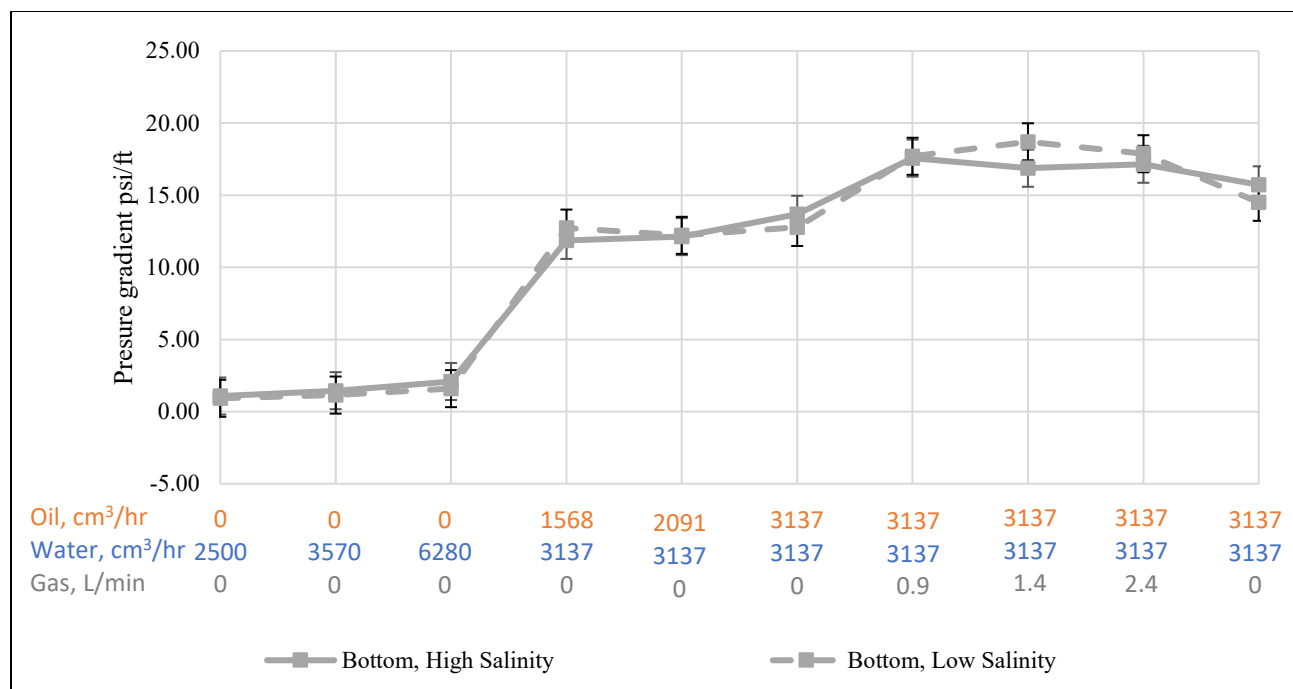


Figure 5-22. Pressure gradient of the near-coupon section of the sand-pack for brine salinity of 350 and 10,000 ppm

5.7 Conclusion

This chapter presented results of the SRT testing of replication attempt of Hycal SRT testing setup. The chapter continued with an investigation of the significance of packing technique, applied axial stress, fluid flow rates, and salinity parameters on test results. Sand production, fines production, and pressure gradients along the sand-pack and across the coupon were used to evaluate the test performance. The results allow the reader to assess the impact of varying each testing parameter on the test performance qualitatively.

Figure 5-23 illustrates a summary of the sand produced by the SRT tests conducted for investigating each testing parameter. The testing results indicate that fluid flow rates are the most influential testing parameter on sand production during SRT testing followed by packing technique, stress magnitude, and salinity in that order. However, more sensitivity testing is needed to establish quantitative relationships between these factors and sand production.

Pressure gradient results indicate packing by moist tamping produced a less compacted but more uniform sand-pack than the packing technique employed by Hycal lab. In addition, the effect of

stress, in the range used here, was found to be minimal on pressure gradients. Low salinity brine increased fines migration accompanied with the higher pressure drop across the sand-pack compared with the high-salinity test.

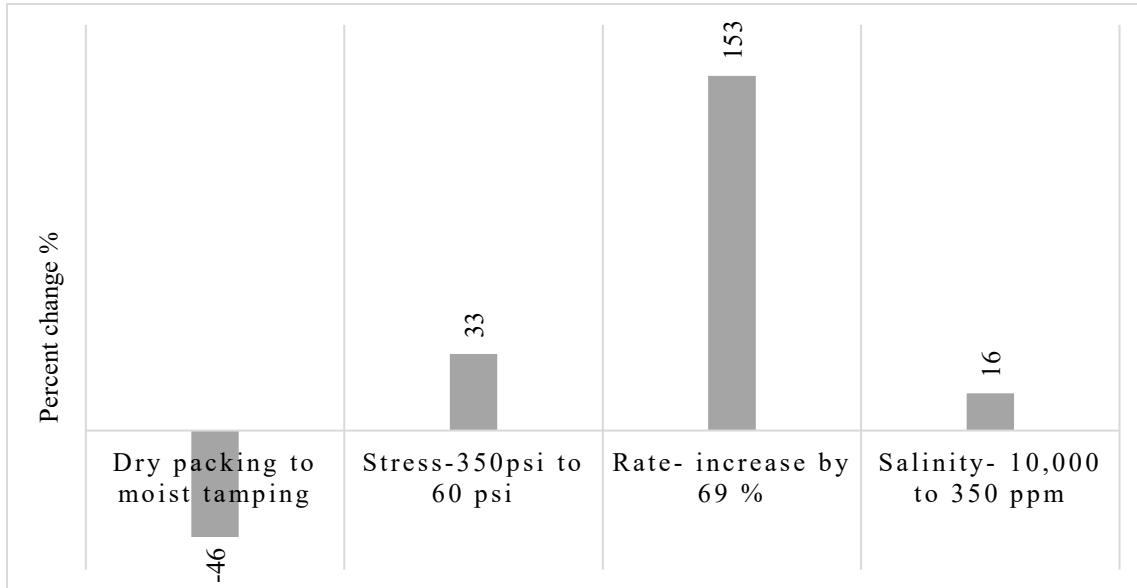


Figure 5-23. Summary of the effect of different testing parameters on the sand production

Chapter 6: Conclusions and Recommendations for Future Work

6.1 Main Results and Contributions

This research developed a new sand control testing facility capable of conducting multiphase flow tests with multi-slot slotted liner coupons under different axial stress magnitudes. A testing procedure was designed to allow the representation of sanding in SAGD conditions while accommodating the differences in various field conditions. The setup was used to evaluate the testing procedure and parameters compared with previous testing parameters in the literature and assess their importance. The sanding performance was assessed based on measuring the cumulative sand produced at the end of the test. The pore and slot plugging were evaluated by comparing the pressure response of the sand-pack and near-coupon region.

The work started by characterizing the samples of oil-sands received from a Long Lake field, in the McMurray Formation. The characterization was conducted in terms of PSD, grain shape, and mineral composition. Following that, the characterization data was used to replicate the oil sand samples by commercial sands. Sieve analysis was conducted to validate the success of replication.

Several conclusions were reached through conducting SRT testing, where testing parameters were gradually changed from Hycal procedure to the new procedure. The sanding test results indicate that fluid flow rate is the most influential testing parameter on sand production during SRT testing followed by the packing technique, stress magnitude, and salinity. Analysis of pressure data revealed that the moist tamping packing technique results in a significant increase in porosity and uniformity of the sand-pack. In addition, the effect of stress was found to be minimal on pressure drop, which was attributed to the high porosity of the sand-pack. Furthermore, lowering salinity from 10,000 ppm to 350 ppm was found to significantly increase fines migration and production, which led to the higher pressure drop across the cell.

6.2 Experimental testing limitations

The major limitations of the developed setup and procedure due to cost and time constraints are listed below:

- The setup is only allowing for linear flow towards the SCD, which prevents accurate capture of near wellbore radial flow convergence around a SAGD well. Ignoring the radial flow regime would result in under-estimating the pressure drop in the setup.
- Channeling between the wall and the sand-pack is a phenomenon reported in the sand control testing literature (Ballard and Beare 2006). This phenomenon will result in lower pressure drop and sand production than expected, especially at high flow rates. To reduce the effect of this problem, highly viscous vacuum grease was applied between the sand-pack and the core holder.
- Currently, nitrogen gas is used to simulate an assumed breakthrough steam quality of 50%. Further thermodynamic simulation and lab testing are required to adjust these assumptions. A further improvement is to use High Temperature-High Pressure (HT-HP) setup to simulate steam breakthrough. Using such an HT-HP setup will capture phenomena such as the steam hammer, which cannot be captured using nitrogen.
- Currently, sand production is quantified at the end of the test as cumulatively produced sand. However, fitting the sand trap with a butterfly or ball valve will allow the isolation and measurement of sand production at each stage.
- The results of the lab testing need to be correlated with field data. This effort was not possible in this work due to the lack of sufficient reliable pressure and sand production field data.

6.3 Recommendations for Future Work

6.3.1 Investigation into how laboratory sand production relates to field production

Currently, all variations of sand control testing are useful to the extent of comparing the relative performance of screens under various flow conditions. This is mainly because the upper limit of sand production in lab testing is all based on undocumented experience and simplistic assumptions of sand transportation. A relationship between the sand produced at the liner and sand reaching the

downhole pump and surface equipment has not been investigated in the literature. Once such a connection is established, the quantification of an upper limit during testing can be meaningful to the well trajectory and field equipment. A possible approach is to use established solids transportation equation under different flow conditions to simulate the transportation of lab-produced sand numerically with specific PSD and then, validate the results against sand production monitoring equipment in the wellbore. Such transport equations are used for cutting transportation during drilling.

6.3.2 Investigating how conducting HT-HP sand control testing differs from the simplified version

A significant assumption during sand control testing is the use of standard laboratory temperatures and pressures to simulate high pressure and temperature fluid performance. This may be enough for evaluating sand production for liquids; however, simulating sand production and erosion due to steam breakthrough cannot be evaluated under lab condition. HT-HP cell can capture steam hammering and temperature effects on the slot size.

6.3.3 Investigating how to practically and accurately quantify fines migration in multiphase flow conditions

Previous researchers studying fines migration in porous media under single-phase brine flow were quickly able to quantify fines concentrations in the sand-pack and effluent (Mahmoudi et al. 2016a). However, the quantification becomes challenging when dealing with the multiphase flow as the fines must be effectively isolated from two different fluids. Achieving this will allow investigation and modeling of fines migration in multiphase flow conditions, which will have applications in production engineering and non-petroleum sectors. One possible approach is to use radioactive fines and track their redistribution along the core using radioactivity measuring devices such as Geiger counter.

6.3.4 Investigating how to practically measure and isolate relative permeability effects from fines migration effects in multiphase flow conditions

Currently, the sand control testing is conducted, and plugging is quantified based on pressure drop measurements. However, no distinction is made between the pressure drop resulting from the effect of relative permeability and the effect of pore plugging by fines migration. A possible

approach is to measure relative permeabilities of a sand core using one of the steady or unsteady state methods to establish the effect of relative permeability. Once the relative permeability curves are established, the effect of fines migration can be isolated from the pressure loss caused by relative permeability effects.

6.3.5 Effect of stress isotropy on sand production

Recent work in sand control testing incorporated the effect of stress on sand production and fines migration. However, no investigation has been carried out on the impact of the level of stress anisotropy on sand production. Stress anisotropy can affect the stability of sand bridges around the sand control liner and thus, sand production.

6.3.6 Effect of slot width, geometry, and density on completion induced skin in injection wells

Currently, most SAGD injection wells are completed using a slotted liner. However, no attempt of quantification of slot density and width on completion induced skin has been reported in the literature. This work will aim first to derive analytical models of flow convergence in injection slots and, then verify the models by numerical simulation using the Computational Fluid Dynamics (CFD) and laboratory testing. The output should be a model capable of predicting the completion induced back pressure in injection wells.

References

- Abass, H.H., Nasr-El-Din, H.A., and BaTaweel, M.H. 2002. "Sand Control: Sand Characterization, Failure Mechanisms, and Completion Methods." In *SPE Annual Technical Conference and Exhibition*, San Antonio, Texas, USA. doi:10.2118/77686-MS.
- Adams, P.R., Davis E.R., Hodge R.M., Burton R.C., Ledlow L., Procyk A.D., and Crissman S.C.. 2009. "Current State of the Premium Screen Industry: Buyer Beware, Methodical Testing and Qualification Shows You Don't Always Get What You Paid For." *SPE Drilling & Completion*, 24(03), 362-372. doi:10.2118/110082-PA.
- AER. 2018. "ST98: Alberta's Energy Reserves & Supply/Demand Outlook." *Government of Alberta*.
- Aggour, M.A., Abu-Khamsin S.A., and Osman E.A. 2007. "A New Method of Sand Control : The Process and Its First Field Implementation" In *SPE/IADC Middle East Drilling and Technology Conference*, Cairo, Egypt. doi:10.2118/108250-MS.
- Agunloye, E., and Utunedi E. 2014. "Optimizing Sand Control Design Using Sand Screen Retention Testing." In *38th Nigeria Annual International Conference and Exhibition*, Lagos, Nigeria. doi:10.2118/172488-MS.
- Al Bahlani, A.M., and Babadagli T. 2008. "A Critical Review of the Status of SAGD : Where Are We and What Is Next ?" In *SPE Western Regional and Pacific Section AAPG Joint Meeting*, Bakersfield, California, USA: Society of Petroleum Engineers. doi:10.2118/113283-MS.
- Anderson, M. 2017. "SAGD Sand Control : Large Scale Testing Results." In *SPE Canada Heavy Oil Technical Conference*, Calgary, Alberta, Canada. doi:10.2118/185967-MS.
- Arthur, J.R.F., and Menzies B. 1972. "Inherent Anisotropy in a Sand." *Géotechnique* 22 (1): 115–28. doi:10.1680/geot.1973.23.1.128.
- Ballard, T., and Beare S. 2013. "Particle Size Analysis For Sand Control Applications." In *SPE European Formation Damage Conference & Exhibition*, Noordwijk, The Netherlands. doi:10.2118/165119-MS.
- Ballard, T., and Beare S. 2012. "An Investigation of Sand Retention Testing with a View to Developing Better Guidelines for Screen Selection." In *SPE International Symposium on Formation Damage Control*, Lafayette, Louisiana, USA. doi:10.2118/151768-MS.
- Ballard, T., and Beare S. 2006. "Sand Retention Testing : The More You Do , the Worse It Gets." In *SPE International Symposium and Exhibition on Formation Damage Control*, Lafayette, Louisiana, USA. doi:10.2118/98308-MS.
- Ballard, T., and Beare S. 2003. "Media Sizing for Premium Sand Screens: Dutch Twill Weaves." In *Proceedings of SPE European Formation Damage Conference*, The Hague, Netherlands. doi:10.2118/82244-MS.
- Ballard, T., Kageson-Loe N., and Mathisen A. 1999. "The Development and Application of a Method for the Evaluation of Sand Screens." In *SPE European Formation Damage*

- Conference*, The Hague, Netherlands. doi:10.2118/54745-MS.
- Barry, M.D., Hecker M.T., Haeberle D.C., Blacklock J., and Yeh D.C. 2008. "Openhole Gravel Packing With Zonal Isolation." In *SPE Annual Technical Conference and Exhibition*, Anaheim, California, USA. doi:10.2118/110460-MS.
- Bayat, H., Rastgou M., Nemes A., Mansourizadeh M., and Zamani P. 2017. "Mathematical Models for Soil Particle-Size Distribution and Their Overall and Fraction-Wise Fitting to Measurements." *European Journal of Soil Science* 68 (3): 345–64. doi:10.1111/ejss.12423.
- Beare, S., and Ballard T. 2013. "Particle Size Analysis For Sand Control Applications." In *SPE European Formation Damage Conference*, Noordwijk, The Netherlands. doi:10.2118/165119-MS.
- Bellarby, J. 2009. "Well Construction Design." *Elsevier*, 56:129–239. doi:10.1016/S0376-7361(08)00203-3.
- Bennion, D.B. 2009. "Protocols for Slotted Liner Design for Optimum SAGD Operation." *Journal of Canadian Petroleum Technology* 48 (11): 21–26. doi:10.2118/130441-PA.
- Bennion, D.B., Gupta S., Gittins S., and Hollies D. 2008. "Protocols for Slotted Liner Design for Optimum SAGD Operation." In *Canadian International Petroleum Conference/SPE Gas Technology Symposium*, Calgary, Alberta. doi:10.2118/130441-PA.
- Bennion, D.B., Ma T., Thomas F.B., and Romanova U.G. 2007. "Laboratory Procedures for Optimizing the Recovery from High Temperature Thermal Heavy Oil and Bitumen Recovery Operations." *Proceedings of Canadian International Petroleum Conference*, Calgary, Alberta. doi:10.2118/2007-206.
- Beshry, M.A., Krawchuk P., Brown G.A., and Brough B. 2006. "Predicting the Flow Distribution on Total E&P Canada's Joslyn Project Horizontal SAGD Producing Wells Using Permanently Installed Fiber-Optic Monitoring." In *SPE Annual Technical Conference and Exhibition*, San Antonio, Texas, USA. doi:10.2118/102159-MS.
- Bhushan, B. 2000 "Modern Tribology Handbook." *CRC press*, Two Volume Set
- Blott, S., and Pye K. 2008. "Particle Shape: A Review and New Methods of Characterization and Classification." *Sedimentology* 55 (1): 31–63. doi:10.1111/j.1365-3091.2007.00892.x.
- Brand, S. 2010. "Results From Acid Stimulation in Lloydminster SAGD Applications." In *SPE International Symposium and Exhibition on Formation Damage*, Lafayette, Louisiana, USA. doi:10.2118/126311-MS.
- Brooks, R., and Tavakol H. 2012. "Experiences in Eliminating Steam Breakthrough and Providing Zonal Isolation in SAGD Wells." *Proceedings of SPE Western Regional Meeting*, Calgary, Alberta, Canada. doi:10.2118/153903-MS.
- Bruno, M.S., Bovberg C.A., and Meyer R.F. 1996. "Some Influences of Saturation and Fluid Flow on Sand Production: Laboratory and Discrete Element Model Investigations." In *SPE Annual Technical Conference*, Denver, Colorado, USA. doi:10.2118/36534-MS.
- Burton, R.C., Chin L., Davis E.R., Enderlin M.B., Fuh G., Hodge R., Ramos G.G., VanffhaDeVerg

- P., Werner M., Mathews W.L., and Petersen S. 2005. "North Slope Heavy - Oil Sand - Control Strategy : Detailed Case Study of Sand Production Predictions and Field Measurements for Alaskan Heavy - Oil Multilateral Field Developments." In *SPE Annual Technical Conference and Exhibition*, Dallas, Texas, USA. doi:10.2118/97279-MS.
- Burton, B., and Hodge R. 1999. "Drilling and Completion of Horizontal Wells Requiring Sand Control." In *SPE/IADC Drilling Conference*, Amsterdam, Netherlands. doi:10.2118/52812-MS.
- Butler, R. 1998. "SAGD Comes of Age!" *Journal of Canadian Petroleum Technology* 37 (7): 9–12. doi:10.2118/98-07-DA.
- Bybee, K. 2003. "Comparison of Cyclic Steam Stimulation and Steam Assisted Gravity Drainage." *Journal of Petroleum Technology* 55 (06): 68–69. doi:10.2118/0603-0068-JPT.
- CAPP. 2018. "Canada's Oil Sands." <https://www.capp.ca/publications-and-statistics/publications/316441>.
- Carlson, M. 2003. "SAGD and Geomechanics." *Journal of Canadian Petroleum Technology* 42 (6): 19–25. doi:10.2118/03-06-DAS.
- Carlson, J., Gurley J., King G., Price-Smith, C., and Waters F. 1992. "Sand Control : Why and How ?" *Oilfield Review* 4 (4): 41–53.
- Chanpura, R.A., Hodge R.M., Andrews J.S., Toffanin E.P., Moen T., and Parlar M. 2011. "A Review of Screen Selection for Standalone Applications and a New Methodology." *SPE Drilling & Completion*, 26(1): 84–95. doi:10.2118/127931-PA.
- Chenault, R.L. 1938. "Experiments on Fluid Capacity and Plugging of Oil-Well Screens." In *Drilling and Production Practice*. Amarillo, Texas: American Petroleum Institute.
- Cho, G., Dodds J., and Santamarina J.C. 2006. "Particle Shape Effects on Packing Density, Stiffness, and Strength: Natural and Crushed Sands." *Journal of Geotechnical and Geoenvironmental Engineering* 132 (5): 591–602. doi:10.1061/(ASCE)1090-0241(2006)132:5(591).
- Civan, F. 2016. "Reservoir Formation Damage." *Gulf Professional Publishing*, Third Edition, 277–94. doi:10.1016/B978-0-12-801898-9.00011-4.
- Clearly, M.P., Melvan J.J., and Kohlhaas C.A. 1979. "The Effect of Confining Stress and Fluid Properties on Arch Stability in Unconsolidated Sands." *SPE Annual Technical Conference and Exhibition*, Las Vegas, Nevada, USA. doi:10.2118/8426-MS.
- Coberly, C.J. 1938. "Selection of Screen Openings for Unconsolidated Sands." *Drilling and Production Practice*, API 37-189.
- Cocco, R., Karri S.B.R., and Knowlton T. 2014. "Introduction to Fluidization." *Chemical Engineering Progress* 110 (11): 21–29.
- Colbert, F.C., Costa A.L., Gachet R.F., Garcia F.M., and Neto A.T.J. 2017. "Sand Control Technology for Extended-Reach Wells : Best Practices from the Longest Gravel Packs Performed Offshore Brazil Gravel Pack Surface Equipment." In Abu Dhabi International

- Petroleum Exhibition & Conference, Abu Dhabi, UAE. doi:10.2118/188517-MS.
- Constien, V.G., and Skidmore V. 2006. "Standalone Screen Selection Using Performance Mastercurves." In *SPE International Symposium and Exhibition on Formation Damage Control*, Lafayette, Louisiana, USA. doi:10.2523/98363-MS.
- Coşkuner, G., and Maini B. 1990. "Effect of Net Confining Pressure on Formation Damage in Unconsolidated Heavy Oil Reservoirs." *Journal of Petroleum Science and Engineering* 4 (2): 105–17. doi:10.1016/0920-4105(90)90019-Y.
- Cowie, B.R. 2013. "Stable Isotope and Geochemical Investigations into the Hydrogeology and Biogeochemistry of Oil Sands Reservoir Systems in Northeastern Alberta, Canada." University of Calgary. doi:10.11575/PRISM/27867.
- Cox, M.R., and Budhu M. 2008. "A Practical Approach to Grain Shape Quantification." *Engineering Geology* 96: 1–16. doi:10.1016/j.enggeo.2007.05.005.
- Dahm, K., and Visco D. 2014 "Fundamentals of Chemical Engineering Thermodynamics". *Nelson Education*.
- Dang, T.Q.C., Chen Z., Nguyen T.B.N., Bae W., and Mai C.L. 2013. "Numerical Simulation of SAGD Recovery Process in Presence of Shale Barriers, Thief Zones, and Fracture System." *Petroleum Science and Technology* 31 (14): 1454–1470. doi:10.1080/10916466.2010.545792.
- Das, S. 2005. "Improving the Performance of SAGD." In *SPE International Thermal Operations and Heavy Oil Symposium*, Calgary, Alberta, Canada. doi:10.2118/97921-MS.
- Devere-Bennett, N. 2015. "Using Prepack Sand-Retention Tests (SRT's) to Narrow Down Liner / Screen Sizing in SAGD Wells." In *SPE Thermal Well Integrity and Design Symposium*, Banff, Alberta, Canada. doi:10.2118/178443-MS.
- Diaz, B.I.M. 2008. "Sand on Demand: An Approach to Improving Productivity in Horizontal Wells under Heavy Oil Primary Production." University of Alberta. doi:10.2118/115625-MS.
- Dusseault, M.B. 2002. "CHOPS - Cold Heavy Oil Production with Sand in the Canadian Heavy Oil Industry" *Alberta Department of Energy*.
- Dvorkin, J.P. 2008. "Can Gas Sand Have a Large Poisson's Ratio?" *Geophysics* 73 (2): E51–57. doi:10.1190/1.2821820.
- Edmunds, N. 2000. "Investigation of SAGD Steam Trap Control in Two and Three Dimensions." *Journal of Canadian Petroleum Technology* 39 (1): 30–40. doi:10.2118/00-01-02.
- Esmaelnejad, L., Siavashi F., Seyedmohammadi J., and Shabanpour M. 2016. "The Best Mathematical Models Describing Particle Size Distribution of Soils." *Modeling Earth Systems and Environment* 2 (4):1–11. doi:10.1007/s40808-016-0220-9.
- Farrow, C., Munro D., and McCarthy T. 2004. "Screening Methodology for Downhole Sand Control Selection." In *SPE Asia Pacific Oil and Gas Conference and Exhibition*. Perth, Australia. doi:10.2118/88493-MS.

- Fattahpour, V., Mahmoudi M., Wang C., Kotb O., Roostaei M., Nouri A., Fermaniuk B., Sauve A., and Sutton C. 2018. "Comparative Study on the Performance of Different Stand-Alone Sand Control Screens." In *SPE International Conference and Exhibition on Formation Damage Control*, Lafayette, Louisiana, USA. doi:10.2118/189539-MS.
- Fattahpour, V., Azadbakht S., Mahmoudi M., Guo Y., Nouri A., and Leitch M. 2016. "Effect of Near Wellbore Effective Stress on the Performance of Slotted Liner Completions in SAGD Operations." In *SPE Thermal Well Integrity and Design Symposium*, Banff, Alberta, Canada. doi:10.2118/182507-MS.
- Fattahpour, V., Moosavi M., and Mehranpour M. 2012. "An Experimental Investigation on the Effect of Grain Size on Oil-Well Sand Production." *Petroleum Science* 9 (3): 343–353. doi:10.1007/s12182-012-0218-5.
- Fonseca, J., O'Sullivan C., Coop M.R., and Lee P.D. 2012. "Non-Invasive Characterization of Particle Morphology of Natural Sands." *Soils and Foundations* 52 (4). 712–722. doi:10.1016/j.sandf.2012.07.011.
- Gates, I.D., and Leskiw C. 2010. "Impact of Steam Trap Control on Performance of Steam-Assisted Gravity Drainage." *Journal of Petroleum Science and Engineering* 75 (1–2). 215–222. doi:10.1016/j.petrol.2010.11.014.
- Gillespie, G., Deem C.K., and Malbrel C.. 2000. "Screen Selection for Sand Control Based on Laboratory Tests," *SPE Asia Pacific Oil and Gas Conference and Exhibition*, Brisbane, Australia. doi:10.2118/64398-MS.
- Göktepe, A.B., and Sezer A. 2010. "Effect of Particle Shape on Density and Permeability of Sands." *Proceedings of the Institution of Civil Engineers - Geotechnical Engineering* 163 (6): 307–320. doi:10.1680/geng.2010.163.6.307.
- Green, D.W. 2008. "Perry's Chemical Engineers' Handbook". *McGraw Hill*.
- Guo, Y. 2018. "Effect of Stress Build-up around SAGD Wellbores on the Slotted Liner Performance." University of Alberta. doi:10.7939/R3V98066B.
- Guo, Y., Roostaei M., Nouri A., Fattahpour V., Mahmoudi M., and Jung H. 2018. "Effect of Stress Build-up around Standalone Screens on the Screen Performance in SAGD Wells." *Journal of Petroleum Science and Engineering* 171: 325–339. doi:10.1016/j.petrol.2018.07.040.
- Haavind, F., Bekkelund S.S., Moen A., Kotlar H.K., Andrews J.S., and Håland T. 2008. "Experience With Chemical Sand Consolidation as a Remedial Sand-Control Option on the Heidrun Field." In *SPE International Symposium and Exhibition on Formation Damage Control*, Lafayette, Louisiana, USA. doi:10.2118/112397-MS.
- Hallman, T., Yung V.Y.B., and Albertson A. 2015. "Analysis of Wellbore Failures and Re-Design of Slotted Liners for Horizontal Wells Applied in a Heavy Oilfield." In *SPE Western Regional Meeting*. Garden Grove, California, USA. doi:10.2118/174072-MS.
- Han, G., and Dusseault M.B. 2002. "Quantitative Analysis of Mechanisms for Water-Related Sand Production." In *SPE International Symposium and Exhibition on Formation Damage Control*, Lafayette, Louisiana, USA. doi:10.2118/73737-MS.

- Handfield, T.C., Nations T.E., and Noonan S.G.. 2009. "SAGD Gas Lift Completions and Optimization: A Field Case Study at Surmont." *Journal of Canadian Petroleum Technology* 48 (11): 51–54. doi:10.2118/117489-PA.
- Hodge, R.M., Burton R.C., Constien V., and Skidmore V. 2002. "An Evaluation Method for Screen-Only and Gravel-Pack Completions." In *International Symposium and Exhibition on Formation Damage Control*, Lafayette, Louisiana, USA. doi:10.2523/73772-MS.
- Hoffmann, G.G., Steinfatt I., and Strohechein A. 1995. "Thermal Recovery Processes and Hydrogen Sulfide Formation." In *SPE International Symposium on Oilfield Chemistry*. San Antonio, Texas, USA. doi.org/10.2118/29016-MS.
- Huang, Y., Yang S., Hall M.R., and Zhang Y. 2018. "The Effects of NaCl Concentration and Confining Pressure on Mechanical and Acoustic Behaviors of Brine-Saturated Sandstone." *Energies* 11 (2): 385. doi:10.3390/en11020385.
- Huang, A.B., Chang W.J., Hsu H.H., and Huang Y.J. 2015. "A Mist Pluviation Method for Reconstituting Silty Sand Specimens." *Engineering Geology* 188: 1–9. doi:10.1016/j.enggeo.2015.01.015.
- Irani, M. 2013. "Understanding the Steam-Hammer Mechanism in Steam-Assisted-Gravity-Drainage Wells." *SPE Journal* 18 (6): 1181–1201. doi:10.2118/165456-PA.
- Rodríguez, J., Edeskär T., Knutsson S. 2013. "Particle Shape Quantities and Measurement Techniques: A Review." *The Electronic Journal of Geotechnical Engineering* 18 : 169–198. id: diva2:976352
- Jafarpour, M., Rahmati H., Azadbakht S., Nouri A., Chan D., and Vaziri H. 2012. "Determination of Mobilized Strength Properties of Degrading Sandstone." *Soils and Foundations* 52 (4): 658–667. doi:10.1016/j.sandf.2012.07.007.
- Janoo, V.C. 1998. "Quantification of Shape, Angularity, and Surface Texture of Base Course Materials." *CRREL Special Report 98-1*
- Jimenez, J. 2008. "The Field Performance of SAGD Projects in Canada." In *International Petroleum Technology Conference*, Kuala Lumpur, Malaysia. doi:10.2523/IPTC-12860-MS.
- Jin, Y., Chen J., Chen M., Zhang F., Lu Y., and Ding J. 2012. "Experimental Study on the Performance of Sand Control Screens for Gas Wells." *Journal of Petroleum Exploration and Production Technology* 2 (1): 37–47. doi:10.1007/s13202-012-0019-9.
- Kaiser, T.M.V. 2002. "Inflow Analysis and Optimization of Slotted Liners." *SPE Drilling & Completion* 17 (4): 200–209. doi:10.2118/80145-PA.
- Kaiser, T.M.V, Wilson S., and Venning L.A. 2000. "Inflow Analysis and Optimization of Slotted Liners." In *International Conference on Horizontal Well Technology*, Calgary, Alberta, Canada. doi:10.2118/65517-MS.
- Kalgaonkar, R., Chang F., Ballan A.N.A., Abadi A., and Tan A. 2017. "New Advancements in Mitigating Sand Production in Unconsolidated Formations Laboratory Procedures Chemical Preparation." In *SPE Kingdom of Saudi Arabia Annual Technical Symposium and Exhibition*,

- Dammam, Saudi Arabia. doi:10.2118/188043-MS.
- Kapadia, P.R., Wang J., Kallos M.S., and Gates I. 2011. "Reactive Thermal Reservoir Simulation: Hydrogen Sulphide Production in SAGD." In *Canadian Unconventional Resources Conference*, Calgary, Alberta, Canada. doi:10.2118/149448-MS.
- Khamehchi, E., Ameri O., and Alizadeh A. 2015. "Choosing an Optimum Sand Control Method." *Egyptian Journal of Petroleum* 24 (2): 193–202. doi:10.1016/j.ejpe.2015.05.009.
- Khilar, K.C., and Fogler H.S. 1998. "Migration of Fines in Porous Media". *Springer Science & Business Media*. Volume 12. doi:10.1007/978-94-015-9074-7.
- Khilar, K.C., and Fogler H.S. 1984. "The Existence of a Critical Salt Concentration for Particle Release." *Journal of Colloid And Interface Science* 101 (1): 214–224. doi:10.1016/0021-9797(84)90021-3.
- Kia, S.F., Fogler H.S., and Reed M.G. 1987. "Effect of PH on Colloidally Induced Fines Migration." *Journal of Colloid And Interface Science* 118 (1): 158–168. doi:10.1016/0021-9797(87)90444-9.
- Krumbein, W.C., and Sloss L.L. 1951. "Stratigraphy and Sedimentation." *Soil Science Society of America Journal*. 71 (5): 401. doi:10.1086/625952.
- Kuerbis, R., and Vaid Y.P. 1988. "Sand Sample Preparation-the Slurry Deposition Method." *Soils and Foundations* 28 (4): 107–118. doi:10.3208/sandf1972.28.4_107.
- Ladd, R.S. 1978. "Preparing Test Specimens Using Undercompaction." *Geotechnical Testing Journal* 1 (1): 16–23. doi:10.1520/GTJ10364J.
- Latiff, A. 2011. "Assessment and Evaluation of Sand Control Methods for a North Sea Field." Imperial College London. doi: <http://hdl.handle.net/10044/1/24371>
- Layne, L.A., and F W Gerwick. 1973. "Wire Wrapped Well Screen." U.S Patent Number: 3,709,293.
- Lees, G. 1964. "A New Method for Determining the Angularity of Particles." *Sedimentology* 3 (1): 2–21. doi:10.1111/j.1365-3091.1964.tb00271.x.
- Leone, J.A., and Scott M.E. 1988. "Characterization and Control of Formation Damage During Waterflooding of a High-Clay-Content Reservoir." *SPE Reservoir Engineering* 3 (04): 1279–1286. doi:10.2118/16234-PA.
- Lightbown, V. 2017. "New SAGD Technologies Show Promise in Reducing Environmental Impact of Oil Sand Production." *Journal of Environmental Solutions for Oil, Gas, and Mining* 1 (2): 1–12.
- Liu, X., and Civan F. 1996. "Formation Damage and Filter Cake Buildup in Laboratory Core Tests : Modeling and Model-Assisted Analysis." *SPE Formation Evaluation* 11 (1): 26–30. doi:10.2118/25215-PA.
- Liu, X., and Civan F. 1994. "Formation Damage and Skin Factor Due to Filter Cake Formation and Fines Migration in the Near-Wellbore Region." In *SPE International Symposium on*

- Formation Damage Control*, Lafayette, Louisiana, USA. doi:10.2118/27364-MS.
- Liu, X., and Civan F. 1995. "Formation Damage by Fines Migration Including Effects of Filter Cake, Pore Compressibility, and Non-Darcy Flow-A Modeling Approach to Scaling From Core to Field." In *SPE International Symposium on Oilfield Chemistry*, San Antonio, Texas, USA. doi:10.2118/28980-MS.
- Liu, X., and Civan F. 1993. "Characterization and Prediction of Formation Damage in Two-Phase Flow Systems." In *SPE Production Operations Symposium*, Oklahoma City, Oklahoma, USA. doi:10.2118/25429-MS.
- Liu, X., Jiang X., Liu J., Li J., and Li W. 2017. "The Effect of the Injection Salinity and Clay Composition on Aquifer Permeability." *Applied Thermal Engineering* 118: 551–60. doi:10.1016/j.applthermaleng.2017.02.098.
- Powers, M.C. 1953. "A New Roundness Scale for Sedimentary Particles." *Journal of Sedimentary Research* 23 (2): 117–19. doi:10.1306/D4269567-2B26-11D7-8648000102C1865D.
- Mahmoudi, M., Fattahpour V., Roostaei M., Kotb O., Wang C., Nouri A., Sutton C., and Fermaniuk B. 2018. "An Experimental Investigation into Sand Control Failure Due to Steam Breakthrough in SAGD Wells." In *SPE Canada Heavy Oil Technical Conference*, Calgary, Alberta, Canada. doi:10.2118/189769-MS.
- Mahmoudi, M., Nejadi S., Roostaei M., Olsen J., Fattahpour V., Lange C.F., Zhu D., Fermaniuk B., and Nouri A. 2017. "Design Optimization of Slotted Liner Completions in Horizontal Wells: An Analytical Skin Factor Model Verified by Computational Fluid Dynamics and Experimental Sand Retention Tests." In *SPE Thermal Well Integrity and Design Symposium*. Banff, Alberta, Canada. doi:10.2118/188167-MS.
- Mahmoudi, M. 2016. "New Sand Control Design Criteria and Evaluation Testing for Steam Assisted Gravity Drainage (SAGD) Wellbores." University of Alberta. doi:10.7939/R3C824S55.
- Mahmoudi, M., Fattahpour V., Nouri A., and Leitch M. 2016a. "An Experimental Investigation of the Effect of PH and Salinity on Sand Control Performance for Heavy Oil Thermal Production." In *SPE Canada Heavy Oil Technical Conference*. Calgary, Alberta, Canada. doi:10.2118/180756-MS.
- Mahmoudi, M., Fattahpour V., Nouri A., Rasool S., and Leitch M. 2016b. "The Effect of Screen Aperture Size on Fines Production and Migration in SAGD Production Wells." In *Heavy Oil Congress*, Calgary, Alberta, Canada. WHOC16 - 612.
- Mahmoudi, M., Fattahpour V., A Nouri A., Yao T., Baudet A.B., Leitch M., and Fermaniuk B. 2016c. "New Criteria for Slotted Liner Design for Heavy Oil Thermal Production." In *SPE Thermal Well Integrity and Design Symposium*. Banff, Alberta, Canada. doi:10.2118/182511-MS.
- Manchuk, J.G., Babak O., and Deutsch C.V. 2013. "Geostatistical Modeling of Particle Size Distributions in the McMurray Formation." *CIM Journal* 4 (2).
- Manuwa, S.I. 2012. "Evaluation of Soil / Material Interface Friction and Adhesion of Akure Sandy

- Clay Loam Soils in Southwestern Nigeria.” *Advances in Natural Science* 5 (1): 41–46. doi:10.3968/j.ans.1715787020120501.1015.
- Marfo, S.A., Appah D., Joel O.F., and Ofori-Sarpong G. 2015. “Sand Consolidation Operations, Challenges and Remedy.” In *SPE Nigeria Annual International Conference and Exhibition*. doi:10.2118/178306-MS.
- Markestad, P., Christie O., Espedal A., and Rorvik O. 1996. “Selection of Screen Slot Width to Prevent Plugging and Sand Production.” In *SPE Formation Damage Control Symposium*. Lafayette, Louisiana, USA. doi:10.2118/31087-MS.
- Matanovic, D., Cikes M., and Moslavac B. 2012. Sand Control in Well Construction and Operation. *Springer Science & Business Media*. doi:10.1007/978-3-642-25614-1.
- Mathisen, A., Aastveit G., and Alteraas E. 2007. “Successful Installation of Standalone Sand Screen in More Than 200 Wells-The Importance of Screen Selection Process and Fluid Qualification.” *Proceedings of European Formation Damage Conference*, Scheveningen, The Netherlands. doi:10.2118/107539-MS.
- Mishra, S., and Ojha K. 2016. “Nanoparticle Induced Chemical System for Consolidating Loosely Bound Sand Formations in Oil Fields.” *Journal of Petroleum Science and Engineering* 147: 15–23. doi:10.1016/j.petrol.2016.05.005.
- Miura, S., and Toki S. 1982. “A Sample Preparation Method and Its Effect on Static and Cyclic Deformation-Strength Properties of Sand.” *Soils and Foundations* 22 (1): 61–77. doi:10.3208/sandf1972.22.61.
- Mohan, K.K., Vaidya R.N., Reed M.G., and Fogler H.S. 1993. “Water Sensitivity of Sandstones Containing Swelling and Non-Swelling Clays.” *Colloids in the Aquatic Environment* 73: 237–254. doi:10.1016/0927-7757(93)80019-B.
- Montero, J., Chissonde S., Kotb O., Wang C., Roostaei M., Nouri A., Mahmoudi M., and Fattahpour V. 2018. “Critical Review of Sand Control Evaluation Testing for SAGD Applications,” In *SPE Canada Heavy Oil Technical Conference*, Calgary, Alberta, Canada. doi:10.2118/189773-MS.
- Morita, N., and Boyd P.A. 1991. “Typical Sand Production Problems: Case Studies and Strategies for Sand Control.” In *SPE Annual Technical Conference and Exhibition*, Dallas, Texas, USA. doi:10.2118/22739-MS.
- Morita, N., Whitfill D.L., Massie I., and Knudsen T.W. 1989a. “Realistic Sand-Production Prediction: Numerical Approach.” *SPE Production Engineering* 4 (1): 15–24. doi:10.2118/16989-PA.
- Morita, N., Whitfill D.L., Fedde O.P., and Levik T.H. 1989b. “Parametric Study of Sand-Production Prediction: Analytical Approach.” *SPE Production Engineering* 4 (01): 25–33. doi:10.2118/16990-PA.
- Muecke, T.W. 1979. “Formation Fines and Factors Controlling Their Movement in Porous Media.” *Journal of Petroleum Technology* 31 (2):144–150. doi:10.2118/7007-PA.

- Mungan, N. 1965. "Permeability Reduction Through Changes in PH and Salinity." *Journal of Petroleum Technology* 17 (12): 1449–1453. doi:10.2118/1283-PA.
- De Nevers, N., and Grahn R. 1991. "Fluid Mechanics for Chemical Engineers." *New York: McGraw-Hill*.
- Nexen CNOOC. 2017. "Long Lake Kinosis Oil Sands Project Annual Performance Presentation." *Alberta Energy Reguator*.
- Oda, M. 1972. "Initial Fabrics and Their Relations To Mechanical Properties of Granular Material." *Soils and Foundations* 12 (1): 17–36. doi:10.3208/sandf1960.12.17.
- O'Hara, M. 2015. "Thermal Operations In The McMurray ; An Approach To Sand Control." In *SPE Thermal Well Integrity and Design Symposium*, Banff, Alberta, Canada. doi:10.2118/178446-MS.
- Ovalle, C., Dano C., Hicher P., and Cisternas M. 2014. "Experimental Framework for Evaluating the Mechanical Behavior of Dry and Wet Crushable Granular Materials Based on the Particle Breakage Ratio." *Canadian Geotechnical Journal* 52 (5): 587–598. doi:10.1139/cgj-2014-0079.
- Oyenevin, M.B. 1988. "Formation Sand Size Prediction From Well-Log Correlations." *Society of Petroleum Engineers*,. SPE 16245-MS.
- Pan, T. 2002. "Fine Aggregate Characterization Using Digital Image Analysis." Louisiana State University and Agricultural and Mechanical College. URL: https://digitalcommons.lsu.edu/gradschool_theses/1771.
- Papamichos, E., Cerasi P., Stenebraten J.F., Berntsen A.N., Ojala I., Vardoulakis I., Brignoli M., Fuh G.F., Han G., Nadeem A., Ray P., and Wold S. 2010. "Sand Production Rate under Multiphase Flow and Water Breakthrough." In *44th U.S. Rock Mechanics Symposium and 5th U.S.-Canada Rock Mechanics Symposium*. Salt Lake City, Utah, USA. ARMA-10-340.
- Papamichos, E., and Malmanger E.M. 1999. "A Sand-Erosion Model for Volumetric Sand Predictions in a North Sea Reservoir." In *Latin American and Caribbean Petroleum Engineering Conference*, Caracas, Venezuela. doi:10.2118/54007-ms.
- Parlar, M., Tibbles R.J., Gadiyar B., and Stamm B. 2016. "A New Approach for Selecting Sand-Control Technique in Horizontal Openhole Completions." *SPE Drilling & Completion* 31 (1): 4–15. doi:10.2118/170691-PA.
- Penberthy, W.L., and Shaughnessy C.M. 1992. "Sand Control." *Society of Petroleum Engineers*.
- Peterson, D., West H.P.D., and Washington B. 2007. "Guidelines for Produced Water Evaporators in SAGD." *IWC*. 7 (68): 1–16.
- Price-Smith, C., Parlar M., Bennett C., Gilchrist J.M., Pitoni E., Burton R.C., Hodge R.M., Troncoso J., Ali S.A., and Dickerson R. 2003. "Design Methodology for Selection of Horizontal Openhole Sand-Control Completions Supported by Field Case Histories." *SPE Drilling & Completion* 18 (3): 235–255. doi:10.2118/85504-PA.
- Procyk, A. Whitlock M., and Ali S. 1998. "Plugging-Induced Screen Erosion Difficult to Prevent."

Oil & Gas Journal 96 (29): 80.

- Ravalec, M.L., Morlot C., Marmier R., and Foulon D. 2009. "Heterogeneity Impact on SAGD Process Performance in Mobile Heavy Oil Reservoirs." *Oil & Gas Science and Technology - Revue de l'IFP* 64 (4): 469–476. doi:10.2516/ogst/2009014.
- Riley, N.A. 1941. "Projection Sphericity." *Journal of Sedimentary Research* 11 (2): 94–95. doi:10.1306/D426910C-2B26-11D7-8648000102C1865D.
- Rhodes, M. 2008. "Introduction to Particle Technology." *John Wiley & Sons*. 2nd edition.
- Roberts, C., and Abbakumov K. 2014. "Key Companies Active in Alberta Oil Sands" U.S. Department of Commerce, Calgary, Alberta, Canada.
- Rodríguez, J., Edeskär T., Knutsson S. 2013. "Particle Shape Quantities and Measurement Techniques - A Review." *Electronic Journal of Geotechnical Engineering* 18: 169–198. URL: https://pure.ltu.se/portal/files/41279547/shape_report_november_2012_A4.pdf.
- Rogers, E.B. 1971. "Sand Control in Oil and Gas Wells." *Oil and Gas Journal*. November: 54-60.
- Romanova, U.G., Piwowar M., and Ma T., 2015. "Sand Control for Unconsolidated Heavy Oil Reservoirs : A Laboratory Test Protocol and Recent Field Observations." In *International Symposium of the Society of Core Analysts*, St. John, Newfoundland and Labrador, Canada.
- Romanova, U.G., Gillespie G., Sladic J., Ma T., Solvoll T.A., and Andrews J.S. 2014. "A Comparative Study of Wire Wrapped Screens vs . Slotted Liners for Steam Assisted Gravity Drainage Operations." *World Heavy Oil Congress*, New Orleans, Louisiana, USA. WHOC14 - 113.
- Romanova, U.G., Ma T. 2013. "An Investigation of the Plugging Mechanisms in a Slotted Liner from the Steam Assisted Gravity Drainage Operations." In *SPE European Formation Damage Conference and Exhibition*, Noordwijk, The Netherlands. doi:10.2118/165111-MS
- Roostaei, M., Nouri A., Fattahpour V., Mahmoudi M., Izadi M., Ghalambor A., and Fermaniuk B. 2018a. "Sand Control Design through Assessment of Mathematical Models Representing Particle Size Distribution of Reservoir Sands." In *SPE International Symposium on Formation Damage Control*, Lafayette, Louisiana, USA. doi:10.2118/189528-MS.
- Roostaei, M., Kotb O., Mahmoudi M., Fattahpour V., Wang C., Nouri A., and Fermaniuk B. 2018b. "An Experimental Investigation into Gravel Pack Performance in Steam-Drive Operations." In *SPE Western Regional Meeting*, Garden Grove, California, USA. doi:10.2118/190125-MS.
- Rousé, P .C., Fannin R.J., and Shuttle D.A. 2008. "Influence of Roundness on the Void Ratio and Strength of Uniform Sand." *Géotechnique* 58 (3): 227–231. doi:10.1680/geot.2008.58.3.227.
- Santarelli, F.J., Detienne J.L., and Zundel J.P. 1989. "Determination of the Mechanical Properties of Deep Reservoir Sandstones to Assess the Likelihood of Sand Production." In *ISRM International Symposium. International Society for Rock Mechanics*, Pau, France. ISRM-IS-1989-100.
- Sarkar, A., and Sharma M. 1990. "Fines Migration in Two-Phase Flow." *Journal of Petroleum*

- Technology* 42 (5): 646–652. doi:10.2118/17437-PA.
- Shahsavari, M.H., and Khomehchi E. 2018. “Optimum Selection of Sand Control Method Using a Combination of MCDM and DOE Techniques.” *Journal of Petroleum Science and Engineering* 171: 229–241. doi:10.1016/j.petrol.2018.07.036.
- Sheng, J. 2013. “Enhanced Oil Recovery Field Case Studies” *Gulf Professional Publishing*. 413–445. doi:10.1016/B978-0-12-386545-8.00017-8.
- Shinohara, K., Oida M., and Golman B. 2000. “Effect of Particle Shape on Angle of Internal Friction by Triaxial Compression Test.” *Powder Technology* 107 (1–2): 131–136. doi:10.1016/S0032-5910(99)00179-5.
- Sidahmed, A.K. 2018. “Optimization of Outflow Control Devices Design in Steam-Assisted Gravity Drainage Models with Wellbore Trajectory Excursions.” University of Alberta. doi:10.7939/R32R3PC88.
- Simon, D.E., McDaniel B.W., and Coon R.M. 1976. “Evaluation of Fluid PH Effects on Low Permeability Sandstones.” In *SPE Annual Fall Technical Conference and Exhibition*, New Orleans, Louisiana, USA. doi:10.2118/6010-MS.
- Singh, P., Ludanova N., and Petegem R.V. 2014. “Advancing Chemical Sand and Fines Control Using Zeta Potential Altering Chemistry by Using Advanced Fluid Placement Techniques.” In *SPE International Symposium and Exhibition on Formation Damage Control*. Lafayette, Louisiana, USA. doi:10.4043/24690-MS.
- Sivagnanam, M., Wang J., and Gates I.D. 2017. “On the Fluid Mechanics of Slotted Liners in Horizontal Wells.” *Chemical Engineering Science* 164: 23–33. doi:10.1016/j.ces.2017.01.070.
- Slack, M.W., Roggensack W.D., Wilson G., and Lemieux R.O. 2000. “Thermal-Deformation-Resistant Slotted-Liner Design for Horizontal Wells.” In *SPE/CIM International Conference on Horizontal Well Technology*, Calgary, Alberta, Canada. doi:10.2118/65523-MS.
- Smart, P. 2013. “Particle Shape Statistics Revisited.” University of Glasgow.
- Sokolov, V.N., and Tchistiakov A.A. 1999. “Physico-Chemical Factors of Clay Particle Stability and Transport in Sandstone Porous Media” In *European Geothermal Conference*, Basel, Switzerland.
- Sparlin, D. 1969. “Fight Sand with Sand - A Realistic Approach to Gravel Packing.” *Fall Meeting of the Society of Petroleum Engineers of AIME*, Denver, Colorado, USA. doi:10.2118/2649-MS.
- Spronk, E.M., Doan L.T., Matsuno Y., and Harschnitz B. 2015. “SAGD Liner Evaluation and Liner Test Design for JACOS Hangingstone.” In *SPE Canada Heavy Oil Technical Conference*, Calgary, Alberta, Canada. doi:10.2118/174503-MS.
- Stein, N., Odeh A.S., and Jones L.G. 1974. “Estimating Maximum Sand-Free Production Rates from Friable Sands for Different Well Completion Geometries.” *Journal of Petroleum Technology* 26 (10): 1156–1158. doi:10.2118/4534-PA.

- Stein, N., and Hilchie D.W. 1972. “Estimating the Maximum Production Rate Possible from Friable Sandstones without Using Sand Control.” *Journal of Petroleum Technology*, 24 (9): 1157–1160. doi:10.2118/3499-PA.
- Stone, T.W., and Bailey W.J. 2014. “Optimization of Subcool in SAGD Bitumen Processes.” *World Heavy Oil Congress*, New Orleans Louisiana, USA.WHOC14-271.
- Suman, G.O., Ellis R.C., and Snyder R.E. 1983. “Sand Control Handbook: Prevent Production Losses and Avoid Well Damage with These Latest Field-proven Techniques.” *Gulf Publishing Company*, 2nd edition.
- Sun, C., Shuang S., Zeng H., Fattahpour V., Mahmoudi M., and Luo J. 2018. “Investigation of Corrosion Properties of a High-Phosphorus Ni-P Coating and Corrosion Resistant Alloys in 3.5 Wt.% NaCl Solution.” In *Corrosion 2018*, Phoenix, Arizona, USA. NACE-2018-11526.
- Sympatec. 2018. “Appendix.” *PAQXOS Software User Manual*.
- Tausch, G.H., and Corley B. 1958. “Sand Exclusion in Oil and Gas Wells.” In *Drilling and Production Practice*, New York, New York, USA.
- Tiffin, D.L, King G.E., Larese R.E., and Britt L.K. 1998. “New Criteria for Gravel and Screen Selection for Sand Control.” In *SPE International Symposium on Formation Damage Control*, Lafayette, Louisiana, USA. doi:10.2118/39437-MS.
- Toma, P., Livesey D., and Heidrick T. 1988. “New Sand-Control Filter for Thermal Recovery Wells.” *SPE Production Engineering* 3 (2): 249–257. doi:10.2118/15057-PA.
- Ueng, T., Wang M., Chen M., Chen C., and Peng L. 2006. “A Large Biaxial Shear Box for Shaking Table Test on Saturated Sand.” *Geotechnical Testing Journal* 29 (1): 1–8. doi:10.1520/GTJ12649.
- Underdown, D.R., Dickerson R.C., and Vaughan W. 1999. “Nominal Sand Control Screen: A Critical Evaluation of Screen Performance.” In *SPE Annual Technical Conference and Exhibition*, Houston, Texas, USA. doi:10.2118/56591-MS.
- University of Florida. 2017. “Fluidization: A Unit Operation in Chemical Engineering.” Unit Operations Laboratory, Department of Chemical Engineering, University of Florida.
- USACE. 1990. “Engineering and Design: Settlement Analysis.” *Engineer Manual 1110-1-1904 Department of the Army U.S. Army Corps of Engineers* 1110-1-1904 EM.
- Vaid, Y.P., and Sivathayalan S. 2000. “Fundamental Factors Affecting Liquefaction Susceptibility of Sands.” *Canadian Geotechnical Journal* 37 (3): 592–606. doi:10.1139/t00-040.
- Valdya, R., and Fogler H. 1992. “Fines Migration and Formation Damage: Influence of PH and Ion Exchange.” *SPE Production Engineering* 7 (4): 325–330. doi:10.2118/19413-PA.
- Vaziri, H., Barree B., Xiao Y., Palmer I., and Kutas M. 2002. “What Is the Magic of Water in Producing Sand?” In *SPE Annual Technical Conference and Exhibition*, San Antonio, Texas, USA. doi:10.2118/77683-MS.
- Vaziri, H.H., Allam R.D., Kidd G.A., Bennett C.L., Grose T.D., Robinson P.A., and Malyn J.

2006. "Sanding: A Rigorous Examination of the Interplay Between Drawdown, Depletion, Startup Frequency, and Water Cut." *SPE Production & Operations* 21 (4): 430–440. doi:10.2118/89895-pa.
- Veeken, C.A.M., Davies D.R., Kenter C.J., and Kooijman A.P. 1991. "Sand Production Prediction Review: Developing an Integrated Approach." In *SPE Annual Technical Conference and Exhibition*, Dallas, Texas, USA. doi:10.2118/22792-MS.
- Wadell, H. 1932. "Volume, Shape, and Roundness of Rock Particles." *The Journal of Geology* 40 (5): 443–451.
- Wadell, H. 1935. "Volume, Shape, and Roundness of Quartz Particles." *The Journal of Geology* 43 (3): 250–280. doi:10.1086/624298.
- Wan, R. 2011. "Advanced Well Completion Engineering". *Gulf Professional Publishing*. 3rd edition. doi:10.1016/B978-0-12-385868-9.00016-6.
- Wang, W., and Coop M.R. 2016. "An Investigation of Breakage Behaviour of Single Sand Particles Using a High-Speed Microscope Camera." *Géotechnique* 66 (12): 984–998. doi:10.1680/jgeot.15.P.247.
- Wen, S., Zhao Y., Liu Y., and Hu S. 2007. "A Study on Catalytic Aquathermolysis of Heavy Crude Oil During Steam Stimulation." In *International Symposium on Oilfield Chemistry*, Houston, Texas, USA. doi:10.2118/106180-MS.
- Wentworth, C.K. 1919. "A Laboratory and Field Study of Cobble Abrasion." *The Journal of Geology* 27 (7): 507–521. doi:10.1086/622676.
- Wentworth, C.K. 1922. "A Scale of Grade and Class Terms for Clastic Sediments." *The Journal of Geology* 30 (5): 377–392. doi:10.1086/622910.
- Weatherford Laboratories. 2015. "Nexen Energy ULC Sand Control Study Field: Long Lake South West Formation: McMurray Internal Report". Unpublished.
- Williams, C.F., Richard B.M., and Horner D. 2006. "A New Sizing Criterion for Conformable and Nonconformable Sand Screens Based on Uniform Pore Structures." In *SPE International Symposium and Exhibition on Formation Damage Control*, Lafayette, Louisiana, USA. doi:10.2118/98235-MS.
- Williamson, H., Babaganov A., and Romanova U. 2016. "Unlocking Potential Of The Lower Grand Rapids Formation, Western Canada: The Role Of Sand Control and Operational Practices in SAGD Performance." In *SPE Canada Heavy Oil Technical Conference*, Calgary, Alberta, Canada. doi:10.2118/180700-MS.
- Witt, K.J., and Brauns J. 1983. "Permeability-Anisotropy Due to Particle Shape." *Journal of Geotechnical Engineering* 109 (9): 1181–1187. doi:10.1061/(ASCE)0733-9410(1983)109:9(1181).
- Wu, B., Choi S.K., Feng Y., Denke R., Barton T., Wong C.Y., Boulanger J., Yang W., Lim S., Zamberi M., Shaffee S., Jadid M.B., Johar Z., and Madon B.B. 2016. "Evaluating Sand Screen Performance Using Improved Sand Retention Test." In *Offshore Technology*

- Conference Asia*, Kuala Lumpur, Malaysia. doi: 10.4043/26434-MS.
- Yang, D., and Macaraeg L. 2013. "Horizontal Well Completion Technology for Improved Heavy Oil Production." In *GeoConvention: Integration*, Calgary, Alberta, Canada.
- Yang, H., and Baudet B.A. 2016. "Characterisation of the Roughness of Sand Particles." *Procedia Engineering* 158: 98–103. doi:10.1016/j.proeng.2016.08.412.
- Yeh, C.S., Clingman S., Dale B.A., Moffett T., Harrison L., Barry M.D., Hecker M.T., and Haerberle D. 2008. "Unlocking the Limits of Extreme Length in Alternate Path Gravel Packing." In *International Petroleum Technology Conference*, Kuala Lumpur, Malaysia. doi:10.2523/IPTC-12549-MS.
- Younessi, A., Rasouli V., and Wu B. 2012. "Proposing a Sample Preparation Procedure for Sanding Experiments." In *Southern Hemisphere International Rock Mechanics Symposium*, Sun City, South Africa. URL: <http://hdl.handle.net/20.500.11937/17695>.
- Zhang, Z. 2017. "An Advanced Sand Control Technology for Heavy Oil Reservoirs." University of Calgary. doi:10.11575/PRISM/27963.
- Zhou, X., Liu D., Bu H., Deng L., Liu H., Yuan P., Du P., and Song H.. 2018. "XRD-Based Quantitative Analysis of Clay Minerals Using Reference Intensity Ratios, Mineral Intensity Factors, Rietveld, and Full Pattern Summation Methods: A Critical Review." *Solid Earth Sciences* 3 (1): 16–29. doi:10.1016/j.sesci.2017.12.002.
- Zhu, D., Leitch M., Wang J., Shi X., Gong L., Aghaie E., Luo J.L., and Zeng H. 2016. "Evaluation of an Advanced Metal Bonded Coating Technology for Improved SAGD Performance Thermal-Chemical Environment of SAGD." In *SPE Latin America and Caribbean Heavy and Extra Heavy Oil Conference*, Lima, Peru. doi:10.2118/181181-MS.

Appendix A: Determining Stress During Saturation

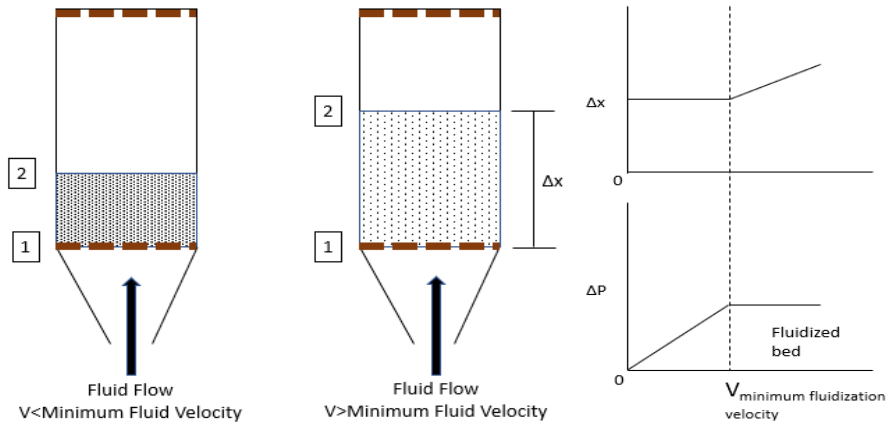


Figure A-1 Modified illustrations of the phenomena of bed fluidization (De Nevers 1999)

Introduction

Fluidization is a process where solids can act as a fluid by injecting fluids upwards through the particle reactor. Fluidization is a process in which solids are caused to behave like a fluid by blowing gas or liquid upwards through the solid-filled reactor (Cocco et al. 2014). It is crucial to suppress this phenomenon by applying stress not to disturb the sand-pack homogeneity produced by the packing. In this section details of calculations of the stress required to prevent fluidization is presented. The procedure is adapted from a manual on fluidization (University of Florida 2017).

Table A-1. Lab constants and assumptions during saturation

Constants						
Particle Density	2.69	g/cm ³				
Length of cell	40	cm				
Diameter of the cell	15	cm				
g	981	cm/s ²				
1 psi	6894.76	pa				
Sphericity	0.885					
D50	44	μm	0.004	cm		
Saturating fluid density (water)	1	g/cc				
Saturating fluid viscosity (μ_f)	1	cp or mPa. S				
Porosity	0.3					
Saturation fluid flow rate	2000	cc/hr	33	cc/min	0.555667	cc/s

$$Area = \pi \frac{D^2}{4} = \pi \frac{15^2}{4} = 177 \text{ cm}^2 \quad (A.1)$$

$$Cell \text{ volume} = D^2 * \pi * \frac{L}{4} = 15^2 * \pi * \frac{40}{4} = 7069 \text{ cm}^3 \quad (A.2)$$

$$Matrix \text{ vol.} = Cell \text{ vol.} * (1 - porosity) = 7069 * (1 - 0.3) = 4948 \text{ cm}^3 \quad (A.3)$$

$$\begin{aligned} Net \text{ weight of grains} &= Weight - Buoyancy = 4085 * 981 * (2.69 - 1) \\ &= 8,187,074 \text{ g.cm/s}^2 = 81.6 \text{ N} \end{aligned} \quad (B.4)$$

$$Superficial \text{ velocity} = \frac{Flow \text{ rate}}{Area} = \frac{0.555667}{177} = 0.003150089 \text{ cm/s} \quad (A.5)$$

Applying Carman-Kozney equation

$$\nabla P = \frac{180 * Superficial \text{ velocity} * \mu_f * (1 - porosity)^2}{(Particle \text{ diameter} * sphericity)^2 * porosity^3} \quad (A.6)$$

$$\nabla P = \frac{180 * 0.003150089 / 100 * 1 / 1000 * (1 - 0.3)^2}{(44 * 0.88 / 100)^2 * 0.3^3} = 67,863 \text{ Pa} \quad (A.7)$$

$$Fluidizing \text{ force} = \nabla P * Area * length = 67,863 * \frac{33.02}{100} * \frac{177}{10,000} = 396 \text{ N} \quad (A.8)$$

Assuming no stress is applied

$$Net \text{ force on grains} = Net \text{ weight of grains} - Fluidizing \text{ force} \quad (A.9)$$

$$Net \text{ force on grains} = 81.6 - 396 = -314 \text{ N} \quad (A.10)$$

$$The \text{ net force on grains is negative indicating fluidization will occur} \quad (A.11)$$

Applying stress of 60 psi

$$Net \text{ force on grains} = Force \text{ induced due to applied stress} + Net \text{ weight of grains} - Fluidizing \text{ force} \quad (A.12)$$

$$Force \text{ induced due to applied stress} = Stress \text{ applied} * Area = 60 * 6894 * 177 / 10,000 = 7,310 \text{ N} \quad (A.13)$$

$$Net \text{ force on grains} = 7310 - 67.6 - 314 = 6,996 \text{ N} \quad (A.14)$$

The net force is positive indicating fluidization will not occur.

Appendix B: Flow Rate Estimation

Table B-1. Lab and field constants and assumptions

Calculation parameters		
Coupon Diameter	17.1	cm
Coupon area	229.7	cm ²
Coupon area	0.023	m ²
Average steam injection rate (provided by Nexen)	270	m ³ /day
Water density	1000	kg/m ³
Mass of water injection	270000	kg/day
Well length (provided by Nexen)	0.8	km
Steam quality	0.5	

Table B-1. Field production information

Field information	
Oil rate, m ³ /d	80
Water rate, m ³ /d	270
Liquid rate, m ³ /d	350
Liquid rate, bbl/d	2201
WOR	3.38
Length of wells, km	0.80
Oil Rate/length, m ² /d	0.10
Water Rate/length, m ² /d	0.34
Liquid Rate/length, m ² /d	0.44
Oil Rate/Liner surface area, m/d	0.18
Water Rate/Liner surface area, m/d	0.60
Liquid Rate/Liner surface area, m/d	0.78
Liquid Rate/Liner surface area, bbl/ft ²	0.46

Estimation of Effective Flow Factor and Corresponding Lab Flow Rates

As discussed in Chapter 4, the effective flow factor is a term used to quantify the uneven production of fluids along the length of a SAGD well. The factor is a function of SCD plugging, uniformity due to completion or reservoir heterogeneity, and length of non-contributing sections of the production well. A study by (Beshry et al. 2006) quantified heterogeneity of fluid production in a SAGD well using distributed temperature sensing data. The results show that non-uniform

flow can cause difference from average production per unit area by as much as 50% in some sections. Another study reported plugging of the slotted liners in SAGD wells can reduce the open to flow area by as much as 90%. Non-contributing sections in SAGD wells are on average around 20% based on the recommendation of industry professionals. Table A-3 shows the fluid flow scenarios simulated during the sand control testing. The information provided above was the basis by which the values of different factors contributing to the effective flow factor were assigned.

Table C-3. Scenarios of effective flow represented in the testing

Effective flow factor calculation				
Scenario	Non-uniform effect	Plugging factor	Blank sections	Effective flow factor
Good SAGD well condition	0.8	0.5	0.8	0.32
Non-uniform flow	0.5	0.5	0.8	0.2
Plugged and non-uniform flow	0.5	0.3	0.8	0.12

Table C-4. Scenarios of effective flow represented in the testing

Scenario	Effective flow	Lab equivalent Oil rate, cc/hr.	Lab equivalent Water rate, cc/hr.	Lab equivalent Liquid rate, cc/hr.
Perfect SAGD well condition	1.0	1171	578	749
Good SAGD well condition	0.32	535	1807	2342
Non-uniform flow	0.20	857	2891	3747
Plugged and non-uniform flow	0.12	1428	4818	6246

Table C-4 shows the different fluid flow scenarios calculated at lab conditions using data from table C-1, C-2, and C-3. These liquid flow rates are then incorporated in the testing procedure to represent SAGD conditions.

Table C-5. Steam rate calculations

Temperature, °C	210
Pressure, kPa	1600
Temp for dry steam, °C	204.384
Density of steam, kg/m ³	8.42
Steam Viscosity, cp	0.016
Steam rate m ³ /d	31,544
Length of wells, km	0.8
Steam Rate/length m ³ /m	39.4
Steam Rate/surface area m ³ /m ²	70.6
Lab equivalent Steam rate, cm ³ /hr.	67,548
Lab equivalent Steam rate, L/min	1.1
Steam quality, %	50
Good scenario Steam rate, L/min	0.9
Non-uniform scenario Steam rate, L/min	1.4
Plugged and non-uniform scenario Steam rate, L/min	2.3

Appendix C: Initial Absolute Permeability

Table C-1 shows the initial permeability of the sand pack for all the tests just after the saturation phase. The difference between the permeability at the top and middle is less than 5% for all the tests. For more details about each test refer to Table 4-2 and Table 4-4.

Table C-1. Initial permeability of the sand pack of each test

Test #	Batch #	Top permeability, md	Middle permeability, md	Difference, %
Rep 1	3	1846	1764	4.5
Rep 2	3	1920	1870	2.7
1	2	1633	1560	4.6
2	3	1664	1746	4.8
3	3	2668	2805	5.0
4	3	2855	2991	4.7
5	3	2847	2945	3.4
6	3	2731	2828	3.5

Appendix D: Friction Approximation Across the Core

Axial load loss in Hycal setup and the University setup is calculated here. The high wall surface area to cross-sectional area ratio for the Hycal setup compared with the same for the University setup results in a higher loss of axial load, hence, a non-uniform stress distribution along the sample. This design element can significantly decrease the stress at the slot opening in Hycal setup, thus, magnify the sand production. Table 1 shows the properties used in the stress calculations.

Table D-1. Mechanical properties of University of Alberta (UofA) and Hycal setup and sands

Sand density UofA	2.68	g/cm ³
Sand density Hycal	2.65	g/cm ³
Young modulus of loose sand, E _{max} (USACE 1990)	3472.2	psi
Young modulus of loose sand, E _{min} (USACE 1990)	1388.89	psi
Poission ratio v _{max} (Dvorkin 2008)	0.237	dimensionless
Poission ratio v _{min} (Dvorkin 2008)	0.115	dimensionless
ID of core UofA	15.24	cm
ID of core Hycal	6.31	cm
Length of core holder Hycal	20	cm
Length of core holder UofA	42	cm
Sand mass in core UofA	11000	g
S _w UofA	0.32	

The equation to calculate Friction factor for stainless steel and unconsolidated sand (Manuwa 2012)

$$Friction\ Factor\ (FF) = 0.0019S_w^3 - 0.0188S_w^2 + 0.735S_w + 0.2951 \quad (D.1)$$

For Moist tamping in UofA testing:

$$\begin{aligned} Friction\ Factor\ (FF) &= 0.0019(0.32)^3 - 0.0188(0.32)^2 + 0.735(0.32) + 0.2951 \\ &= 0.53 \quad (D.2) \end{aligned}$$

For Hycal testing:

$$\begin{aligned} Friction\ Factor\ (FF) &= 0.0019(0)^3 - 0.0188(0)^2 + 0.735(0) + 0.2951 \\ &= 0.2951 \quad (D.3) \end{aligned}$$

$$\varepsilon_{axial} = \frac{dL}{L_{original}}$$

$$= \frac{\text{plunger length w/o stress} - \text{plunger length w stress}}{\text{Length of coreholder} - (\text{Total plunger length} - \text{plunger length w stress} + \text{thickness of diffuser})}$$

$$= \frac{4.03 - 3.85}{47.6 - (10.2 - 3.85 + 0.1)} = 0.004374241 \quad (D.4)$$

$$\sigma_r = \frac{E}{(1 - 2\nu) * (1 + \nu)} * (\varepsilon_{axial} * \nu) \quad (D.5)$$

$$\sigma_{r_max} = \frac{3472.2}{(1 - 2(0.237)) * (1 + 0.237)} * (0.004374241 * 0.237) = 5.53 \text{ psi}$$

$$= 38,143 \text{ Pa} \quad (D.6)$$

$$\sigma_{r_min} = \frac{1388.89}{(1 - 2(0.115)) * (1 + 0.115)} * (0.004374241 * 0.115) = 0.81 \text{ psi}$$

$$= 5,611 \text{ Pa} \quad (D.7)$$

$F = \text{friction factor} * \text{normal force}$

$$= \text{friction factor} * (\sigma_r * \text{Area of core exposed to sand}) \quad (D.8)$$

$\text{Area of core exposed to sand} = (ID_{coreholder} * \pi) * \text{Length of sandpack}$

$$= \frac{(15.24 * \pi) * 42}{10,000} = 0.2011 \text{ m}^2 \quad (D.9)$$

$$F = \text{friction factor} * (\sigma_r * L_{core} - dL_{due to axial force}) \quad (D.10)$$

$dL_{due to axial force}$ can be estimated from end of test expansion using dial gauge

$$F_{min} = 0.53 * \sigma_{r_min} = 0.53 * (\sigma_r * \text{Area of core exposed to sand})$$

$$= 0.53 * (5,611 * 0.2011) = 338 \text{ N} \quad (D.11)$$

$$F_{max} = 0.53 * \sigma_{r_max} = 0.53 * (\sigma_r * \text{Area of core exposed to sand})$$

$$= 0.53 * (38,143 * 0.2011) = 3,068 \text{ N} \quad (D.12)$$

$$F_{sand \text{ weight}} = \text{mass of sand} * g = 11,120 * \frac{9.81}{1000} = 109 \text{ N} \quad (D.13)$$

$$F_{Load\ frame\ at\ 60\ psi} = 9,807\ N \quad (D.14)$$

$$F_{net_min} = F_{Load\ frame} - F_{min} + F_{sand\ weight} = 9,807 - 338 + 109 = 9,586\ N \quad (D.15)$$

$$F_{net_max} = F_{Load\ frame} - F_{max} + F_{sand\ weight} = 9,807 - 3,068 + 109 = 6,856\ N \quad (D.16)$$

UofA setup the friction losses with applied load of 350 psi:

$$\varepsilon_{axial} = \frac{dL}{L_{original}} = 0.00812065 \quad (D.17)$$

$$F_{Load\ frame\ at\ 60\ psi} = 44,482\ N \quad (D.18)$$

$$F_{net_min} = 40,398\ N \quad (D.19)$$

$$F_{net_max} = 43,981\ N \quad (D.20)$$

$$\begin{aligned} \text{Load losses due to friction} &= \frac{(F_{Load\ frame\ at\ 350\ psi} - F_{net_min}) \times 100}{F_{Load\ frame\ at\ 350\ psi}} \\ &= \frac{(44,482 - 40,398) \times 100}{44,482} = 9.18\ \% \quad (D.21) \end{aligned}$$

Hycal setup the friction losses with applied load of 350 psi:

$$\varepsilon_{axial_assumed} = \frac{dL}{L_{original}} = 0.00812065 \quad (D.22)$$

$$F_{Load\ frame\ at\ 350\ psi} = 6,098\ N \quad (D.22)$$

$$F_{net_min} = 618\ N \quad (D.23)$$

$$F_{net_max} = 4,202\ N \quad (D.24)$$

$$\begin{aligned} \text{Load losses due to friction} &= \frac{(F_{Load\ frame\ at\ 350\ psi} - F_{net_min}) \times 100}{F_{Load\ frame\ at\ 350\ psi}} \\ &= \frac{(6,098 - 618) \times 100}{6,098} = 68.76\ \% \quad (D.25) \end{aligned}$$